DETERMINATION OF THE COMPLEX MODULUS OF A SOLID PROPELLANT AND RANDOM VIBRATION ANALYSIS OF LAYERED VISCOELASTIC CYLINDERS WITH FINITE ELEMENT METHOD

by

Hsing-Juin Lee

Dissertation submitted to the Faculty of the
Virginia Polytechnic Institute and State University
in partial fulfillment of the requirements for the degree of
DOCTOR OF PHILOSOPHY
in
Engineering Mechanics

APPROVED:

R. A. Heller, Chairman

T. Herbert

T. Kuppusamy

L. G. Kraige

A. C. Loos

March, 1987

Blacksburg, Virginia

DETERMINATION OF THE COMPLEX MODULUS OF A SOLID PROPELLANT AND RANDOM VIBRATION ANALYSIS OF LAYERED VISCOELASTIC CYLINDERS WITH FINITE ELEMENT METHOD

BY

Hsing-Juin Lee

(ABSTRACT)

Aeronautical structures, such as aircraft or missiles, are usually highly sophisticated systems often subjected to random vibration environment. Thus, in various design, development, and production stages, laboratory random vibration testing of sampled solid rocket motors on electromagnetic or hydraulic shakers are routinely performed as an important experiment-oriented quality control strategy. Nevertheless, it is crucial to understand the dynamic structural behavior of these layered viscoelastic cylinders such as solid rocket motors under random vibration tests analytically.

In this study, a methodology has been developed to deal with the random vibration of a general class of composite structures with frequency-dependent viscoelastic material properties as represented by the example of solid rocket motors. The method combines the finite element method, structural dynamics, strain energy approach, and random vibration analysis concepts. The method is a more powerful technique capable of treating sophisticated random vibration problems

with complicated geometry, nonhomogeneous materials, and frequency-dependent stiffness and damping properties.

Before the random vibration analysis could proceed, a microcomputer-based dynamic mechanical analyzer system was used together with time-temperature superposition principle to obtain the frequency-dependent dynamic viscoelastic properties of the solid propellant. The strain energy approach has been used to calculate the frequency-dependent equivalent viscoelastic damping which is in turn judiciously represented by a combination of viscous damping and structural damping to accommodate this frequency dependent material property.

Modal analysis data together with half power band width calculated at each natural frequency are highly useful guides in the harmonic analysis to achieve computational efficiency. On one hand, the technique used in this study has a hybrid taste in the sense that it makes use of best features and capabilities of both modal analysis and harmonic analysis to achieve the goal of random vibration analysis in addition to the power of finite element technique. The displacement, acceleration and stress power spectra have been obtained for significant points on the rocket model together with their root mean square values. These data can be used for various analyses, testing, design, and other purposes as discussed in later sections of this study.

ACKNOWLEDGEMENTS

The author would like to express his deep and sincere gratitude to his advisor, Professor R. A. Heller for his valuable guidance, personal encouragements, patience and support during his course of doctoral study. Gratitude is also extended to Professors T. Herbert, T. Kuppusamy, L. G. Kraige, A. C. Loos, A. Myklebust, N. Dowling, M. W. Hyer, and M. P. Kamat for their highly appreciated instruction and encouragement.

Special thanks is extended to Professors D. Frederick, J. H. Sword, and all other members of Engineering Science and Mechanics Department for their support and providing an excellent learning and research environments.

Thanks are also due to his wife Mann-Hsi for her help, patience, and understanding during his good and hard times, and to his parents, Mr. and Mrs. Su-Sheng Lee for their incessant love thru all the years.

TABLE OF CONTENTS

LIST OF FIGURES

LIST OF TABLES

1.0 Introduction

1.1 Ideology

Aeronautical structures, such as aircraft or missiles, are usually highly sophisticated systems often subjected to severe natural and dynamic environments. These flight vehicles may experience rapid temperature changes, high humidity and corrosive conditions in addition to random vibration and shock. They have to be designed with high performance and reliability goals in mind. Many missile systems, no matter whether air launched, land vehicle, ship or submarine launched, are constantly subjected to random enviromental vibration. Thus, in various design, development, and production stages, laboratory random vibration testing of sampled solid rocket motors on electromagnetic or hydraulic shakers are routinely performed as an important experiment-oriented quality control strategy, and in many cases, must be performed to satisfy contract specification. Nevertheless, it is crucial to understand the dynamic structural behavior of these layered viscoelastic cylinders such as solid rocket motors under random vibration tests analytically, in order to acquire important data for enhancing test strategy,

failure anlysis, feedback to design, and solving controversies of detailed test arrangements.

1.2 Methodology

In this study, a method has been developed to deal with the random vibration of a general class of composite structures with frequency-dependent viscoelastic material properties as represented by the example of solid rocket motors. The method combines the finite element method, structural dynamics, strain energy approach, random vibration analysis concepts, and computing power. This method is a more powerful technique capable of treating sophisticated random vibration problems with complicated geometry, nonhomogeneous materials, frequency-dependent stiffness and damping properties.

1.3 Test Requirements

Viscoelastic materials are widely used in mechanical, aerospace, and other industries. Their dynamic behavior in sinusoidal motion is analyzed with the aid of the complex elastic modulus, i.e. storage modulus and loss modulus. Storage modulus is the real part of the complex elastic modulus, loss modulus is the imaginary part. Both are functions of frequency, and temperature. Unlike the viscous damping which is restricted to be linearly proportional to

velocity, the loss modulus may be a more generalized and realistic description of material damping in that, it can be any function of frequency.

Before the random vibration analysis could proceed, a microcomputer-based dynamic mechanical analyzer system [1] was used together with time-temperature superposition principle to obtain the frequency-dependent dynamic viscoelastic properties of the solid propellant in addition to the sandwich beam/finite element experimental method to obtain data at relatively higher frequencies for soft materials.

To determine these important dynamic properties for a viscoelastic material such as solid rocket propellants, there are various methods of vibration testing and equipment available [2,3,4]. In this study, a Du Pont dynamic mechanical analyzer [1,4,5], together with a TI professional microcomputer and associated analysis software are used. Due to the relatively narrow effective frequency range of the dynamic mechanical analyzer, test results are further processed with the aid of the time-temperature superposition principle (TTSP) [6,7] to extend the frequency range. Then a least square regression technique is used to obtain a 3-D quadratic surface model for modulus as a function of temperature and frequency. This data processing step is performed with SAS software [8,9,10] on a mainframe computer. Test

results , the surface model of modulus, and various contours are also presented later. This microcomputer-based testing system together with the data processing capability of the mainframe computer, is a useful combination for sophisticated dynamic testing.

1.4 Technical Comments

In this study, a solid rocket motor is simulated by a layered cylinder with viscoelastic core. The steel casing is modeled by shell finite elements and the viscoelastic core is modeled by three dimensional solid elements. One end of this layered cylindrical model is clamped to the support which is subjected to specified random excitation in terms of acceleration power spectrum and root mean square acceleration.

The modal analysis has been performed first to understand the the natural frequencies and mode shapes of the rocket model. Due to the more realistic 3-D model, instead of a beam model assumed in some other study [11], the mode shapes include ring modes and axial modes in addition to the usual bending modes. The strain energy approach has been used together with finite element method to calculate the frequency-dependent equivalent viscoelastic damping which is in turn judiciously represented by a combination of viscous damping

and structural damping to accommodate this frequency dependent material property.

Modal analysis data together with half power band width calculated at each natural frequency are highly useful guides in the harmonic analysis in order to achieve computational efficiency. On one hand, the technique used in this study has a hybrid sense in that it makes use of the best features and capabilities of both modal analysis and harmonic analysis to achieve the goal of random vibration analysis in addition to the power of finite element technique. On the other hand, vibration experiments and computational power were closely weaved together in the study to establish a useful analysis mechanism.

Then the finite element model is used to calculate the discrete frequency response function of stresses and displacement at significant points on the structure. The displacement, acceleration and stress power spectra have been obtained for significant points on the rocket model together with their root mean square values. Moreover, the displacement, acceleration and stress power spectra can later be used for various analysis, testing, design and other purposes as discussed in Chapter 7.

2.0 Literature Review

Viscoelastic materials are widely used in mechanical, aerospace, and other industries. Their dynamic behavior in sinusoidal motion is analyzed with the aid of the complex elastic modulus. This subject has long been investigated by Leaderman [12], Flugge [13], and others. Christensen [14] generalized the theory, Ferry [6] applied it to polymers and developed the time temperature superposition principle with others. Read and Dean [3] review various experimental techniques and instruments to determine the dynamic viscoelastic properties. Lear and Gill [15,16] discuss the theory of dynamic mechanical analyzers, which is basically a computer-aided single degree of freedom testing system. Snowdon [7] generalizes the concept of viscoelastic damping and applies to mechanical systems subjected to shock and vibration, especially various configurations of beams with different boundary conditions. Nicholas and Heller [17] investigate the theory of sandwich beam with viscoelastic core and develope associated experimental and data processing techniques to determine the complex shear modulus by free vibration of the cantileved sandwich beam. The sandwich beam technique generally is used to obtain dynamic data of the

soft viscoelastic core at higher frequencies. In recent years, there has been growing interest in the application of finite element methods to vibration of sandwich beams and multiple layered structures; Johnson and Kienholz [18] use finite element methods and the strain energy approach [19] to predict the modal damping of laminated beams. Soni [20,21] and Lu also have work in this area. Shock and Vibration Digest has a series of survey articles on vibration control with viscoelastic material by Nakra [22-24]. Damping Technology Information Services at Wright-Patterson AFB may be a useful damping data source also.

The finite element method together with support vibration of clamped sandwich beams on an electromagnetic shaker has been used in this study to determine the dynamic modulus and loss modulus of a solid propellant; the data are compared with the results obtained on the dynamic mechanical analyzer.

Concerning vibration analysis, Timoshenko, Thomson [25], Meirovitch [26], Steidel [27] and others presented texts on its theory and application. Curtis [28] discussed the practice of vibration testing. Harris and Crede published a notable handbook of shock and vibration. Pilkey [29] presents reviews and summaries on shock and vibration computer programs. D. J. Gorman [30] authored a book on free vibration of beams and shafts with various boundary configurations.

Rieger [31] had a literature review of vibration engineering. Crandall [32,33], Roberson [34], Lin [35], Newland [36], Elishakoff [37], Shin and Au-Yang [38], Bolotin [39], Huang and Spanos [40] had works on random vibration or random fatigue life prediction. Neverthless, none of these publications have made a serious attempt to tap the power of the finite element method for use in random vibration analysis of composite structures with frequency-dependent material properties. The problem of layered cylinders with frequency dependent viscoelastic material and subjected to random support excitation is investigated with the finite element methods in one part of this study.

Since the classical paper by Turner, Clough, Martin and Topp [41], over thirty years ago, the finite element method [42,43] has been under intensive investigation; there are many books and papers devoted to its theory and application in addition to a number of journals covering this subject. In its early stage; finite element methodology was used for static structural analysis by the aerospace industry; since then it has evolved into a general variationally based numerical technique for solving various differential equations. This method, enhanced by fast-advancing computer technology, has been successfully used for structural mechanics, fracture mechanics, fluid mechanics, heat transfer, electromagnetics, and other ever-increasing new fields. Due to the vast pool

of related papers, there are survey article by Pilkey [44] and others. The quadrilateral shell element used for rocket motor casing in this study is based on a formulation by Batoz [45], while the 3-D finite element for the propellant core is employed by Wilson, Taylor and others [46]. The wave front solution scheme is described by Irons [47] and others.

In this information age, the knowledge of available computer software resources [48,49], such as IMSL [50], SAS [8-10], ANSYS [51,52], and NASTRAN is no longer limited to a small number of previleged groups. These software resources can be used judiciously to relieve reserachers of wasting effort on writing repetitive routine computer programs, thus they can use their time more wisely on creative thinking. In this study, a few computer programs have been written in the languages of Fortran, ANSYS engineering analysis system and SAS to facilitate tests and analysis; some of them are listed in the appendix.

3.0 Configuration and Theoretical Background of the Dynamic Mechanical Analysis System

3.1 System Description

The testing equipment used to determine the complex modulus include a Du Pont dynamic mechanical analyzer DMA982 [Figs. 3.1-3.3], a module interface, a TI professional microcomputer [1] with 10-megabyte hard disk, and associated peripherals. The system measures changes in the dynamic viscoelastic properties resulting from changes in temperature and frequency. It can test material ranging from very soft, such as adhesives and propellant, to very hard, such as steel and ceramic. The allowable storage modulus can range from 1 MPa to 210 GPa. This resonant frequency instrument applies sophisticated data reduction routines to generate test results in either graphical or tabular format.

The Du Pont DMA982 analyzer generates small amplitude, low strain bending vibrations in the tested sample [Figs. 3.3.,3.4, 3.5] [1,15]. Two parallel arms of the DMA, to which the specimen is attached oscillate in a horizontal plane about two pivots. They are restrained by torsional

springs and are driven sinusoidally at a preset small amplitude by an electromagnetic driver at the end of one arm. The system will follow any change in resonant frequency and make up the energy loss due to damping, to maintain the preset amplitude. The natural frequency is a measure of the storage modulus, and the amount of electric compensation of energy is a measure of the loss modulus of the material.

The DMA982 analyzer has a mechanics chamber which contains the flexure pivots, two oscillating arms and clamp sets, an electromagnetic driver, and a linear variable differential transformer (LVDT). The LVDT measures the amplitude of oscillation of the arms, sending a signal to the interface module and then to the computer. The sample chamber contains a radiant heater and a coolant distribution system; a sample thermocouple transmits the temperature signal to the computer.

The DMA analyzer can test a wide temperature range from -150 deg to 500 deg C, with damping ratios between 0.01 to 1.0, amplitude between 0.1 to 1.0 mm and specimen length between 6 to 65 mm. The maximum allowable sample thickness is 12 mm and maximum width is 15 mm. The appropriate sample dimension can be selected within the given range to make the system

natural frequency between 10 to 40 Hz and a damping signal above 10 mv, for optimum test results [1].

3.2 Theoretical Background

For a viscously damped torsional vibration system with a single degree of freedom, the equation of motion [27,53] is given as

$$J\frac{d^2\Phi}{dt^2} + C_t\frac{d\Phi}{dt} + K_t\Phi = M(t) \qquad [3.1]$$

where

J	Mass moment of inertia
Φ	Angular displacement
C_t	Damping constant
K_t	Torsional Stiffness
M	Moment, a time function

Similarly for structural damping , the equation of motion [25,26] becomes

$$J\frac{d^2\Phi}{dt^2} + K_t(1 + i\gamma_1)\Phi = M(t) \qquad [3.2]$$

where γ_1 is the structural damping ratio.

The DMA982 analyzer can be modeled as a torsional vibration system with damping supplied primarily by the viscoelastic

test specimen clamped between two parallel oscillating arms [Fig. 3.5][15, 54]. With a small angular displacement of Φ, the sample will experience a dispalcement Δx of the arms as shown. This displacement contains two contributions; one due to the sample, the other primarily due to the pivot distortion. The theoretical procedure presented in this section is a revised derivation following Lear [15].

$$\Delta x = F\{(\frac{L^3}{12EI} + \frac{\alpha L}{AG}) + J_c\} \qquad [3.3]$$

where

F	Shear force at ends of sample
E	Young's modulus of sample
I	Area moment of inertia of sample cross-section
α	Shear factor of the sample cross-section
G	Shear modulus of sample
J_c	compliance of pivot
A	Sample cross-section area
L	Sample length between clamps

or

$$F = \frac{1}{\{(\frac{L^3}{12EI} + \frac{\alpha L}{AG}) + J_c\}}\Delta x$$
$$= K\ \Delta x$$

where $\Delta x \approx B\Phi$. The total moment acting on the arms and produced by the sample is

$$
\begin{aligned}
M &= [K(B\Phi)]L + FD + FD \\
&= [K(B\Phi)]L + [K(B\Phi)]2D \\
&= [K(B\Phi)](L + 2D) \\
&= [K(B\Phi)]B \\
&= KB^2\Phi
\end{aligned}
\qquad [3.4]
$$

Thus, the equation of motion for DMA [13,55];

$$
2J\frac{d^2\Phi}{dt^2} + \frac{B^2}{\{(\frac{L^3}{12E^{\times}I} + \frac{\alpha L}{AG^{\times}}) + J_c^{\times}\}}\Phi + 2K_{ts}^{\times}\Phi = M(t) \qquad [3.5]
$$

where J is the mass moment of inertia of one oscillating arm about its pivot, and

$$
\begin{aligned}
E^{\times} &= E_1 + iE_2 \\
G^{\times} &= G_1 + iG_2 \\
J_c^{\times} &= J_{c1} - iJ_{c2} \\
K_{ts}^{\times} &= K_{ts1} + iK_{ts2}
\end{aligned}
\qquad [3.6]
$$

are complex quantities to represent the viscoelastic properties of the system. $K_{ts}^{\times}$ is the complex modulus for each torsional spring at pivots. $E^{\times}$ and $G^{\times}$ are related by the Poisson's ratio as

$$
E^{\times} = 2(1 + \nu)G^{\times} \qquad [3.7]
$$

Substituting eqs. [3.6] and [3.7] into eq. [3.5] and reorganizing it [15];

$$2J\frac{d^2\Phi}{dt^2} + \frac{B^2A}{L}\left\{\frac{(G_1\beta + G_2\gamma) + i(G_2\beta - G_1\gamma)}{\beta^2 + \gamma^2}\right\}\Phi + 2(K_{ts1} + iK_{ts2})\Phi = M(t) \qquad [3.8]$$

results. Where

$$\beta = \alpha + \frac{L^2A}{24(1+\nu)I} + \frac{A}{L}(J_{c1}G_1 + J_{c2}G_2) \qquad [3.9]$$

$$\gamma = \frac{A}{L}(J_{c1}G_2 + J_{c2}G_1) \qquad [3.10]$$

or, separating the real and imaginary parts,

$$2J\frac{d^2\Phi}{dt^2} + \left\{\frac{B^2A}{L(\beta^2+\gamma^2)}(G_1\beta + G_2\gamma) + 2K_{ts1}\right\}\Phi + i\left\{\frac{B^2A}{L(\beta^2+\gamma^2)}(G_2\beta - G_1\gamma) + 2K_{ts2}\right\}\Phi = M(t) \qquad [3.11]$$

where the first bracket term is K_{t1}, and the second bracket term is K_{t2}, they are the real and imaginary parts of $K_t^{\times}$ respectively.

The angular displacement can be expressed as

$$\Phi^{\times} = \frac{M_0}{(K_{t1} - 2J\omega^2) + iK_{t2}} \quad , \qquad [3.12]$$

where Mo is the amplitude of M(t).

The DMA analyzer detects the natural frequency

$$\omega^2 = \frac{K_{t1}}{2J} \qquad [3.13]$$

Then from equation [3.11]

$$\omega^2 = \frac{1}{2J}\left\{\frac{B^2A}{L(\beta^2+\gamma^2)}(G_1\beta + G_2\gamma) + 2K_{ts1}\right\} \qquad [3.14]$$

or

$$G_1 = (2J\omega^2 - 2K_{ts1})\frac{(\beta^2+\gamma^2)L}{\beta B^2 A} - \frac{\gamma}{\beta}G_2 \qquad [3.15]$$

Also at resonance, the angular displacement

$$\Phi_0 = \frac{M_0}{K_{t2}} \qquad [3.16]$$

or

$$\Phi_0 = \frac{M_0}{\left\{\frac{B^2A}{L(\beta^2+\gamma^2)}(G_2\beta - G_1\gamma) + 2K_{ts2}\right\}} \qquad [3.17]$$

or

$$G_2 = \left(\frac{M_0}{\Phi_0} - 2K_{ts2}\right)\frac{(\beta^2+\gamma^2)L}{\beta B^2 A} + \frac{\gamma}{\beta}G_1 \qquad [3.18]$$

where Mo is related to the voltage signal V of electromagnetic driver by some system constants [15].

Since β and γ are functions of G1 and G2, equations [3.15] and [3.18] are quadratic in terms of G1 and G2. Solution for them may be obtained by iteration. Test results and data processing will be discussed in the next chapter.

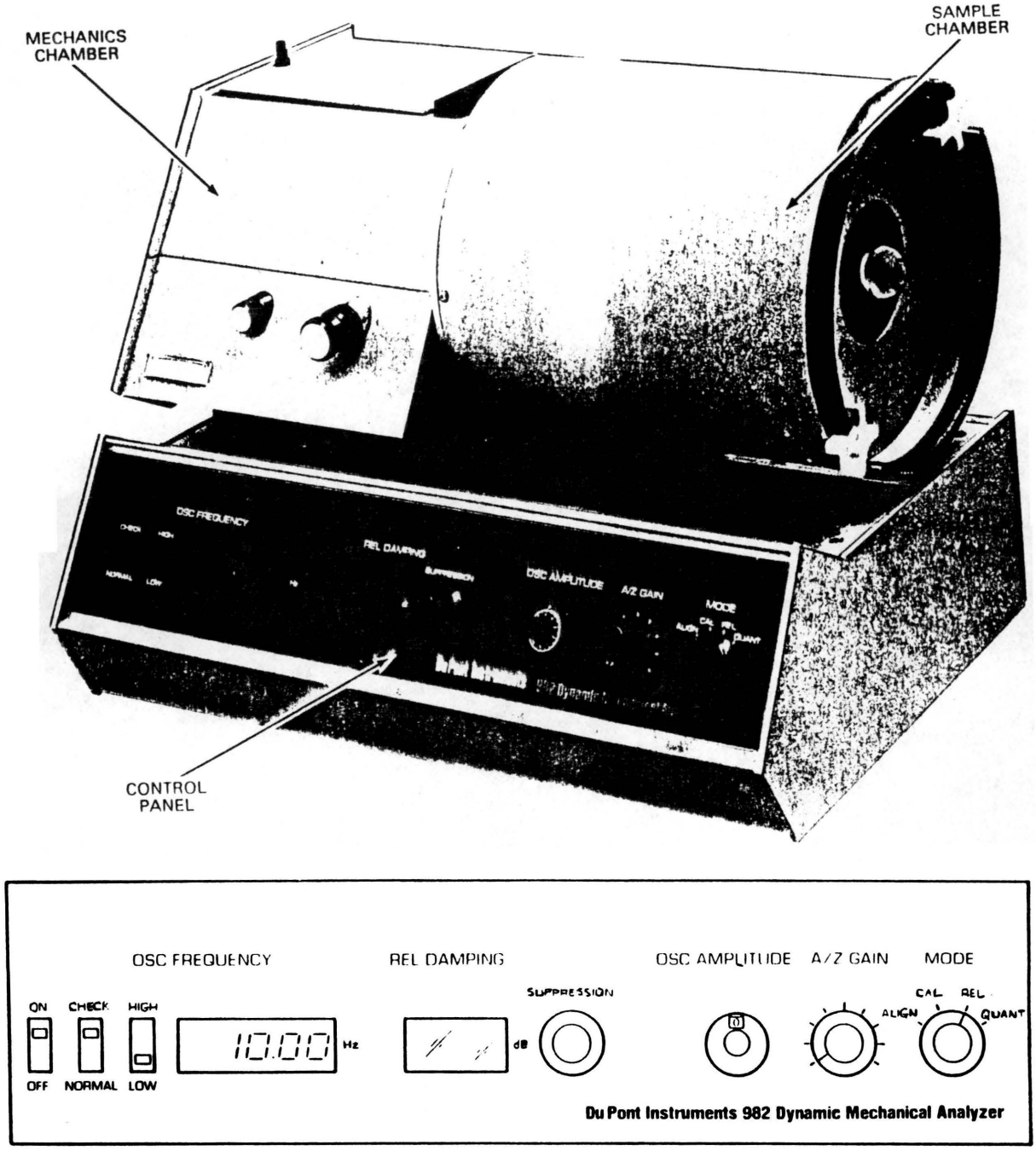

Figure 3.1 Du Pont Dynamic Mechanical Analyzer 982 and Control Panel [1]

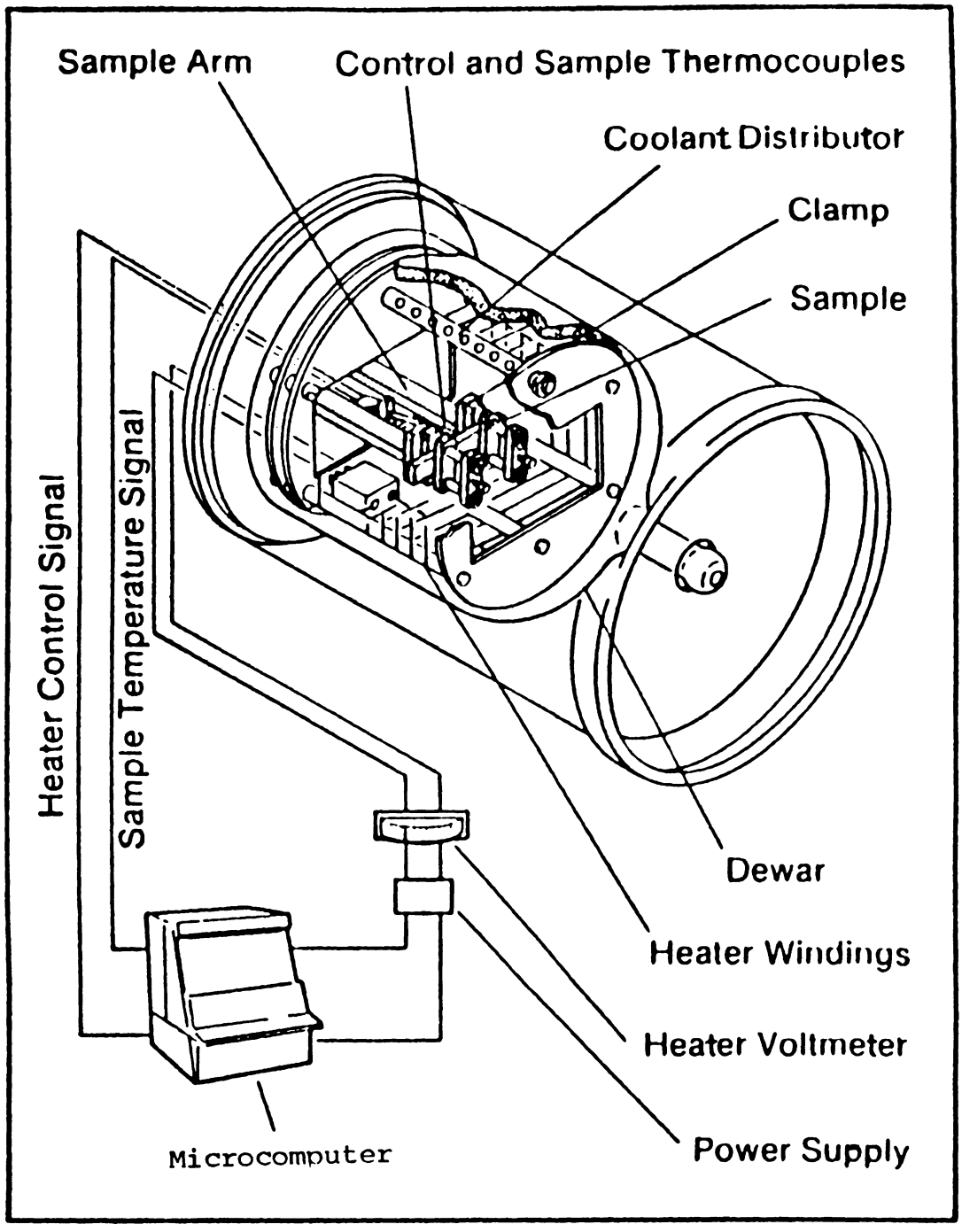

Figure 3.2 DMA982 Sample Chamber [4]

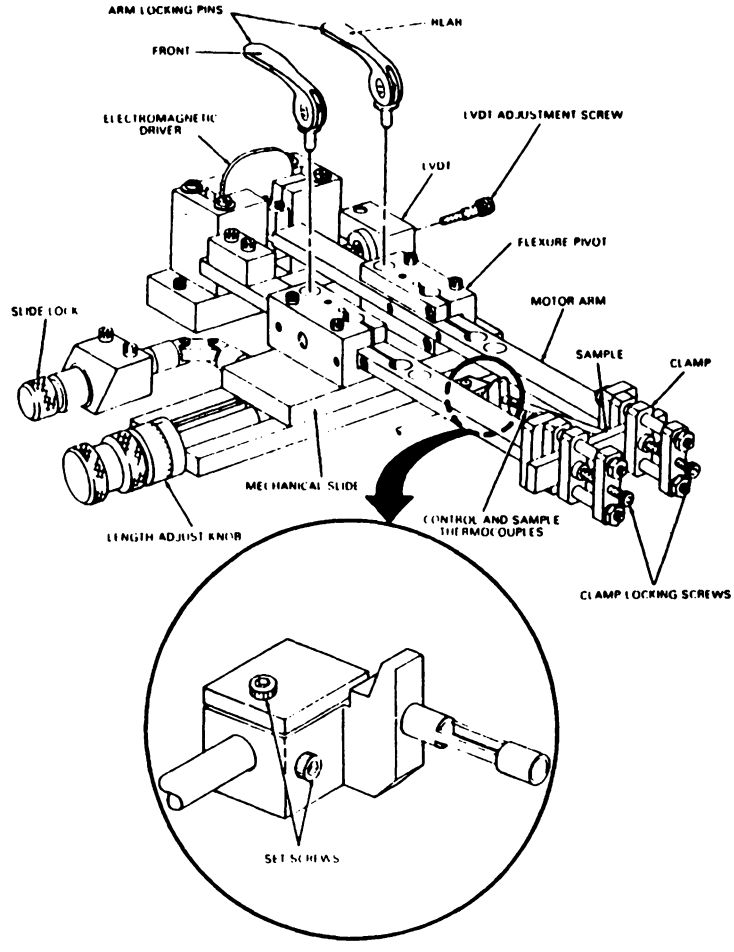

Figure 3.3 DMA982 Mechanics Chamber [1]

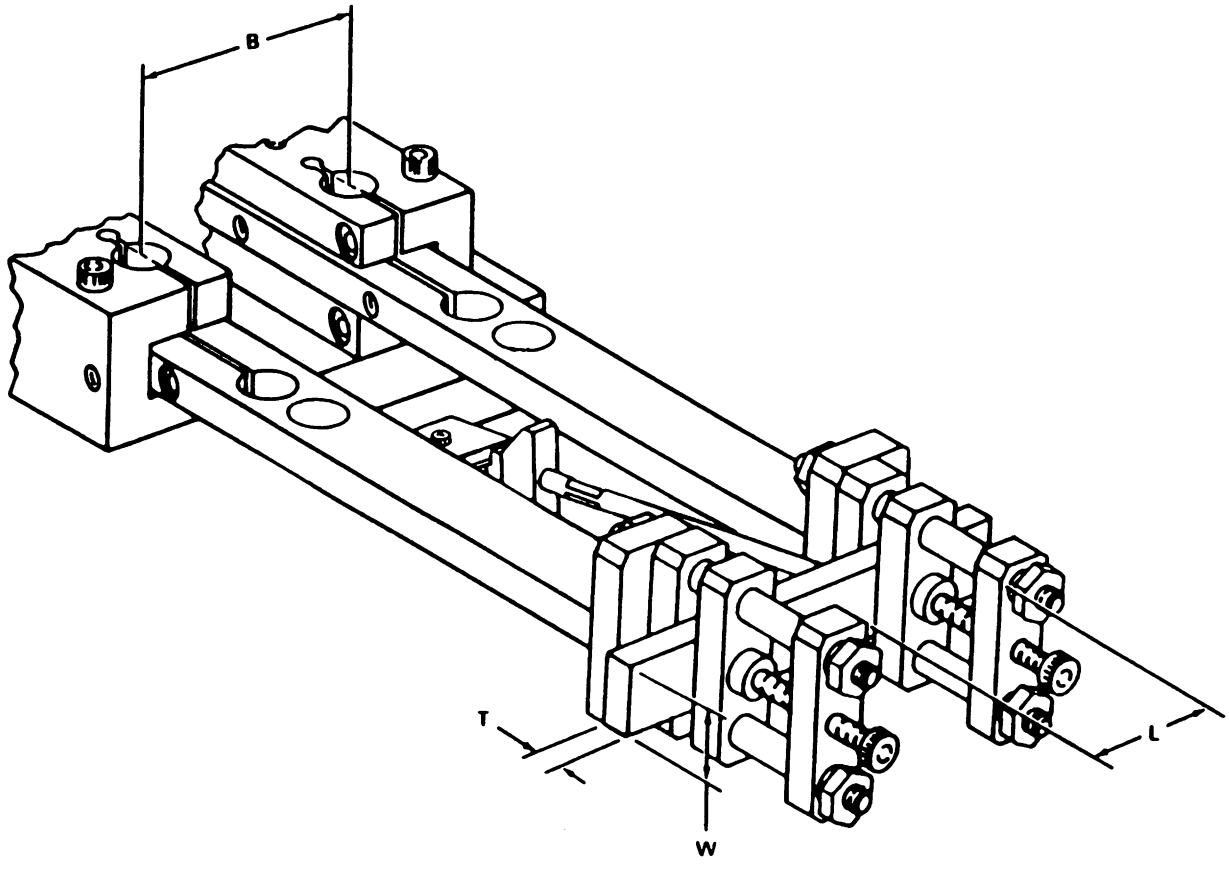

Figure 3.4 DMA982 Pivots, Oscillation Arms, and Sample Dimensions [1]

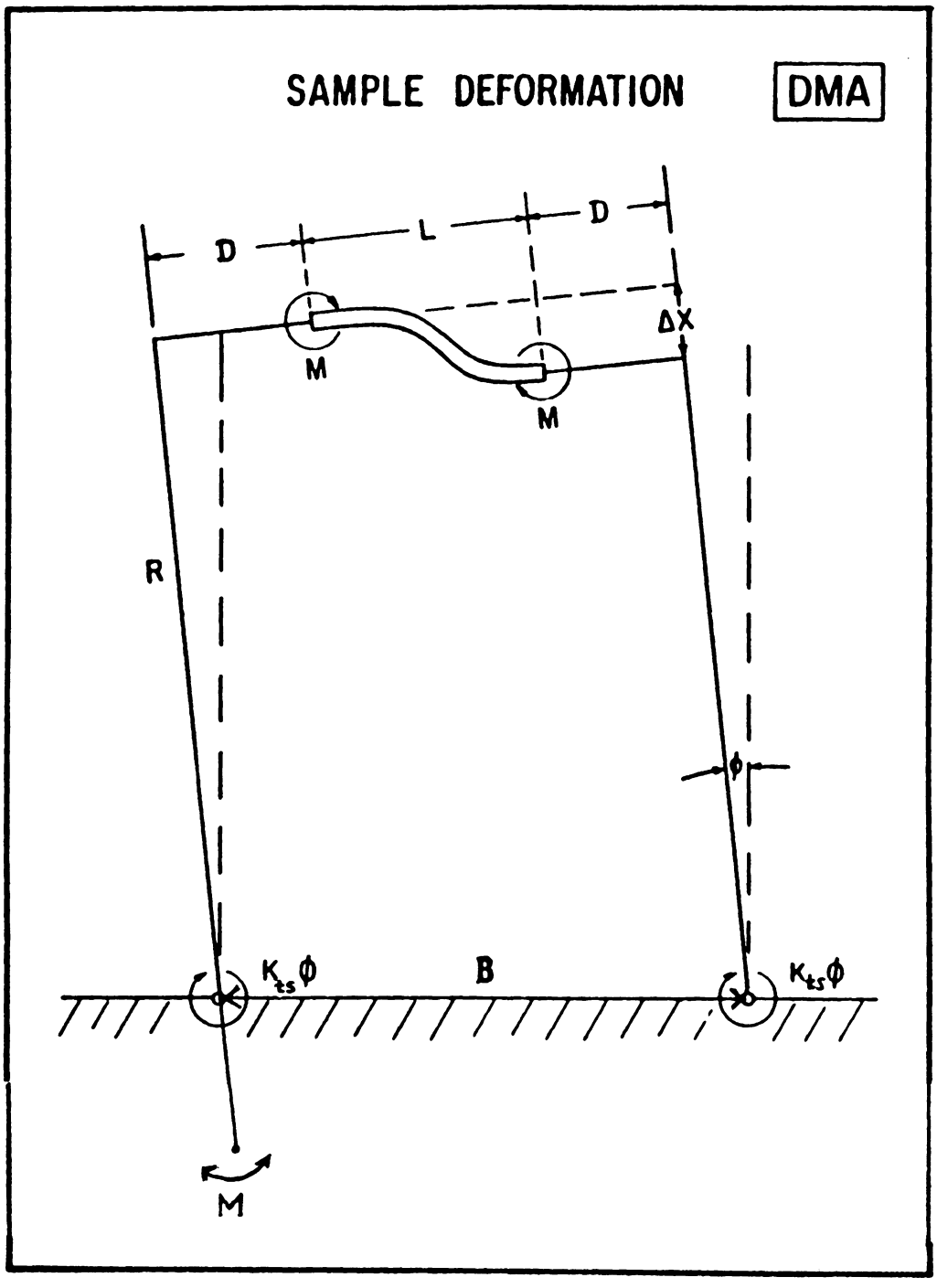

Figure 3.5 Simplified Mechanics Model for figure 3.4 [1, 56]

4.0 Dynamic Mechanical Testing and Data Processing

4.1 Dynamic Mechanical Technique [54]

After the appropriate dimensions of a test sample are selected, and the specimen is installed in the sample chamber of the DMA982, the chamber temperature can be cooled to a specified degree by supplying liquid nitrogen at 78 degrees K. By natural heat transfer, the chamber temperature will rise up to about 256 degrees K, then the DMA heating system takes over control. The temperature process is controlled by a user written program with the DMA thermal analysis software. During testing, the natural frequency and damping voltage signal are continuously stored on the hard disk of the micro-computer and later processed to generate the storage modulus and loss modulus as a function of frequency and temperature. A few test results and associated specimen data are shown in Figs. 4.1-4.8.

Since the frequency range of the DMA982 is very limited, it is desirable to extend the test results to a wider frequency range, this may be accomplished with the use of Time-Temperature Superposition Principle (TTSP) and associated WLF

equation presented by Williams and others [1]. The revised WLF equation for viscoelastic shift function of TPH8208 propellant [57] can be expressed as;

$$\log(a_T) = \frac{-C_1(T - T_s)}{C_2 + (T - T_s) + C_3(T - T_s)^2} \qquad [4.1]$$

where T is the test temperature, Ts = 244.11 degrees K is the reference temperature, C1 = 20.5, C2 = 206.7, and C3 = 0.01325 are constant coefficients [57] with appropriate dimensions to make the shift function nondimensional. The allowable temperature range is between 219 degrees and 338 degrees K. Usually the TTSP is used to transfer data tested at a constant temperature, but due to the nature of data from DMA982 as a result of temperature sweep, it is convenient to write a Fortran program to shift the test data to the reference temperature and then to the desired temperature. A three dimensional best-fit surface can be obtained by regression on the scattered data over a widened frequency range [Figs. 4.9, 4.12, 4.13] [Table 4.1] using the plotting software: SAS/Graph of Statistics Analysis System (SAS) [8-10]. A procedure of SAS Statistics is used to regress the moduli to obtain quadratic surfaces of the form;

$$\begin{aligned} LNE1 = {} & \beta_0 + \beta_1(INVT) + \beta_2(LNFRQ) + \beta_3(INVT)^2 \\ & + \beta_4(LNFRQ)^2 + \beta_5(INVT)(LNFRQ) + \beta_6\varepsilon \end{aligned} \qquad [4.2]$$

where LNE1 = ln(E1), INVT = 1/(temperature deg K), LNFRQ = ln(frequency), and ε is the error term. A similar relation was developed for ln(E2).

The acquired beta coefficients are listed as;

	ln E1	ln E2
βo	-1.0815	-16.93
$\beta 1$	-2209.7	5318.9
$\beta 2$	2.1	3.5
$\beta 3$	949179	0
$\beta 4$	-0.0411	-0.0717
$\beta 5$	-413.6	-747.4

Moreover, contours of the 3D storage modulus, loss modulus and curves of constant temperature can be plotted as shown in Figs. [4.10, 4.11, 4.14, 4.15] by the Gcontour and other procedures of SAS/Graph.

4.2 Sandwich Beam/Finite Element Technique

On the other hand, in this study a sandwich beam/finite element technique was developed to obtain the viscoelastic properties of the propellant at relatively higher frequencies as a check on the results of the dynamic mechanical technique. A typical sandwich beam model [Fig. 4.16] consists of a propellant beam with thin upper and lower steel cover plates which are used to raise the rigidity and natural fre-

quencies of the soft propellant beam. The technique can be briefly described as follows;

(a) A vibration test of the cantilevered sandwich beam on a electromagnetic shaker can be performed to identify the first natural frequency and the associated mode shape. The amplification ratio between the free tip of the beam and the support point can also be obtained with the aid of acceleration readings at both points.

(b) A 2-D finite element model of the sandwich beam can be constructed by using beam elements for the two steel cover plates and 2-D elements for the propellant core.

(c) The first natural frequency can be obtained by the computer program [A3] written in the language of ANSYS engineering analysis system [51,52]. Using an iterative technique, the storage modulus of the propellant can be varied in order to attain the first natural frequency obtained from the shaker test. As a result, the storage modulus of the propellant is obtained at the first natural frequency.

(d) A harmonic response analysis [A4] can be performed using the finite element model. By varying the equivalent viscoelastic damping of the beam, the measured amplification

ratio between the free tip and the support point as vibration test can be obtained. Hence the equivalent viscoelastic damping of the sandwich beam at the first natural frequency is obtained.

(e) The strain energy ratio between the steel covers and the propellant core can be obtained [A5]. Then the strain energy approach [19,18] can be used to calculate the the loss modulus of the propellant at the first natural frequency by the following equation;

$$\eta_e = (\eta_p)_e + (\eta_s)_e = \eta_p \frac{(SE)p}{(SE)p + (SE)s} + \eta_s \frac{(SE)s}{(SE)p + (SE)s} \qquad [4.3]$$

where (SE) means strain energy, η is the viscoelastic damping ratio, the subscript e means equivalent, subcripts p and s indicate propellant beam and steel cover plates respectively.

The above technique has been used for two sandwich beams of different thicknesses. They show agreeable results [Figs. 4.11, 4.15] with the data from the dynamic mechanical technique with difference in the range of 5% to 14% for frequencies between 150 and 180 Hz. More tests and research may be performed to refine the above useful technique.

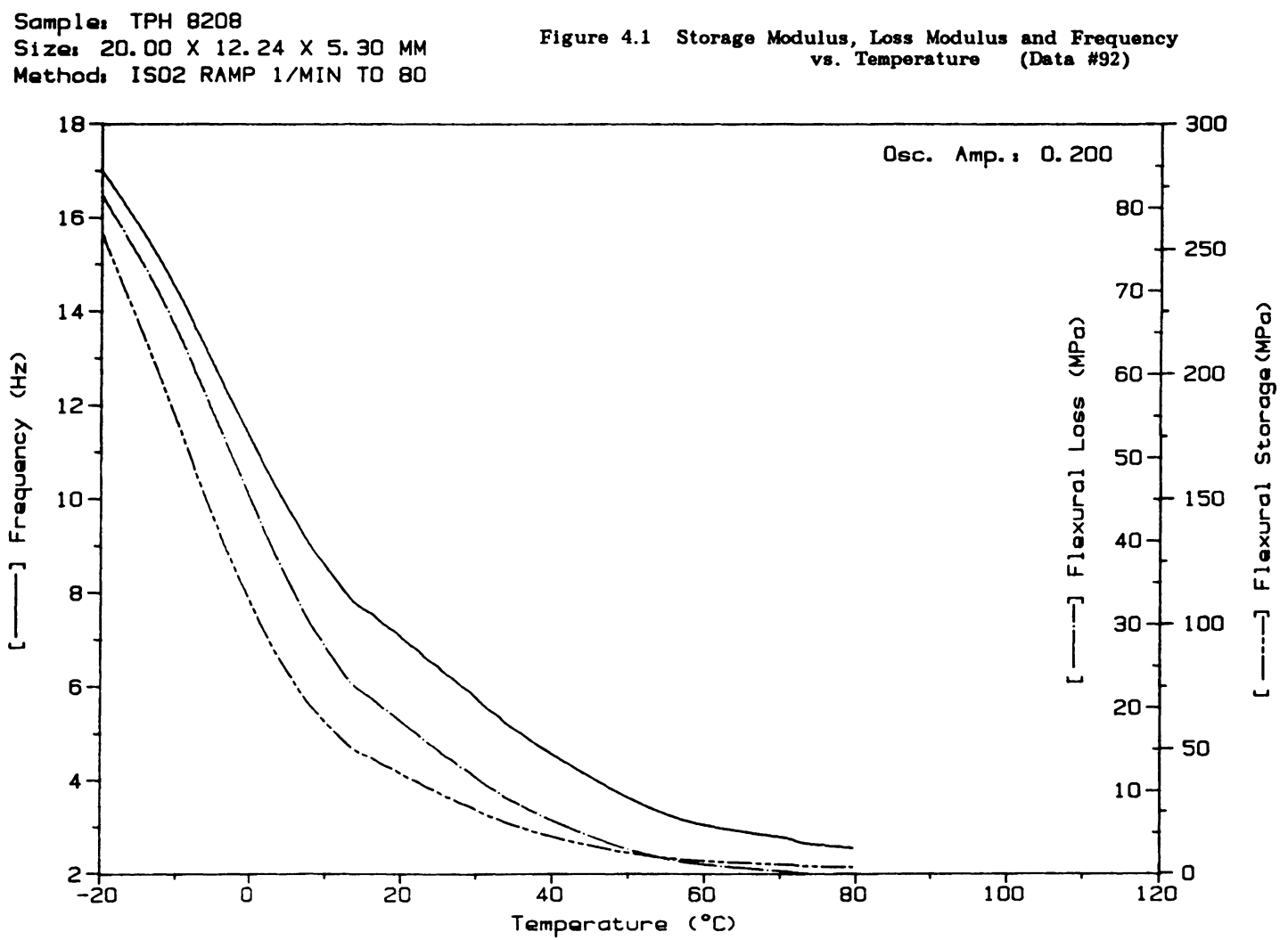

Figure 4.1 Storage Modulus, Loss Modulus and Frequency vs. Temperature (Data #92)

Sample: TPH 8208
Size: 20.00 X 12.24 X 5.30 MM
Method: ISO2 RAMP 1/MIN TO 80

Figure 4.2 Damping Ratio and Frequency vs. Temperature (Data 92)

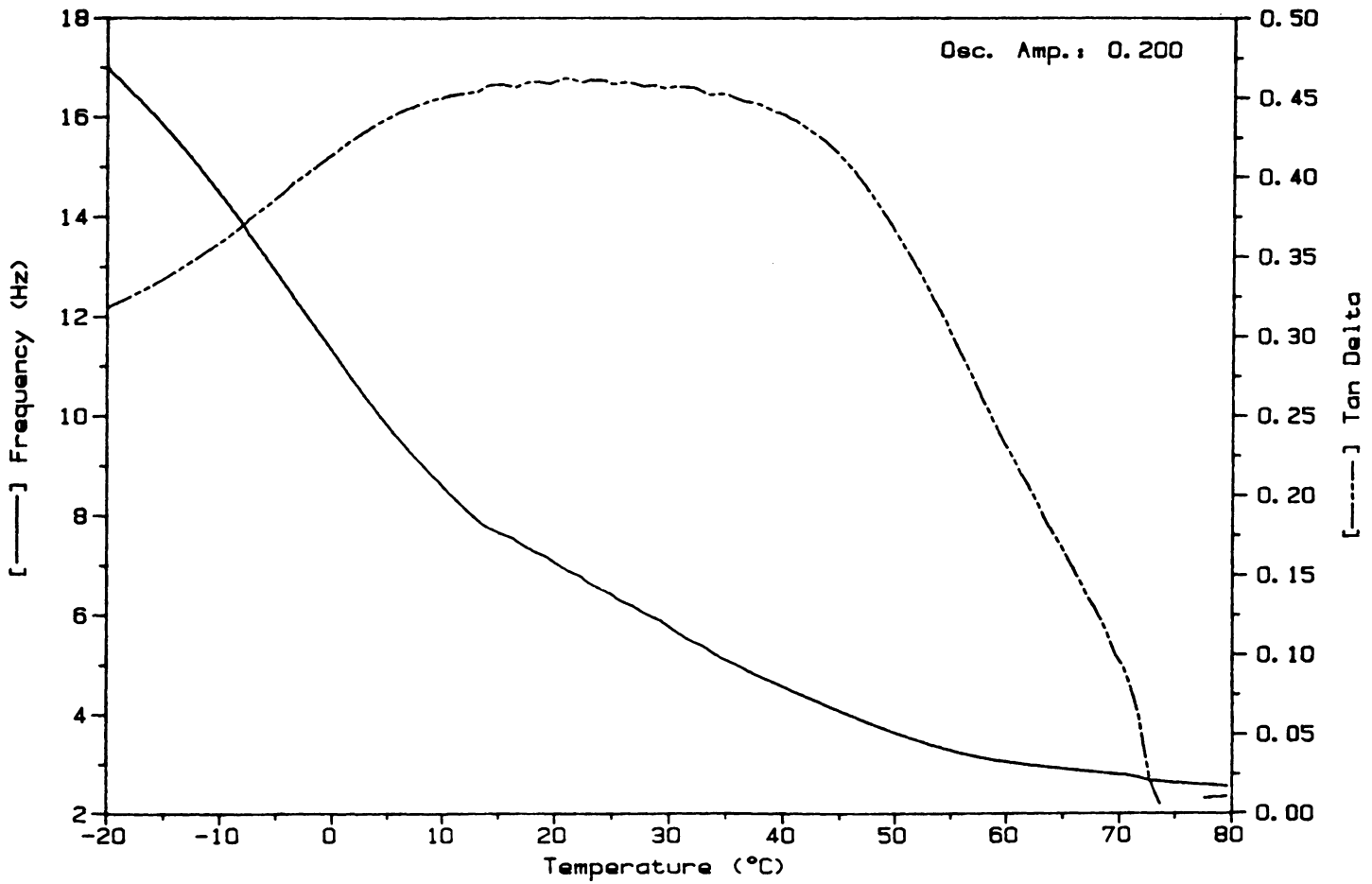

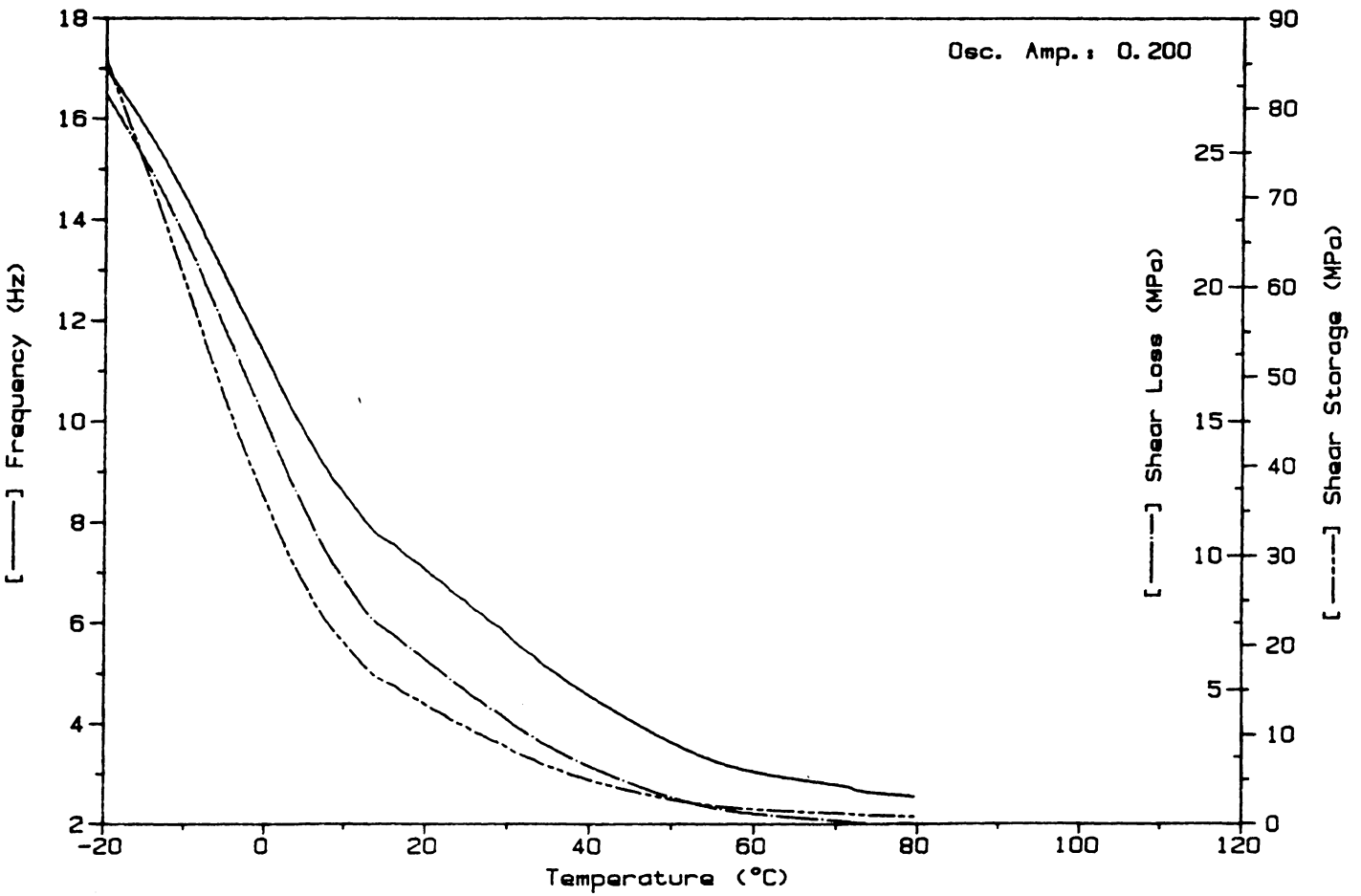

Figure 4.3 Shear Storage Modulus, Shear Loss Modulus and Frequency vs. Temperature (Data #92)

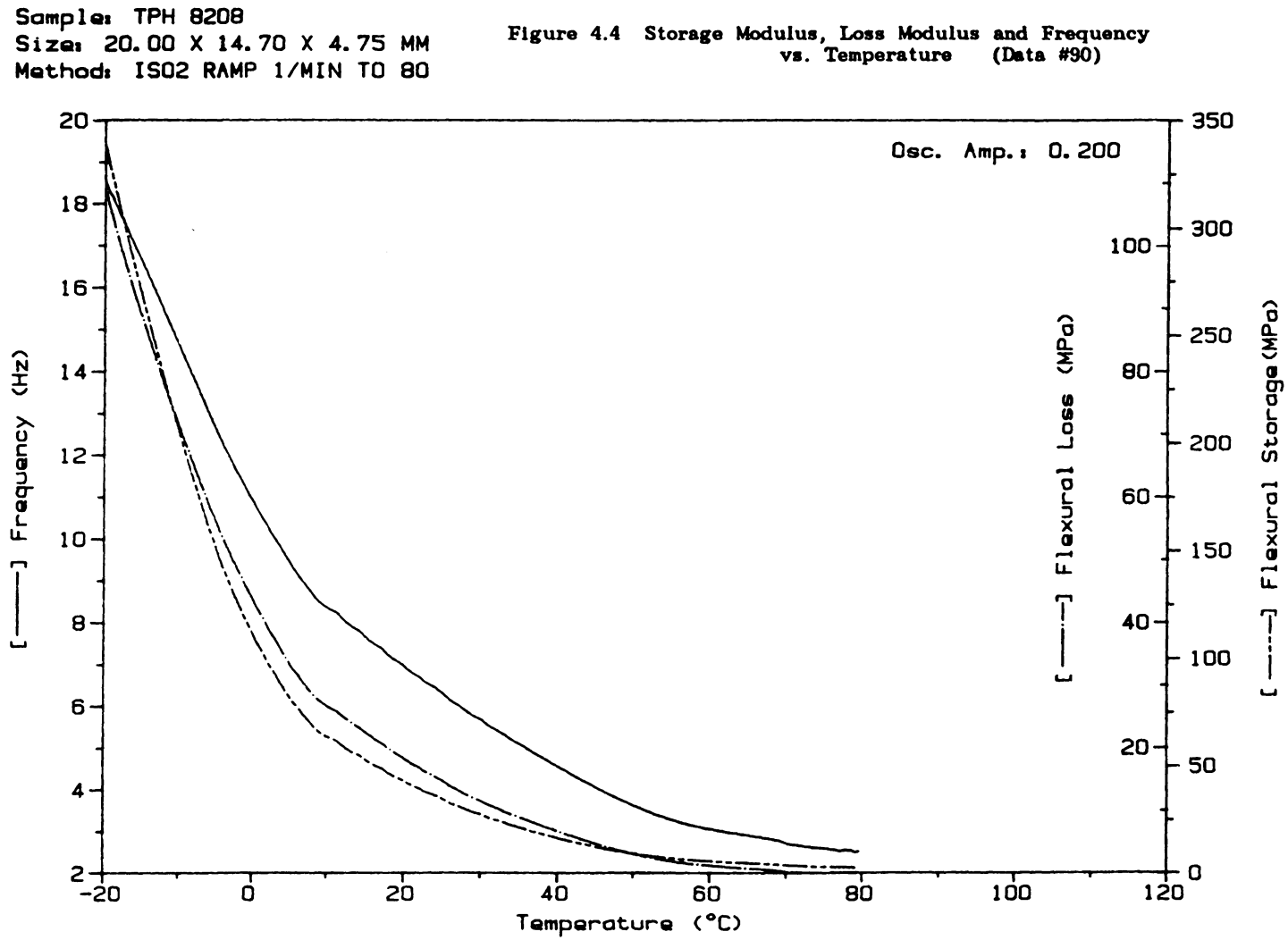

Figure 4.4 Storage Modulus, Loss Modulus and Frequency vs. Temperature (Data #90)

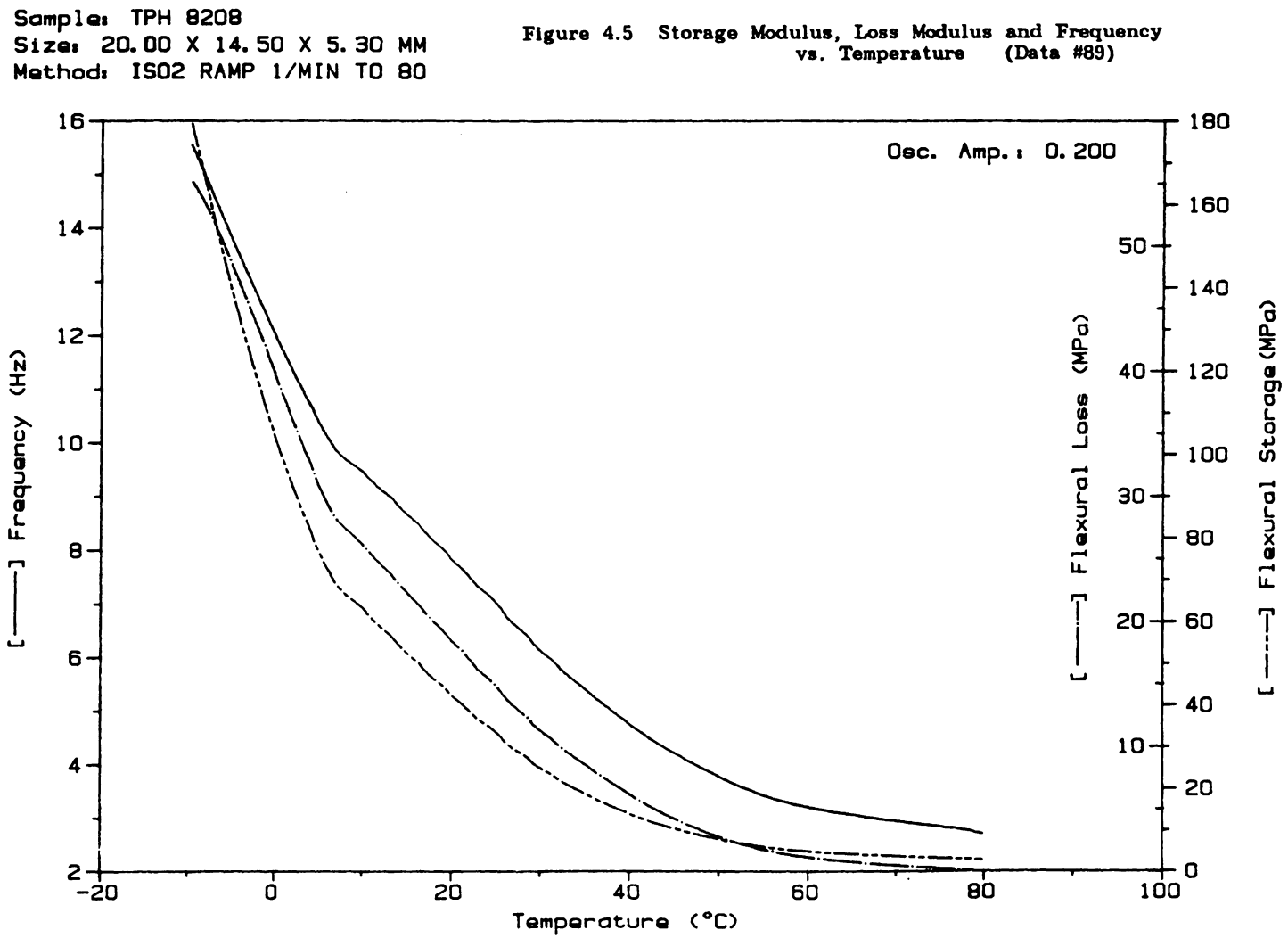

Figure 4.5 Storage Modulus, Loss Modulus and Frequency vs. Temperature (Data #89)

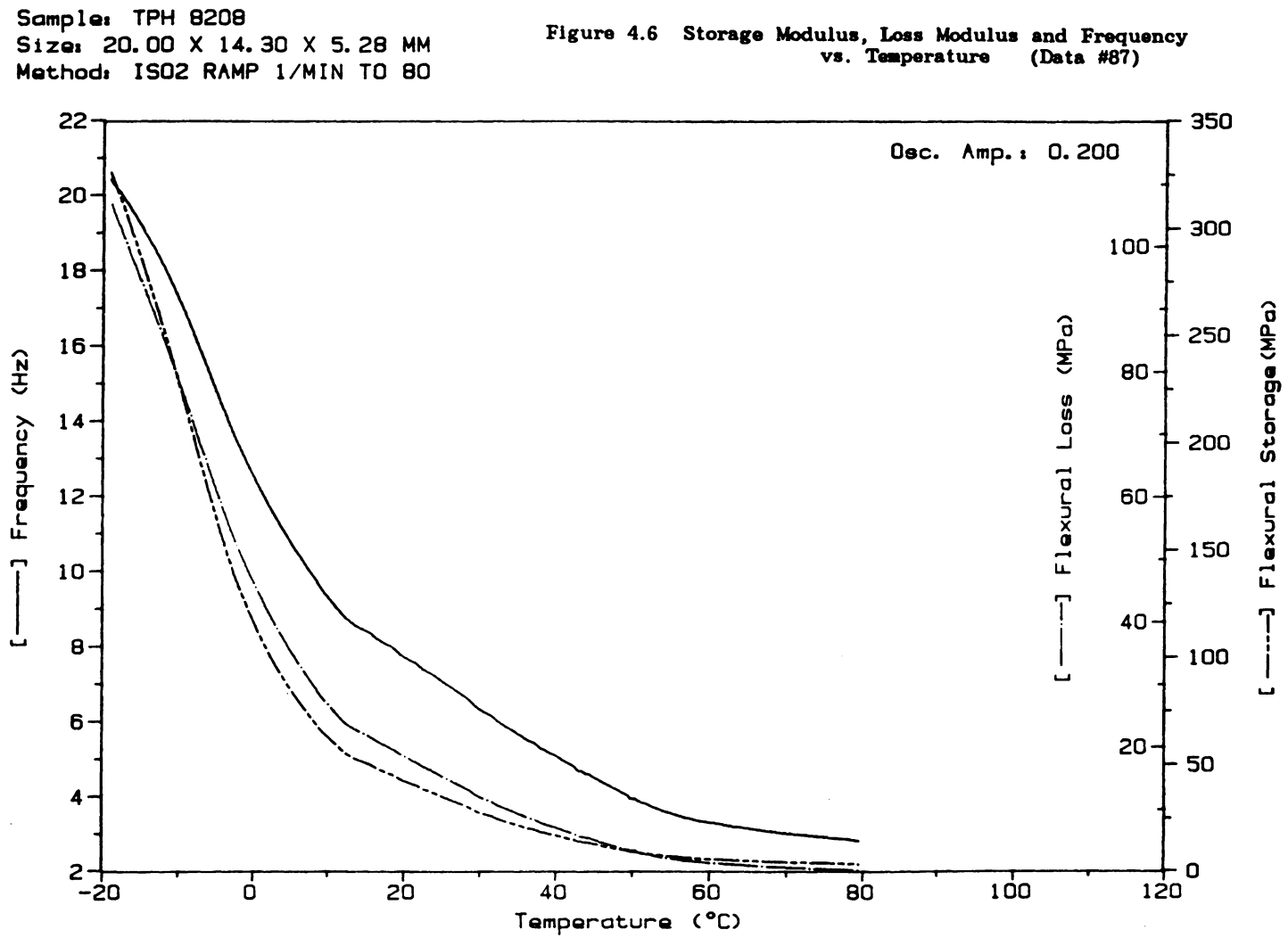

Figure 4.6 Storage Modulus, Loss Modulus and Frequency vs. Temperature (Data #87)

Sample: TPH 8208
Size: 20.00 X 14.30 X 5.28 MM
Method: ISO2 RAMP 1/MIN TO 80

Figure 4.7 Damping Ratio and Frequency vs. Temperature (Data 87)

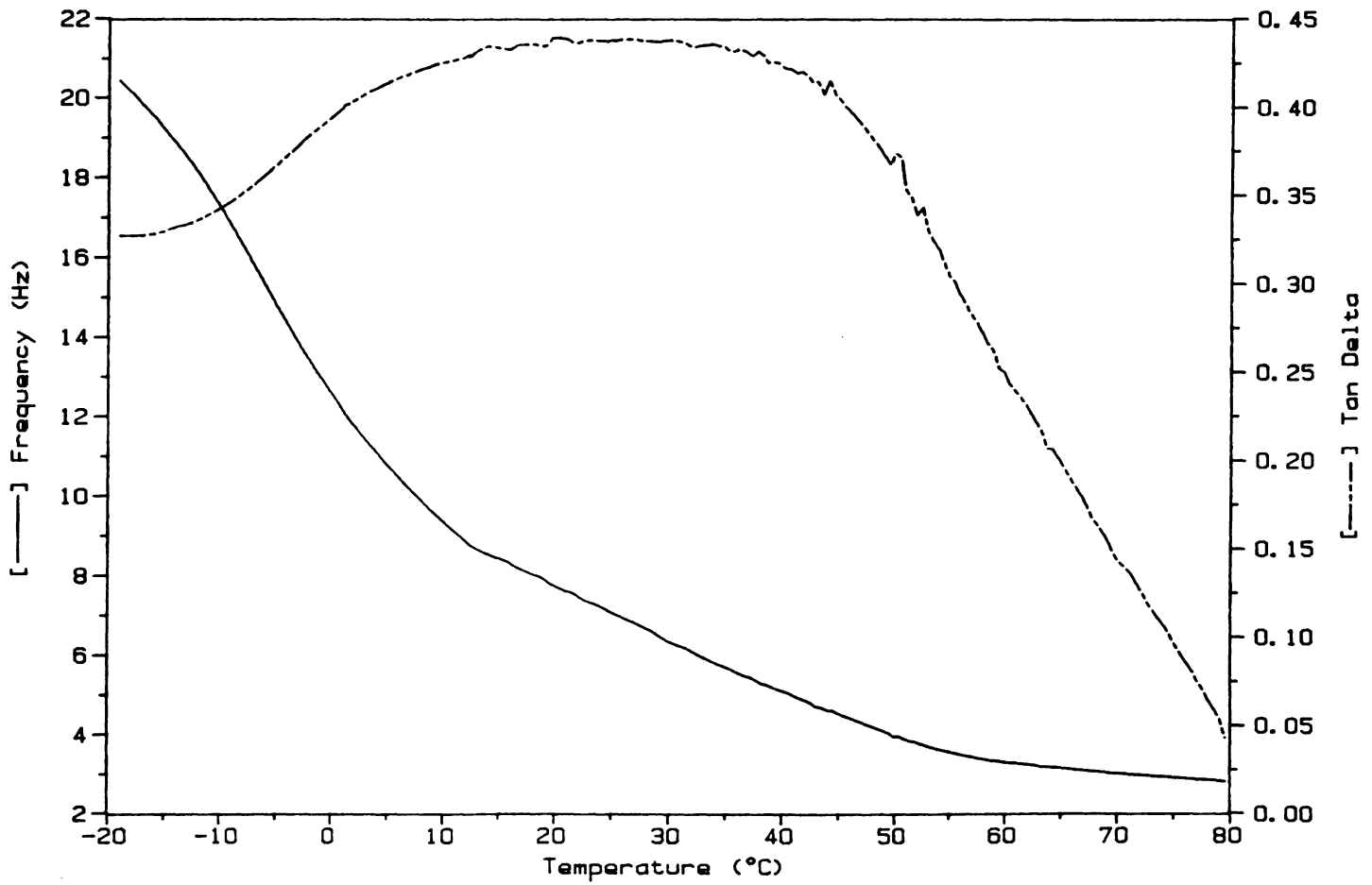

Sample: TPH 8208
Size: 25.00 X 14.10 X 6.40 MM
Method: ISO3 RAMP 1/MIN TO 80

Figure 4.8 Storage Modulus, Loss Modulus and Frequency vs. Temperature (Data #83)

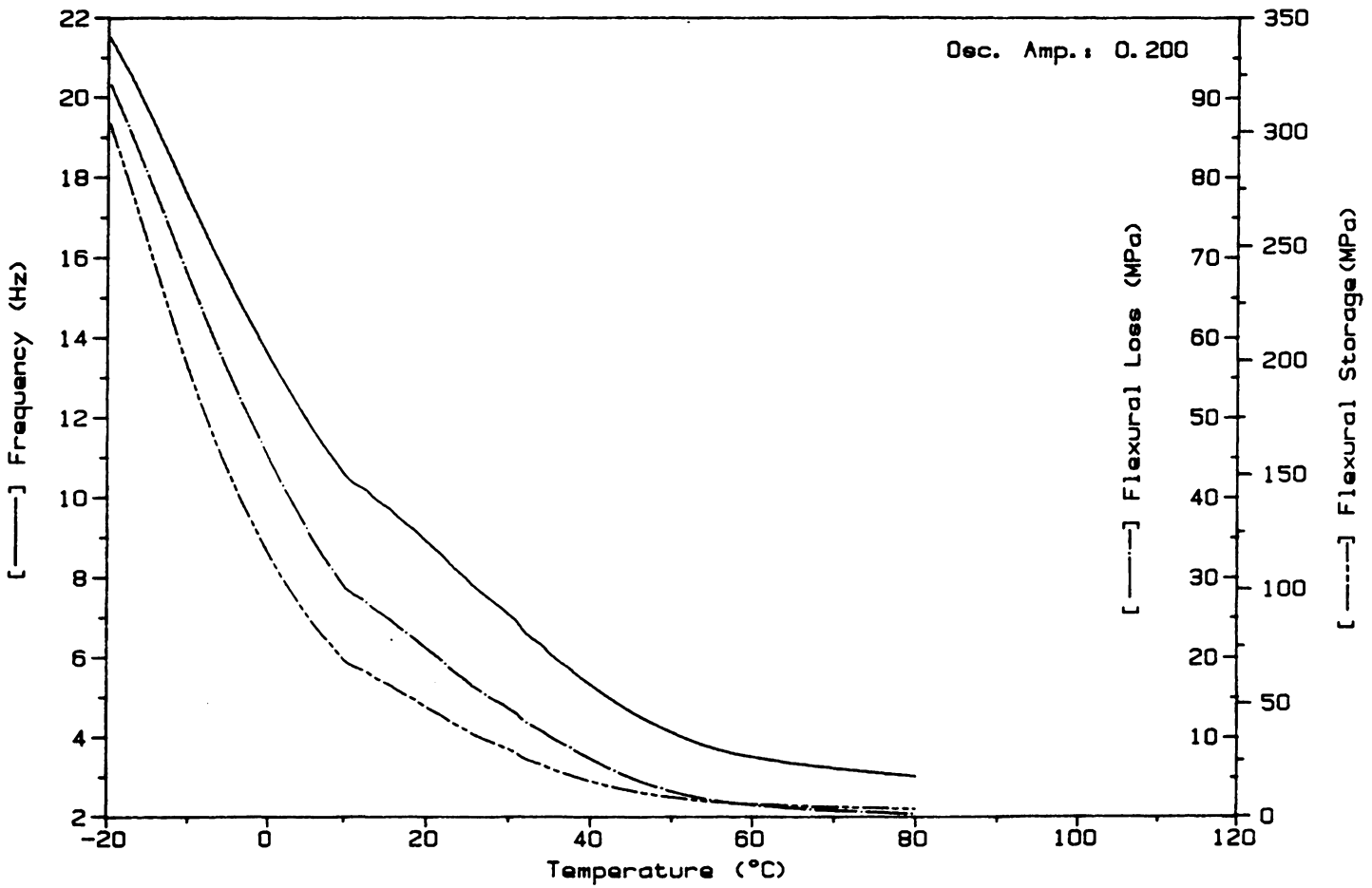

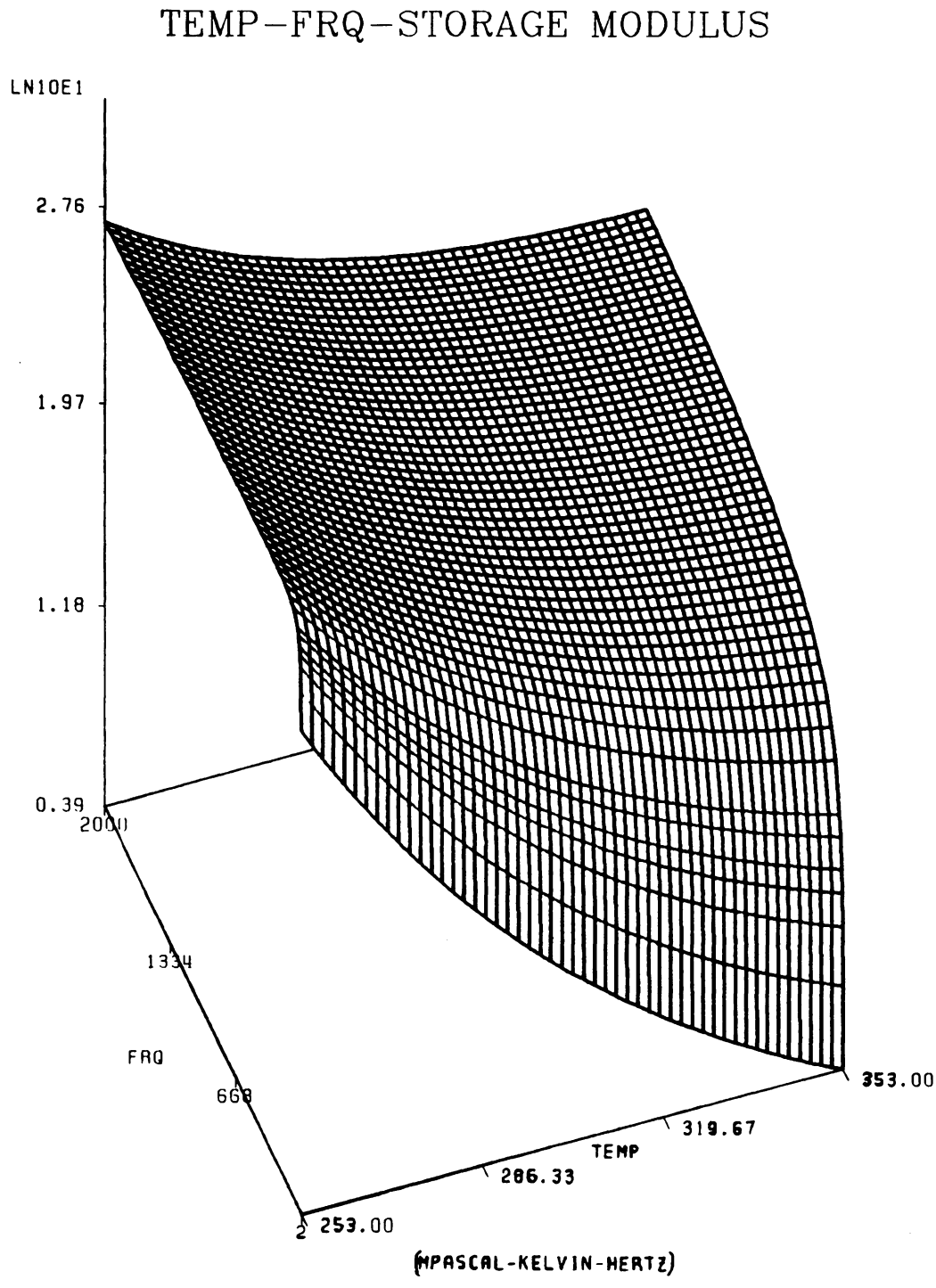

Figure 4.9 3-D Surface Model of (Log E1)

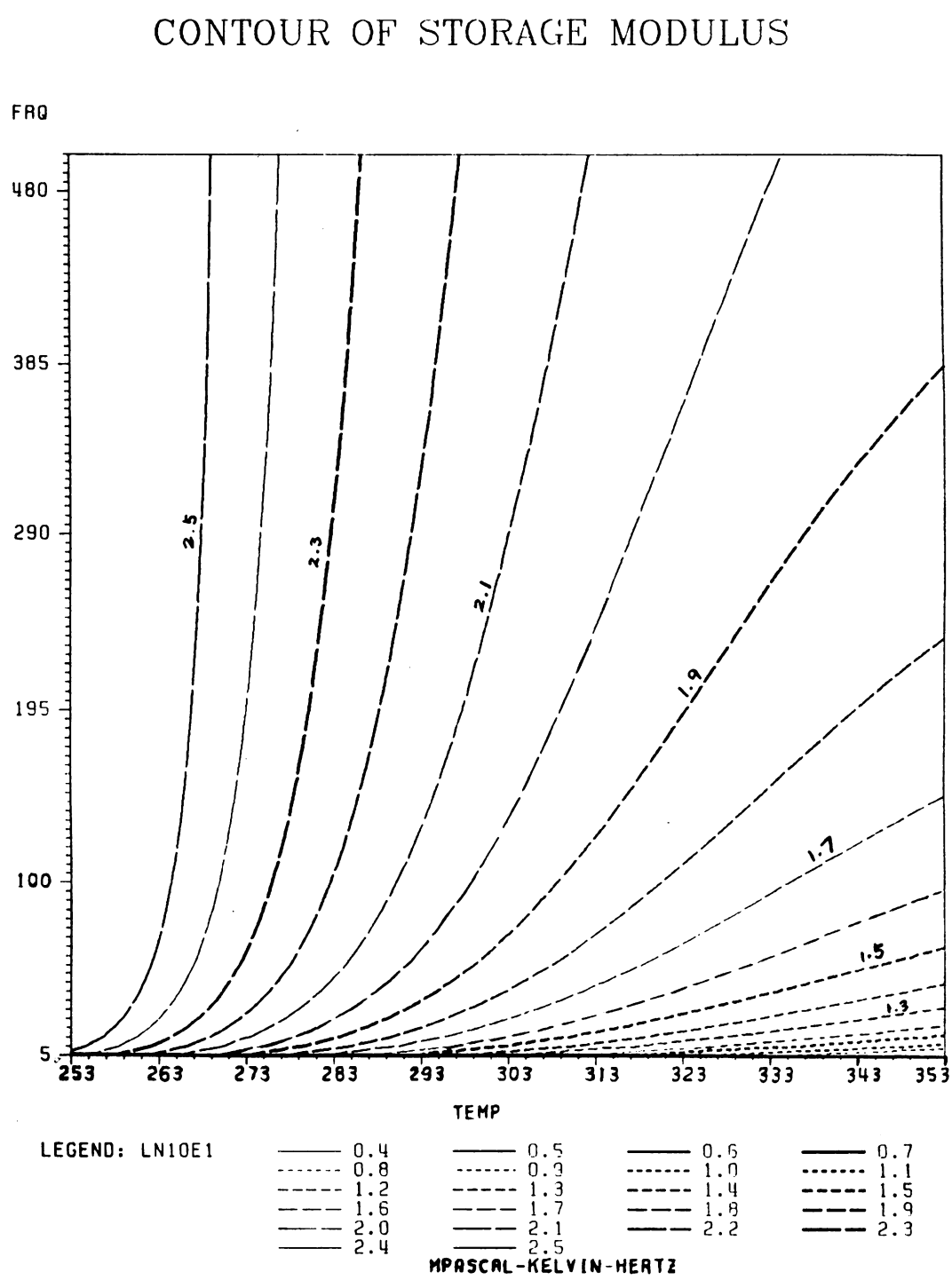

Figure 4.10 Contour of (log E1)

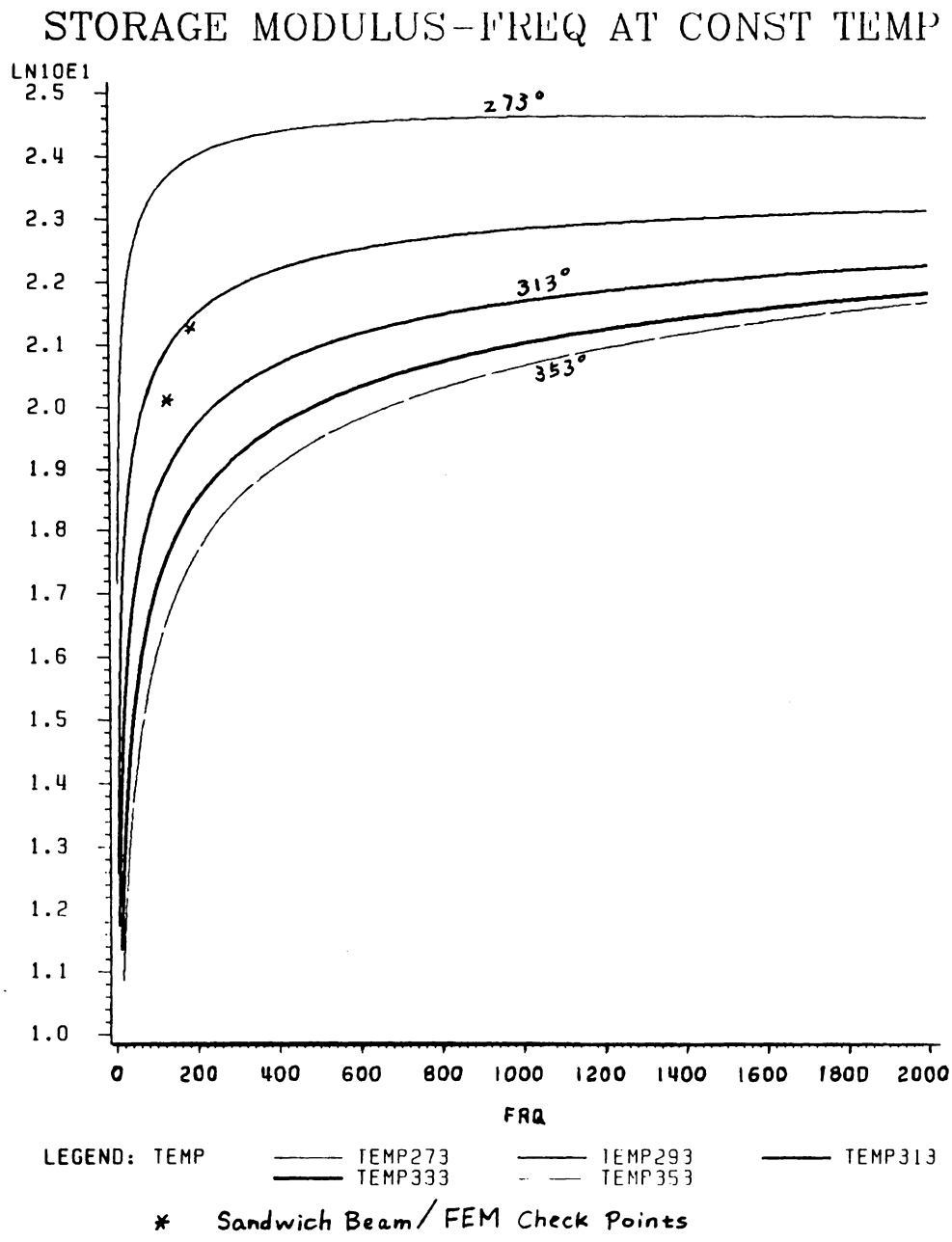

Figure 4.11 (log E1) vs. Frequency at Constant Temperature

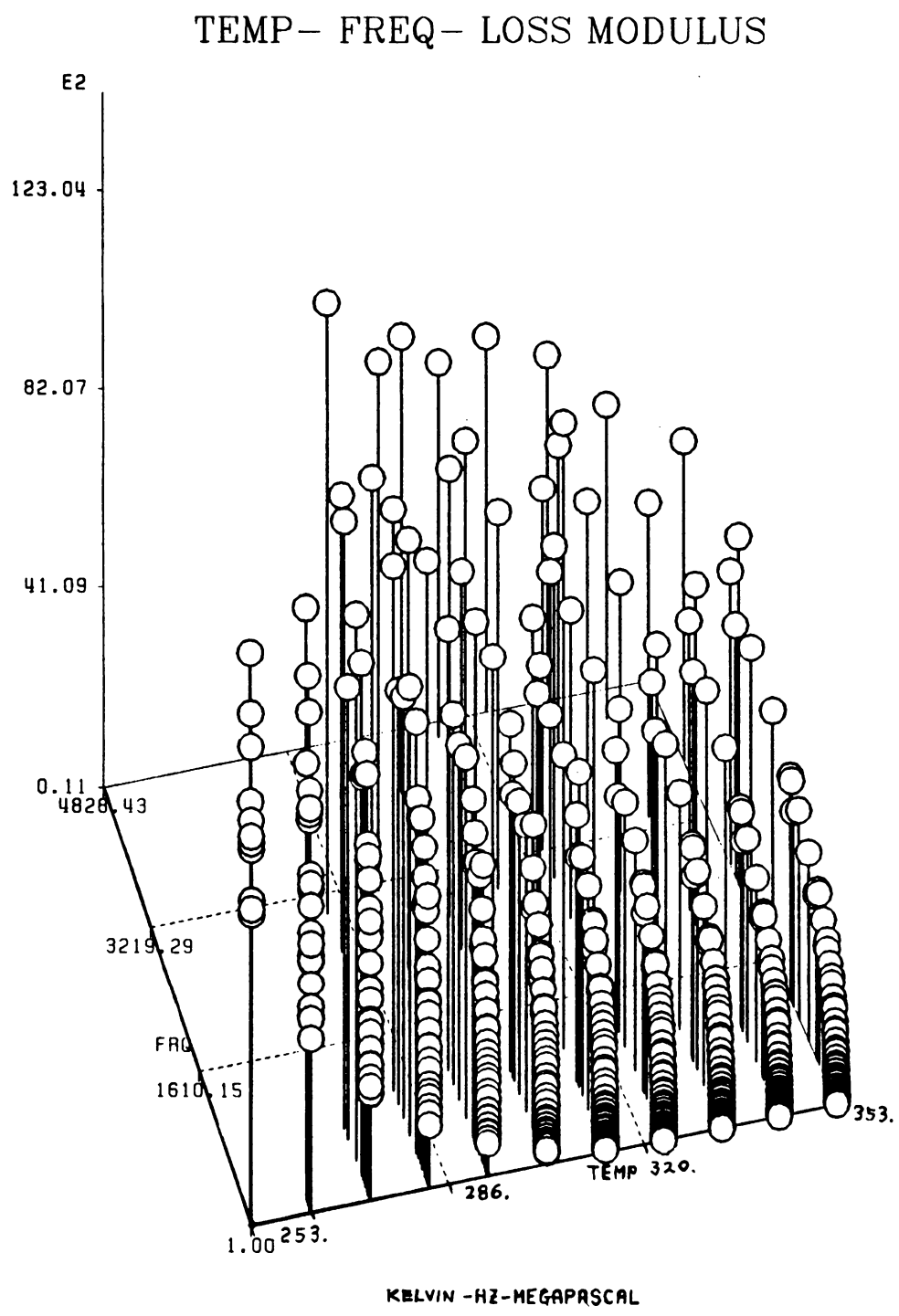

Figure 4.12 Scattered Data Points of Loss Modulus after TTSP

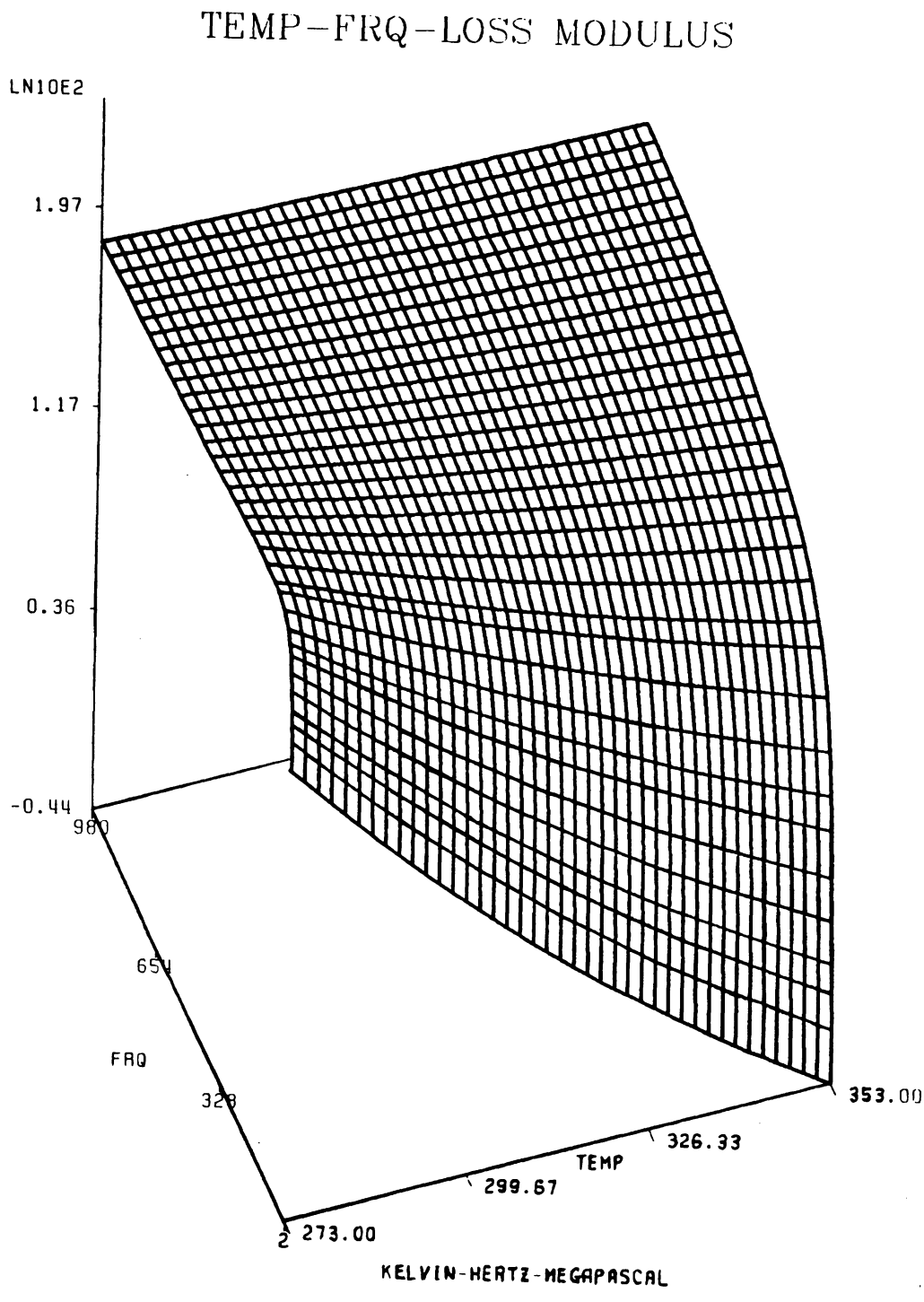

Figure 4.13 3-D Surface Model of (Log E1)

CONTOUR OF LOSS MODULUS

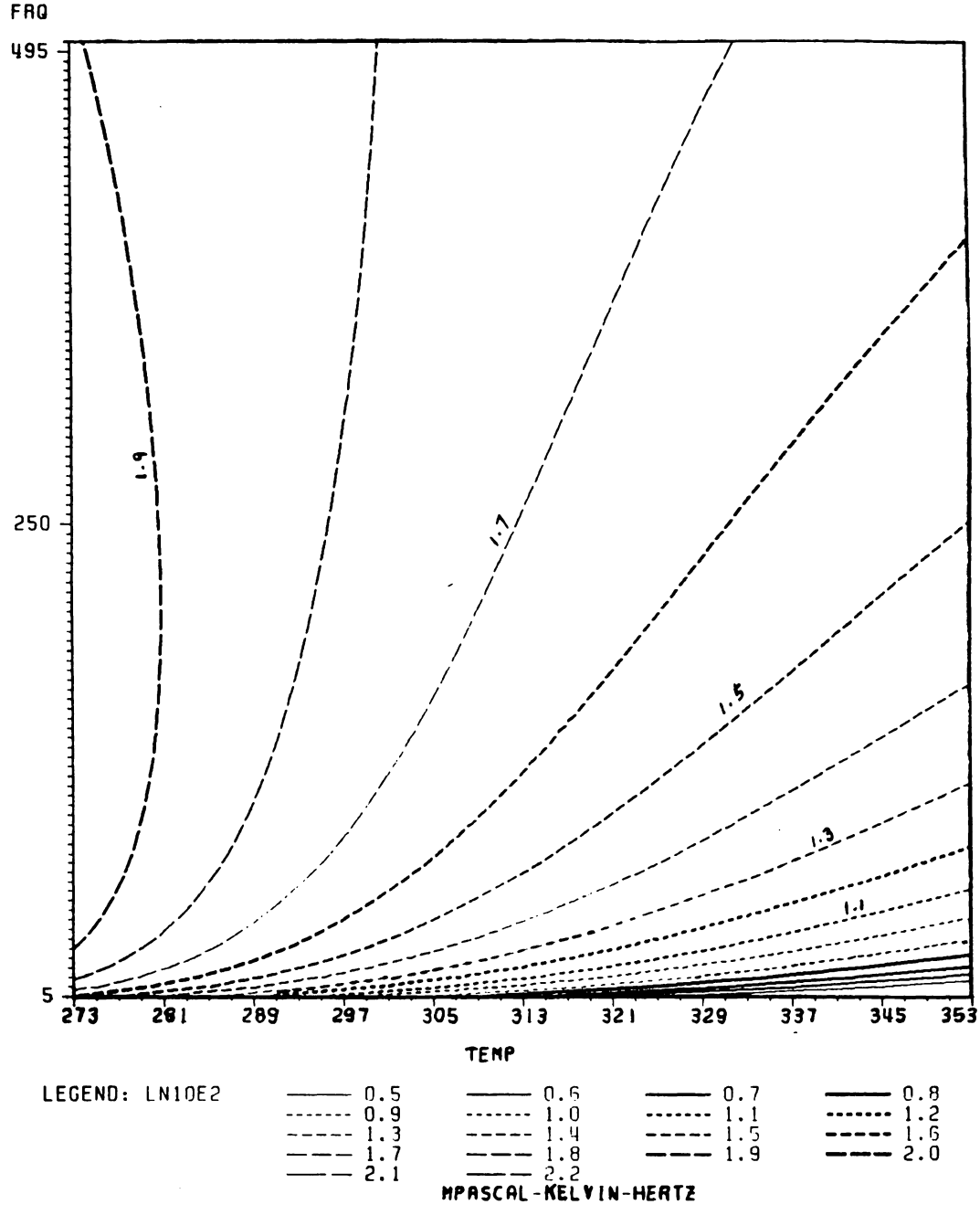

Figure 4.14 Contour of (log E2)

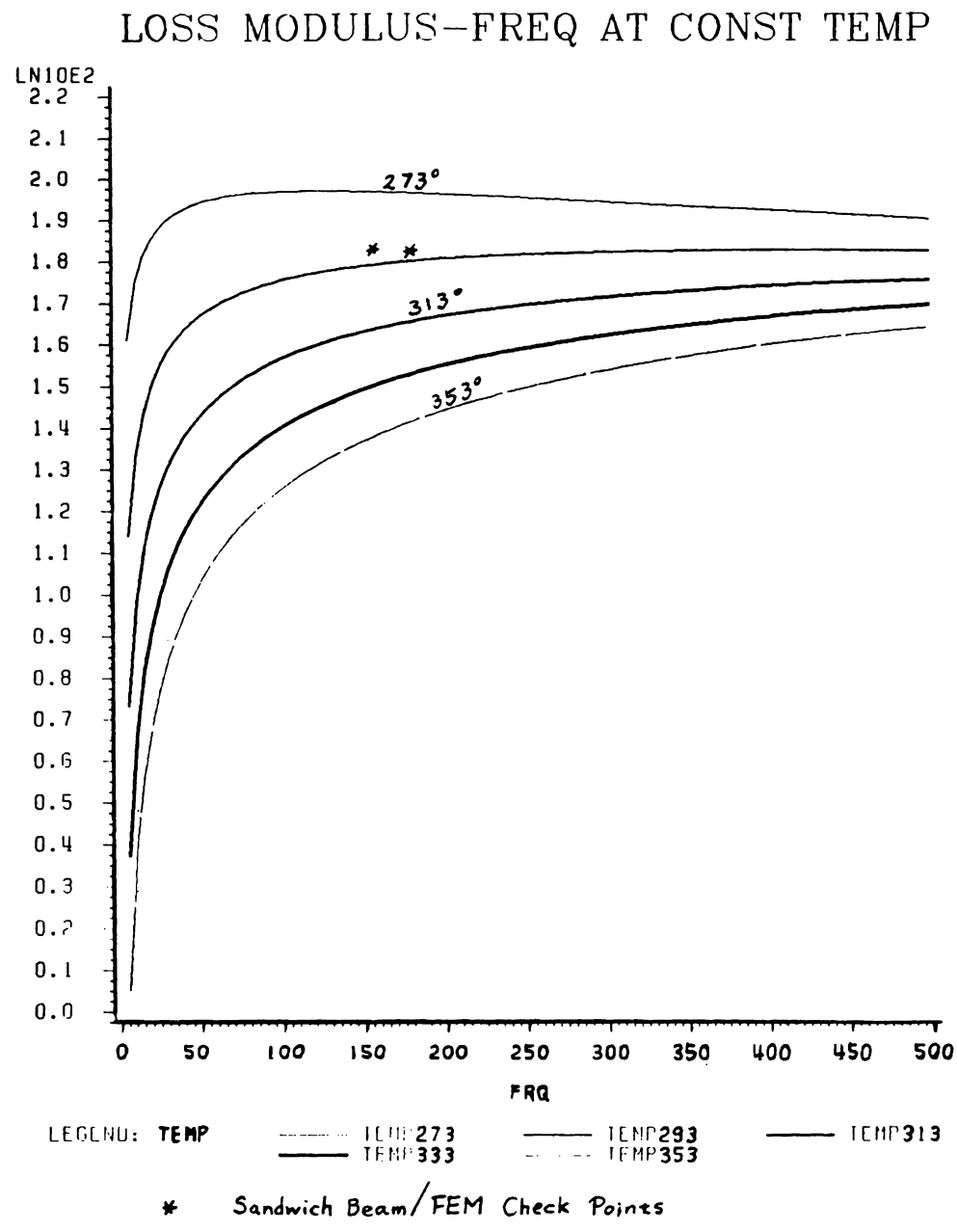

Figure 4.15 (log E2) vs. Frequency at Constant Temperature

Table 4.1 E1, E2 and Damping Rate of Propellant TPH 8208

OBS	TEMP (K deg)	FRQ (Hz)	E1 (Mpasca)	E2 (Mpascal)	DMPRT
1	253	2	204.295	84.241	0.412348
2	253	10	357.102	140.662	0.393898
3	253	20	425.369	154.958	0.364290
4	253	40	487.073	158.427	0.325263
5	253	60	517.675	155.032	0.299478
6	253	80	536.136	150.321	0.280379
7	253	100	548.333	145.472	0.265298
8	253	120	556.811	140.815	0.252895
9	253	140	562.881	136.443	0.242401
10	253	160	567.295	132.370	0.233335
11	253	180	570.524	128.582	0.225375
12	253	200	572.874	125.057	0.218298
13	253	220	574.556	121.771	0.211939
14	253	240	575.721	118.700	0.206176
15	253	260	576.478	115.823	0.200914
16	253	280	576.909	113.121	0.196080
17	253	300	577.076	110.577	0.191616
18	253	320	577.028	108.177	0.187472
19	253	340	576.804	105.907	0.183610
20	253	360	576.432	103.757	0.179998
21	253	380	575.939	101.715	0.176608
22	253	400	575.343	99.774	0.173416
23	253	420	574.662	97.924	0.170403
24	253	440	573.909	96.160	0.167552
25	253	460	573.095	94.473	0.164848
26	253	480	572.230	92.860	0.162277
27	253	500	571.321	91.314	0.159830
28	263	2	98.347	40.942	0.416302
29	263	10	189.997	81.909	0.431108
30	263	20	236.285	97.540	0.412808
31	263	40	282.473	107.798	0.381623
32	263	60	307.884	110.404	0.358589
33	263	80	324.617	110.564	0.340599
34	263	100	336.640	109.713	0.325906
35	263	120	345.742	108.398	0.313523
36	263	140	352.876	106.867	0.302846
37	263	160	358.608	105.244	0.293478
38	263	180	363.299	103.594	0.285147
39	263	200	367.193	101.953	0.277656
40	263	220	370.460	100.342	0.270859
41	263	240	373.224	98.772	0.264646
42	263	260	375.579	97.249	0.258930
43	263	280	377.595	95.774	0.253641
44	263	300	379.328	94.348	0.248725
45	263	320	380.821	92.972	0.244136
46	263	340	382.110	91.643	0.239835
47	263	360	383.224	90.361	0.235792
48	263	380	384.185	89.123	0.231978
49	263	400	385.013	87.927	0.228373
50	263	420	385.726	86.771	0.224955
51	263	440	386.336	85.654	0.221708
52	263	460	386.855	84.573	0.218616
53	263	480	387.294	83.527	0.215668
54	263	500	387.662	82.514	0.212850
55	273	2	51.898	20.9785	0.404225
56	273	10	110.003	49.6244	0.451118
57	273	20	142.376	63.5157	0.446113
58	273	40	177.141	75.4472	0.425916
59	273	60	197.640	80.6020	0.407823
60	273	80	211.864	83.1730	0.392577

Table 4.1 E1, E2 and Damping Rate of Propellant TPH 8208 (cont'd)

OBS	TEMP (K deg)	FRQ (Hz)	E1 (Mpasca)	E2 (Mpascal)	DMPRT
61	273	100	222.554	84.4721	0.379559
62	273	120	230.984	85.0587	0.368245
63	273	140	237.853	85.2137	0.358262
64	273	160	243.584	85.0939	0.349341
65	273	180	248.450	84.7931	0.341288
66	273	200	252.642	84.3706	0.333953
67	273	220	256.293	83.8656	0.327225
68	273	240	259.503	83.3044	0.321015
69	273	260	262.348	82.7056	0.315252
70	273	280	264.885	82.0820	0.309879
71	273	300	267.160	81.4433	0.304848
72	273	320	269.211	80.7962	0.300122
73	273	340	271.067	80.1457	0.295667
74	273	360	272.754	79.4956	0.291456
75	273	380	274.291	78.8487	0.287464
76	273	400	275.696	78.2070	0.283672
77	273	420	276.983	77.5721	0.280061
78	273	440	278.166	76.9449	0.276615
79	273	460	279.254	76.3264	0.273323
80	273	480	280.257	75.7171	0.270170
81	273	500	281.184	75.1174	0.267147
82	283	2	29.614	11.2694	0.380544
83	283	10	68.419	31.1486	0.455266
84	283	20	91.901	42.6329	0.463899
85	283	40	118.665	54.1536	0.456358
86	283	60	135.302	60.1679	0.444692
87	283	80	147.291	63.8392	0.433421
88	283	100	156.582	66.2511	0.423107
89	283	120	164.108	67.8982	0.413741
90	283	140	170.389	69.0439	0.405214
91	283	160	175.746	69.8432	0.397410
92	283	180	180.391	70.3938	0.390229
93	283	200	184.472	70.7606	0.383584
94	283	220	188.096	70.9886	0.377407
95	283	240	191.341	71.1096	0.371638
96	283	260	194.269	71.1472	0.366231
97	283	280	196.927	71.1188	0.361143
98	283	300	199.354	71.0379	0.356341
99	283	320	201.579	70.9148	0.351796
100	283	340	203.629	70.7577	0.347483
101	283	360	205.524	70.5729	0.343380
102	283	380	207.282	70.3657	0.339469
103	283	400	208.916	70.1402	0.335733
104	283	420	210.441	69.8998	0.332159
105	283	440	211.866	69.6475	0.328733
106	283	460	213.202	69.3853	0.325444
107	283	480	214.456	69.1154	0.322282
108	283	500	215.636	68.8393	0.319238
109	293	2	18.068	6.3161	0.349579
110	293	10	45.232	20.1831	0.446208
111	293	20	62.895	29.4054	0.467533
112	293	40	84.068	39.7596	0.472944
113	293	60	97.814	45.8196	0.468438
114	293	80	108.020	49.8925	0.461882
115	293	100	116.119	52.8294	0.454958
116	293	120	122.812	55.0399	0.448164
117	293	140	128.497	56.7517	0.441659
118	293	160	133.422	58.1038	0.435487
119	293	180	137.756	59.1869	0.429650
120	293	200	141.615	60.0630	0.424129

Table 4.1 E1, E2 and Damping Rate of Propellant TPH 8208 (cont'd)

OBS	TEMP (K deg)	FRQ (Hz)	E1 (Mpasca)	E2 (Mpascal)	DMPRT
121	293	220	145.085	60.7763	0.418903
122	293	240	148.230	61.3593	0.413947
123	293	260	151.100	61.8362	0.409240
124	293	280	153.735	62.2259	0.404760
125	293	300	156.166	62.5428	0.400489
126	293	320	158.419	62.7987	0.396409
127	293	340	160.515	63.0028	0.392505
128	293	360	162.471	63.1629	0.388764
129	293	380	164.303	63.2851	0.385174
130	293	400	166.023	63.3746	0.381722
131	293	420	167.642	63.4358	0.378401
132	293	440	169.170	63.4723	0.375199
133	293	460	170.614	63.4873	0.372111
134	293	480	171.982	63.4834	0.369127
135	293	500	173.281	63.4628	0.366243
136	303	2	11.676	3.6779	0.314984
137	303	10	31.508	13.4578	0.427127
138	303	20	45.249	20.7853	0.459354
139	303	40	62.467	29.7930	0.476937
140	303	60	74.067	35.5261	0.479648
141	303	80	82.899	39.6323	0.478078
142	303	100	90.046	42.7610	0.474878
143	303	120	96.049	45.2392	0.471003
144	303	140	101.219	47.2555	0.466864
145	303	160	105.755	48.9283	0.462657
146	303	180	109.791	50.3370	0.458481
147	303	200	113.422	51.5372	0.454386
148	303	220	116.718	52.5694	0.450397
149	303	240	119.733	53.4639	0.446527
150	303	260	122.507	54.2437	0.442780
151	303	280	125.075	54.9271	0.439155
152	303	300	127.461	55.5284	0.435649
153	303	320	129.689	56.0594	0.432258
154	303	340	131.777	56.5294	0.428978
155	303	360	133.738	56.9463	0.425804
156	303	380	135.587	57.3168	0.422729
157	303	400	137.335	57.6463	0.419750
158	303	420	138.990	57.9394	0.416861
159	303	440	140.561	58.2003	0.414058
160	303	460	142.055	58.4323	0.411336
161	303	480	143.478	58.6384	0.408692
162	303	500	144.837	58.8212	0.406121
163	313	2	7.931	2.2169	0.279540
164	313	10	22.956	9.2090	0.401152
165	313	20	33.980	15.0215	0.442072
166	313	40	48.350	22.7402	0.470327
167	313	60	58.351	27.9965	0.479798
168	313	80	66.133	31.9486	0.483093
169	313	100	72.538	35.0822	0.483643
170	313	120	77.991	37.6526	0.482784
171	313	140	82.743	39.8114	0.481144
172	313	160	86.956	41.6568	0.479054
173	313	180	90.740	43.2557	0.476702
174	313	200	94.172	44.6564	0.474199
175	313	220	97.313	45.8942	0.471615
176	313	240	100.206	46.9962	0.468997
177	313	260	102.886	47.9834	0.466373
178	313	280	105.383	48.8725	0.463762
179	313	300	107.717	49.6769	0.461178
180	313	320	109.909	50.4076	0.458629

Table 4.1 E1, E2 and Damping Rate of Propellant TPH 8208 (cont'd)

OBS	TEMP (K deg)	FRQ (Hz)	E1 (Mpasca)	E2 (Mpascal)	DMPRT
181	313	340	111.974	51.0737	0.456121
182	313	360	113.924	51.6827	0.453657
183	313	380	115.772	52.2410	0.451240
184	313	400	117.527	52.7541	0.448869
185	313	420	119.196	53.2266	0.446546
186	313	440	120.788	53.6626	0.444270
187	313	460	122.309	54.0656	0.442040
188	313	480	123.764	54.4386	0.439856
189	313	500	125.159	54.7843	0.437717
190	323	2	5.624	1.3788	0.245176
191	323	10	17.387	6.4513	0.371036
192	323	20	26.477	11.0766	0.418348
193	323	40	38.758	17.6498	0.455388
194	323	60	47.557	22.3906	0.470818
195	323	80	54.538	26.1006	0.478575
196	323	100	60.368	29.1373	0.482661
197	323	120	65.392	31.6965	0.484713
198	323	140	69.816	33.8979	0.485531
199	323	160	73.773	35.8210	0.485558
200	323	180	77.355	37.5212	0.485055
201	323	200	80.628	39.0391	0.484190
202	323	220	83.642	40.4049	0.483070
203	323	240	86.436	41.6420	0.481769
204	323	260	89.039	42.7691	0.480341
205	323	280	91.476	43.8009	0.478822
206	323	300	93.767	44.7495	0.477240
207	323	320	95.928	45.6249	0.475615
208	323	340	97.973	46.4354	0.473961
209	323	360	99.913	47.1881	0.472291
210	323	380	101.758	47.8888	0.470613
211	323	400	103.518	48.5429	0.468934
212	323	420	105.198	49.1547	0.467259
213	323	440	106.806	49.7281	0.465592
214	323	460	108.348	50.2664	0.463936
215	323	480	109.828	50.7727	0.462293
216	323	500	111.251	51.2495	0.460665
217	333	2	4.141	0.8824	0.213098
218	333	10	13.620	4.6171	0.339004
219	333	20	21.300	8.3184	0.390541
220	333	40	32.022	13.9089	0.434362
221	333	60	39.909	18.1492	0.454764
222	333	80	46.277	21.5835	0.466401
223	333	100	51.665	24.4712	0.473652
224	333	120	56.359	26.9599	0.478363
225	333	140	60.529	29.1428	0.481469
226	333	160	64.289	31.0832	0.483494
227	333	180	67.716	32.8262	0.484762
228	333	200	70.868	34.4050	0.485482
229	333	220	73.787	35.8453	0.485793
230	333	240	76.507	37.1669	0.485795
231	333	260	79.055	38.3858	0.485559
232	333	280	81.451	39.5148	0.485138
233	333	300	83.712	40.5645	0.484572
234	333	320	85.854	41.5440	0.483889
235	333	340	87.889	42.4604	0.483115
236	333	360	89.827	43.3204	0.482267
237	333	380	91.676	44.1292	0.481361
238	333	400	93.445	44.8917	0.480407
239	333	420	95.140	45.6118	0.479416
240	333	440	96.768	46.2933	0.478396

Table 4.1 E1, E2 and Damping Rate of Propellant TPH 8208 (cont'd)

OBS	TEMP (K deg)	FRQ (Hz)	E1 (Mpasca)	E2 (Mpascal)	DMPRT
241	333	460	98.332	46.9392	0.477352
242	333	480	99.839	47.5523	0.476290
243	333	500	101.292	48.1353	0.475215
244	343	2	3.151	0.5796	0.183957
245	343	10	10.985	3.3694	0.306736
246	343	20	17.616	6.3523	0.360597
247	343	40	27.157	11.1142	0.409263
248	343	60	34.346	14.8924	0.433593
249	343	80	40.244	18.0470	0.448443
250	343	100	45.294	20.7625	0.458393
251	343	120	49.736	23.1486	0.465426
252	343	140	53.716	25.2766	0.470561
253	343	160	57.329	27.1962	0.474388
254	343	180	60.643	28.9433	0.477272
255	343	200	63.708	30.5453	0.479454
256	343	220	66.562	32.0231	0.481100
257	343	240	69.234	33.3934	0.482327
258	343	260	71.747	34.6696	0.483221
259	343	280	74.120	35.8628	0.483849
260	343	300	76.368	36.9821	0.484259
261	343	320	78.506	38.0353	0.484490
262	343	340	80.543	39.0289	0.484572
263	343	360	82.489	39.9685	0.484530
264	343	380	84.353	40.8591	0.484384
265	343	400	86.140	41.7048	0.484150
266	343	420	87.858	42.5093	0.483841
267	343	440	89.512	43.2759	0.483467
268	343	460	91.105	44.0075	0.483039
269	343	480	92.644	44.7067	0.482565
270	343	500	94.131	45.3758	0.482050
271	353	2	2.4674	0.3899	0.158008
272	353	10	9.0888	2.5032	0.275419
273	353	20	14.9247	4.9255	0.330026
274	353	40	23.5591	8.9947	0.381791
275	353	60	30.2121	12.3578	0.409034
276	353	80	35.7491	15.2438	0.426410
277	353	100	40.5433	17.7807	0.438561
278	353	120	44.7977	20.0484	0.447532
279	353	140	48.6375	22.1008	0.454397
280	353	160	52.1463	23.9760	0.459782
281	353	180	55.3835	25.7025	0.464082
282	353	200	58.3927	27.3020	0.467559
283	353	220	61.2073	28.7918	0.470398
284	353	240	63.8536	30.1855	0.472730
285	353	260	66.3523	31.4943	0.474653
286	353	280	68.7206	32.7276	0.476241
287	353	300	70.9726	33.8931	0.477552
288	353	320	73.1200	34.9975	0.478630
289	353	340	75.1730	36.0464	0.479512
290	353	360	77.1399	37.0447	0.480227
291	353	380	79.0283	37.9967	0.480798
292	353	400	80.8446	38.9061	0.481245
293	353	420	82.5944	39.7762	0.481585
294	353	440	84.2827	40.6100	0.481831
295	353	460	85.9139	41.4100	0.481995
296	353	480	87.4919	42.1786	0.482086
297	353	500	89.0202	42.9179	0.482114

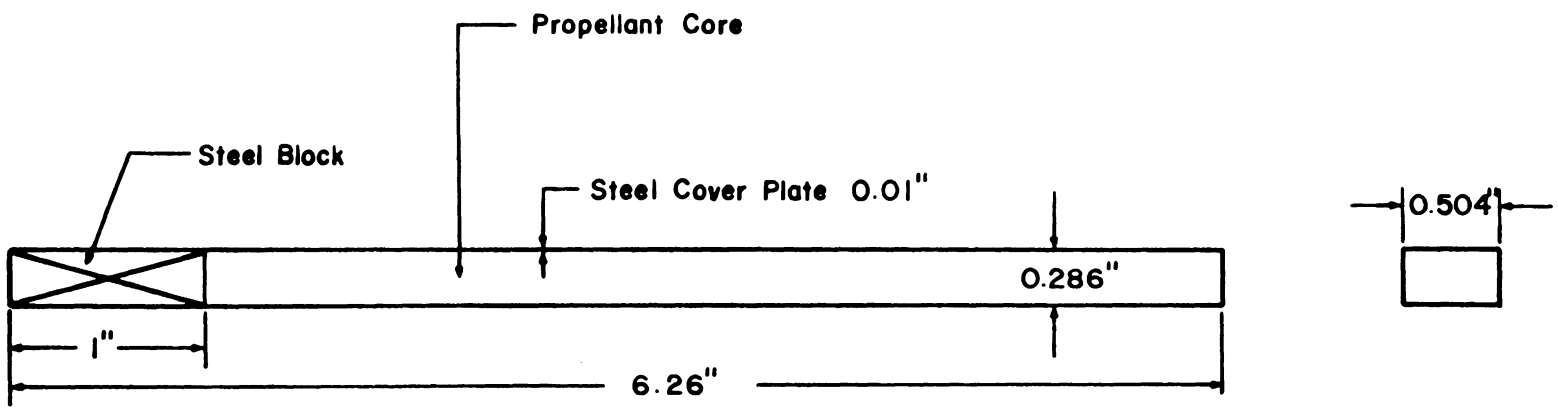

Figure 4.16 Configuration of a Sandwich Beam

5.0 Finite Element Modeling and Modal Analysis of the Solid Rocket Motor

5.1 Preliminary Remarks

Before proceeding to the random vibration analysis of a rocket motor in next chapter, it is useful to understand its undamped natural frequencies and mode shapes, thus to recognize significant regions of the rocket motor under random excitation and select the appropriate density of frequency stations around natural frequencies in order to achieve computational effectiveness. The finite element model of the cantilevered rocket motor [Fig. 5.1,5.2] consists of ninety-nine flat shell elements for the 1.52 mm thick cylindrical steel casing and ninety-nine 3-D solid elements for the propellant. Nodal positions, element listing, and constrained nodes are shown in Table 5.1-5.3. The 4-node quadrilateral shell element has three translational and three rotational degrees of freedom at each node. It has both bending and in-plane membrane stiffness capability. The 3-D solid element has three translational degrees of freedom at each of its eight nodes. These finite elements have been commonly used [45,46]. The frequency-independent elastic

modulus of the steel casing can be assumed to be 207 GPa, the viscoelastic damping ratio is assumed to be 0.001 at the temperature of 20 degrees C. The frequency-dependent viscoelastic properties of the propellant at the same temperature are listed in Table 4.1. All the following analyses are performed for material properties at 20 degrees C.

5.2 General Concept of Finite Element Method

Since its inception over thirty years ago [41], finite element method has become a general variation-based numerical method for effective engineering analysis [58]. The basic concept is to divide the given continuum into a number of regions called finite elements. Concerning structural dynamics, the motion at any point in each element is approximately represented by displacements of selected nodes on the boundary or in the element with assumed interpolation displacement model;

$$\{U(x,y,z)\} = [N(x,y,z)]\{q\} \qquad [5.1]$$

where {U} is the displacement vector of any point in the element, [N] is the interpolation displacement model matrix, and {q} is the nodal displacement vector. By this discretization process, the infinite degrees of freedom of each element have been reduced to a finite number of degrees

of freedom. With the aid of variational principles of mechanics, each element equation of motion can be obtained. After assembly of all the elements in a given structural system and imposing the boundary conditions, the global equations of motion in matrix form can be solved effectively for nodal displacements by modern digital computer. Consequently, the displacement data can be postprocessed to obtain acceleration, strain and stress at desired points of the system. Indeed, the finite element method can be conceived as a natural way to treat a continuous body as built up of cells called elements. In this manner, complicated geometry, nonhomogeneous material, and various boundary conditions may be treated effectively.

5.3 Finite Element Method and Structural Dynamics

Hamilton's variational principle can be used here to derive the element equations of motion [53,59,43]. This principle states that the variation of the kinetic energy, potential energy and work done by nonconservative forces on a given dynamic system between any two time instants must be stationary. In mathematical form, it can be expressed as

$$\delta\int_{t_1}^{t_2}(T - V + W_{nc})dt = 0 \qquad [5.2]$$

where T is the total kinetic energy, V is the total potential energy, and W_{nc} is the nonconservative work done on the system. Or in more detailed form

$$\delta \int_{t_1}^{t_2}(\iiint_V(\frac{1}{2}\rho\{\dot{U}(p,t)\}^T\{\dot{U}(p,t)\} - \frac{1}{2}\{\xi(p,t)\}^T[C]\{\xi(p,t)\} + \{U(p,t)\}^T\{F_b\})dv + \iint_S\{U(p,t)\}^T\{F_s\}ds)dt = 0 \quad [5.3]$$

where ρ is the density, ξ is the strain, $\{F_b\}$ indicates the body force vector, $\{F_s\}$ is the surface force vector. In terms of elmement nodal displacements, Hamilton's principle can be written as

$$\delta \int_{t_1}^{t_2}((\iiint_V(\frac{1}{2}\rho\{\dot{q}(t)\}^T[N]^T[N]\{\dot{q}(t)\} - \frac{1}{2}\{q(t)\}^T[B]^T[C][B]\{q(t)\} + \{q(t)\}^T[N]^T\{F_b\})dv) + \iint_S\{q(t)\}^T[N]^T\{F_s\}ds)dt = 0 \quad [5.4]$$

where the [B] matrix relates the strain vector to the displacement vector at a point, and the [C] matrix is the constitutive matrix relating the stress vector and the strain vector. The kinetic energy term can be further simplified as follows

$$\delta\int_{t_1}^{t_2}(\iiint_V\frac{1}{2}\rho\{\dot{q}(t)\}^T[N]^T[N]\{\dot{q}(t)\}dv)dt = \int_{t_1}^{t_2}\{\delta\dot{q}(t)\}^T(\iiint_V\rho[N]^T[N]\{\dot{q}(t)\}dv)dt \quad [5.5]$$

After integration by parts with respect to time, it becomes

$$[\{\delta q\}^T(\iiint_V \rho[N]^T[N]dv)\{\dot{q}\}]_{t1}^{t2} - \int_{t1}^{t2}\{\delta q\}^T(\iiint_V \rho[N]^T[N]dv)\{\ddot{q}(t)\}dt \quad [5.6]$$

Since at instants t1 and t2, $\delta q = 0$, thus the first part in the above equation vanishes. Equation [5.4] becomes

$$\int_{t1}^{t2}\{\delta q\}^T((\iiint_V \rho[N]^T[N]dv)\{\ddot{q}(t)\} + (\iiint_V [B]^T[C][B]dv)\{q(t)\} - \iiint_V [N]^T\{F_b\}dv - \iint_S [N]^T\{F_s\}ds)dt = 0 \quad [5.7]$$

Since the virtual displacements are arbitrary, the expression in the parenthesis must vanish for the above equation to be satisfied.

$$(\iiint_V \rho[N]^T[N]dv)\{\ddot{q}\} + (\iiint_V [B]^T[C][B]dv)\{q(t)\} = \iiint_V [N]^T\{F_b\}dv + \iint_S [N]^T\{F_s\}ds \quad [5.8]$$

in concise matrix form, the above elemental equation can be written as

$$[M]\{\ddot{q}\} + [K]\{q\} = \{F_e\} \quad [5.9]$$

the right hand side is the equivalent nodal force vector. After the assembly of all the elemental equations, the global equations in the similar matrix form can be obtained. Without nodal forces, the above matrix equation becomes an eigenvalue problem

$$\omega^2[M]\{Q\} = [K]\{Q\} \qquad [5.10]$$

Due to the symmetry about the Y-Z plane, only one half of the layered cylinder is used to build the finite element model with 782 degrees of freedom. For this structural system with an overall viscoelastic damping ratio less than 0.02, the undamped natural frequencies and mode shapes do not differ significantly from their damped couterparts [25,27,55]. The frequency-dependent stiffness matrix [K] can be updated for higher modes as deemed necessary. The subspace iteration method [60] was used to obtain the eigenvalues and eigenvectors. Computer programs in the language of ANSYS engineering analysis system [51,52] have been written [A.7, A.8] to obtain the first few natural frequencies and mode shapes of the undamped rocket motor. The first natural frequency is at 92.7 Hz, the mode shape is basically in bending as shown in Fig. 5.3. The second one is also a bending mode at 489.8 Hz [Fig. 5.4]. The third one is a ring mode at 740 Hz [Fig. 5.5]. The fourth one is an axial mode at 763 Hz [Fig.5.6]. The fifth one is a ring mode with more complicated flexural shape as shown in Fig. 5.7.

5.4 Comparison with the Beam Model

A convenient check of the complicated finite element modeling and processing procedures, can be performed by using the closed-form solution of Euler beam model simulating the rocket motor. Due to Euler's assumptions that beam cross section planes remain plane, normals remain normal, and no consideration for the rotatory inertia, the first natural frequency is expected to be somewhat higher than the true value. Thus it can be considered as an upper bound for the first natural frequency obtained from the finite element model. The equation of motion for Euler beam can be expressed as

$$EI\frac{d^4y}{dz^4} - \rho\omega^2 y = 0 \qquad [5.11]$$

with the clamped boundary conditions

$$\begin{aligned} y &= 0 \quad at \quad z = 0 \\ \frac{dy}{dz} &= 0 \quad at \quad z = 0 \\ \frac{d^2y}{dz^2} &= 0 \quad at \quad z = l \\ \frac{d^3y}{dz^3} &= 0 \quad at \quad z = l \end{aligned} \qquad [5.12]$$

The equation of motion and associated boundary conditions have been solved for natural frequencies and corresponding mode shapes. The first natural frequency for the clamped beam model can be calculated as

$$f_1 = \frac{3.515}{2\pi}\sqrt{\frac{EI}{(\rho l)l^3}} = 97.5Hz$$

which is approximately 5% higher than the 92.7 Hz obtained from finite element model. Except for relatively long beams, higher natural frequencies obtained from the Euler beam model are usually not good for checking purposes. Another finite element model consisting of 20 beam elements with shear effect has also been used to check the shell finite element model. The first natural frequency is 93.2 Hz which is closer to the 92.7 Hz due to the inclusion of shear effects. Additionally, the second natural frequency is 3.7% off the 489.8 Hz obtained from the shell-solid finite element model.

Moreover, harmonic response peaks at these bending natural frequencies presented in a number of plots in chapter six can be used as additional checks. Hence, with reasonable results from the analytical approach, the beam finite element approaches and the harmonic response approach, the shell-solid finite element modeling and processing procedures are acceptable.

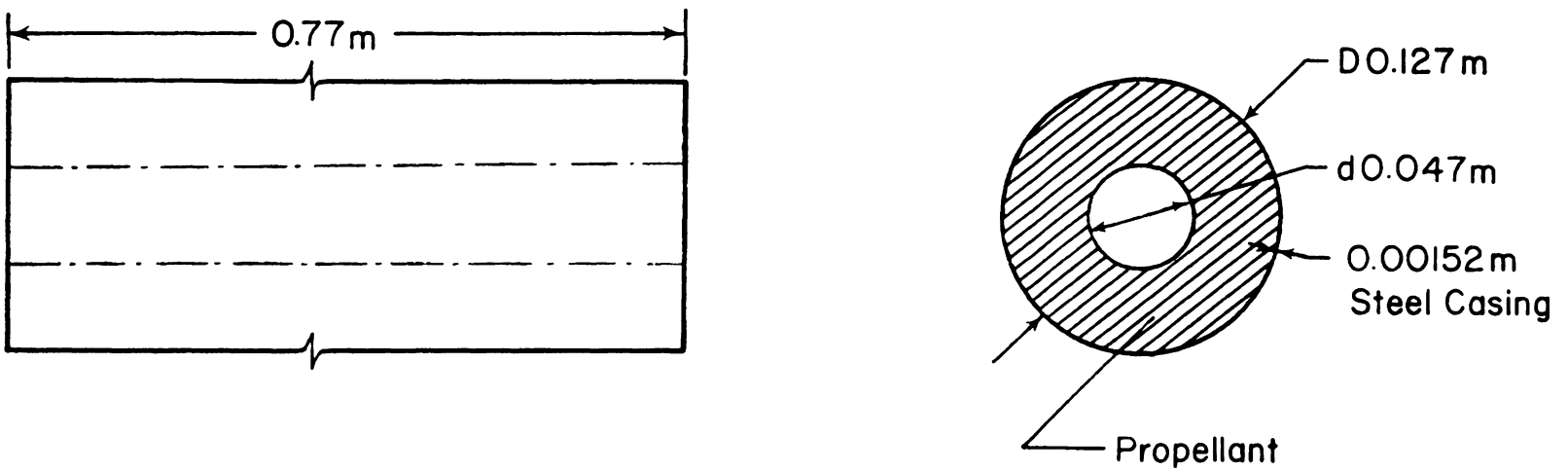

Figure 5.1 Dimensions of the Rocket Motor

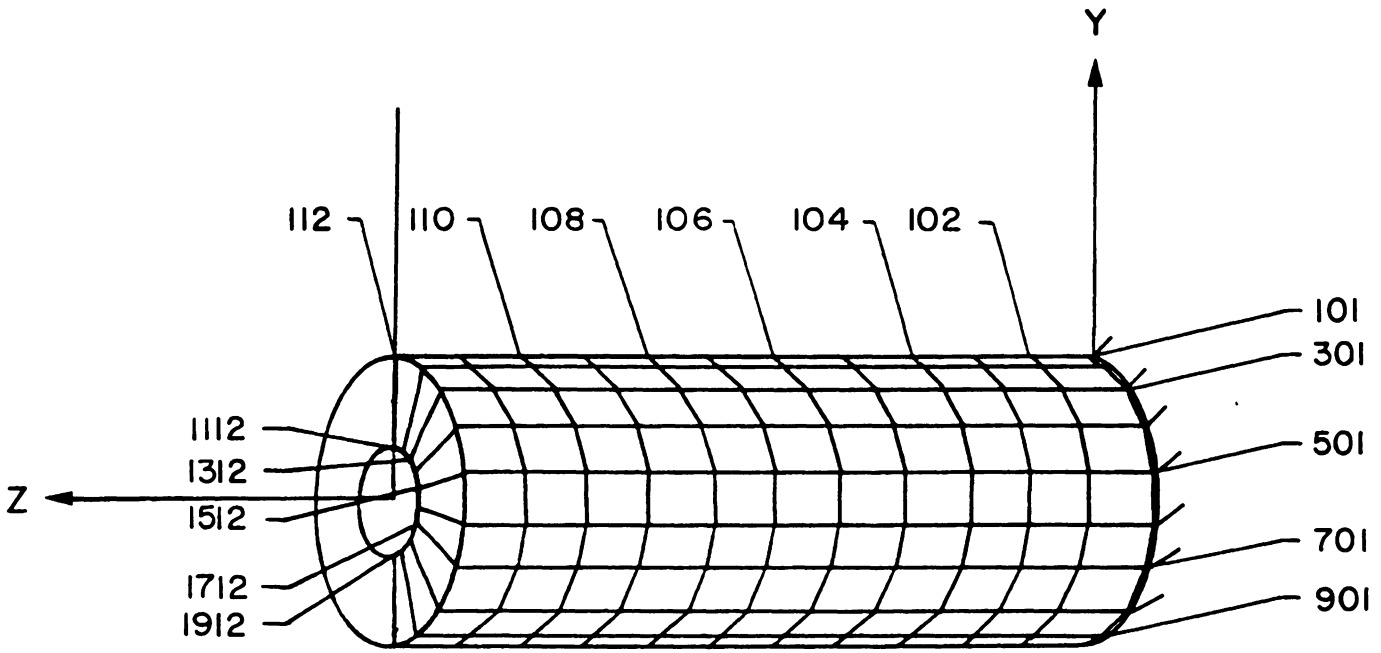

Figure 5.2 Finite Element Modeling of the Rocket Motor

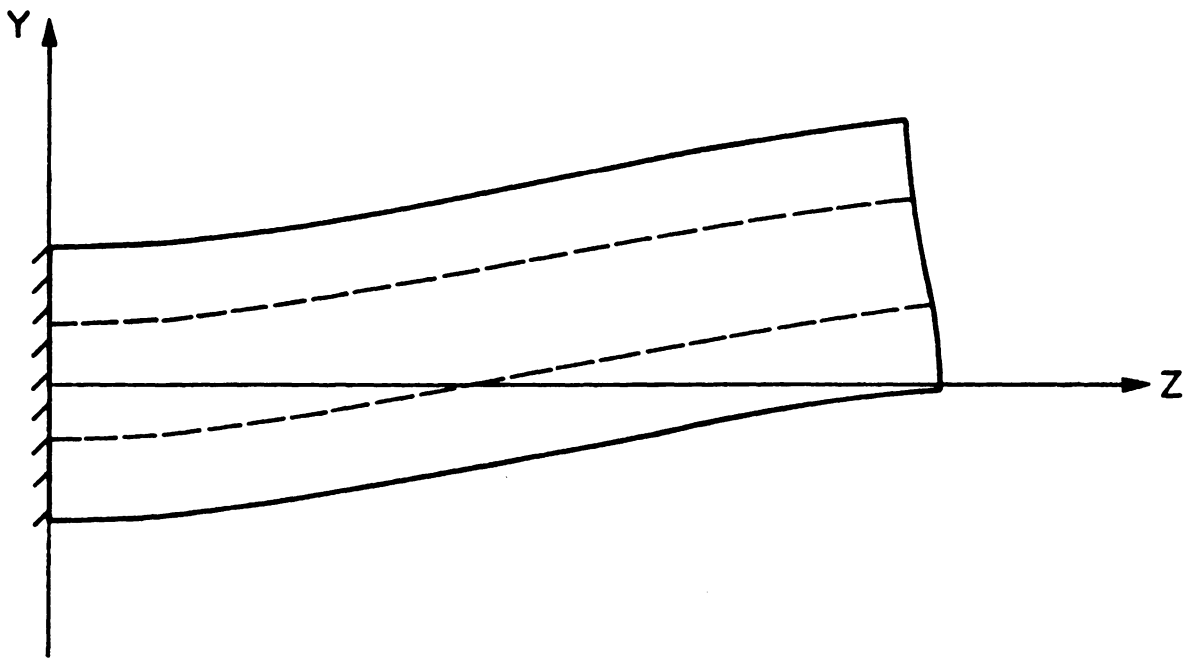

Figure 5.3 Mode Shape #1 at 92.7 Hz

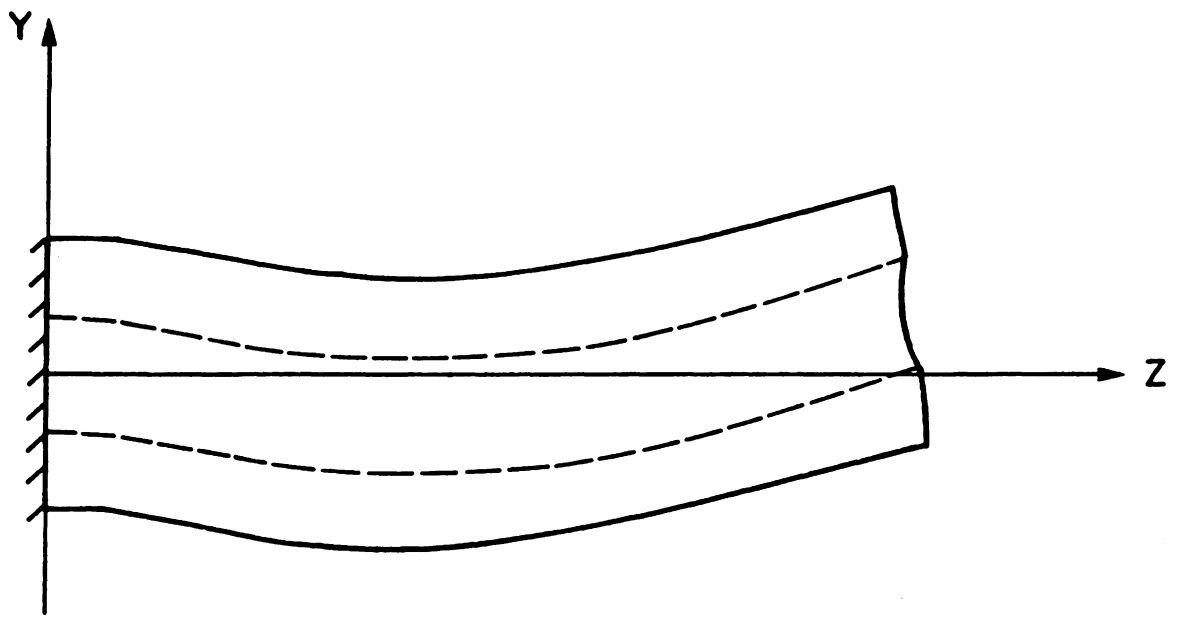

Figure 5.4 Mode Shape #2 at 489.8 Hz

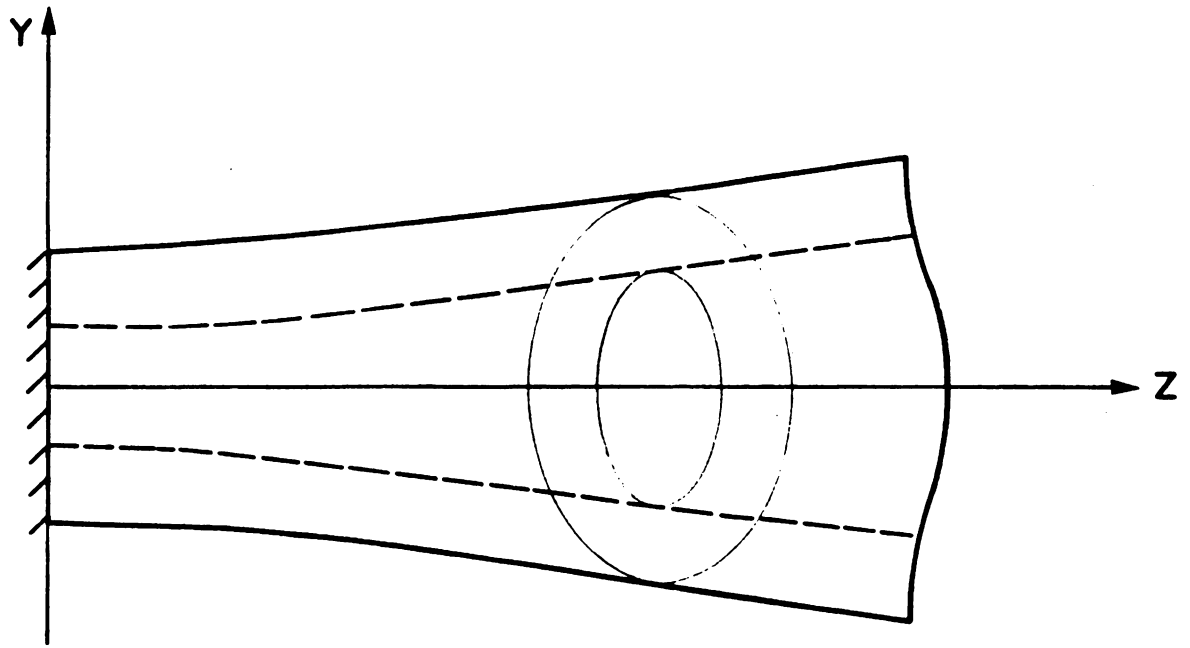

Figure 5.5 Mode Shape #3 at 740 Hz

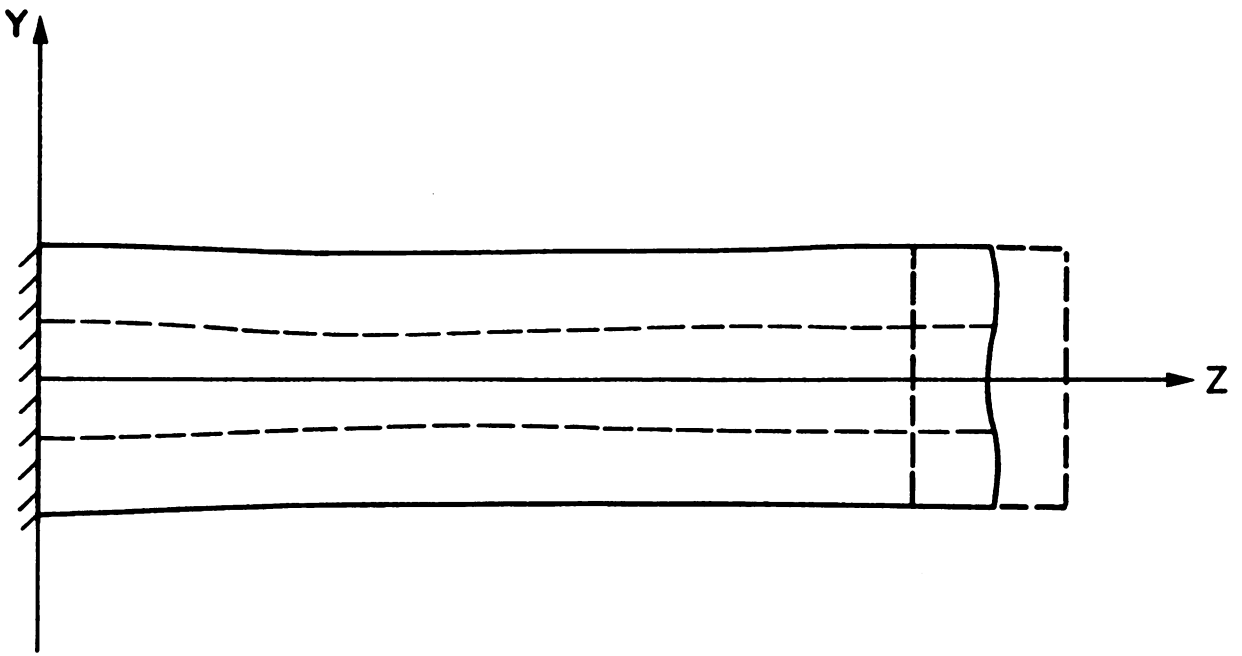

Figure 5.6 Mode Shape #4 at 753. Hz

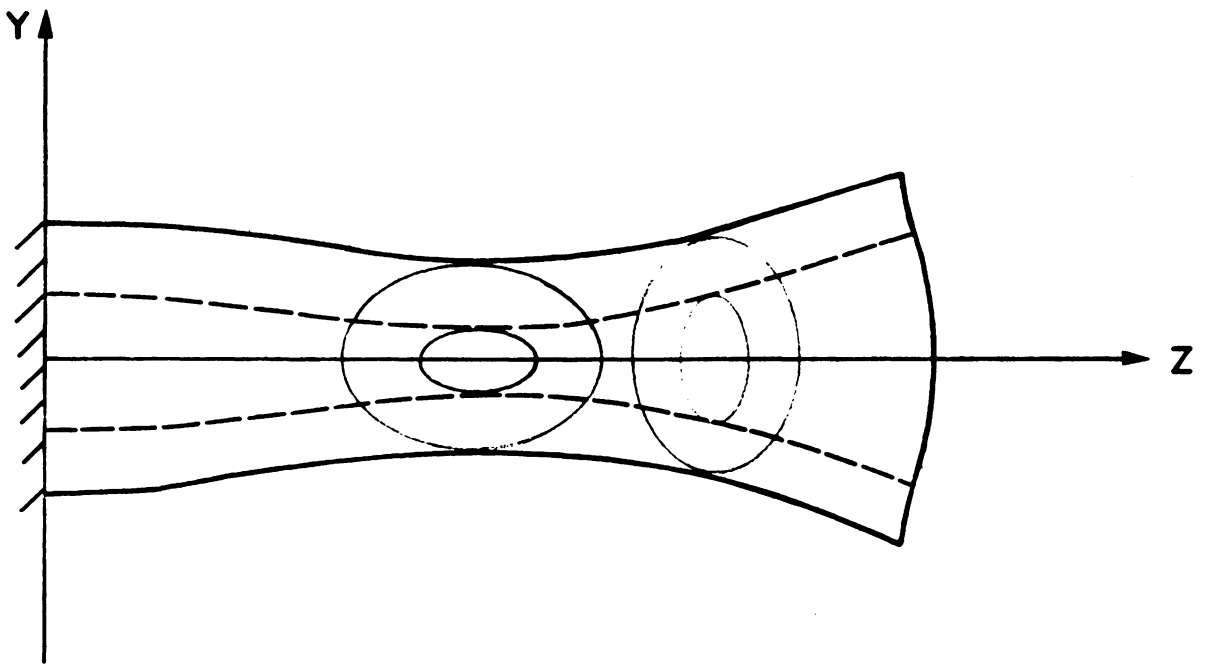

Figure 5.7 Mode Shape #5 at 779.5 Hz

Table 5.1 Node position

NODE	r	θ	z	NODE	r	θ	z
101	0.62740E-01	90.000	0.00000E+00	401	0.62740E-01	30.000	0.00000E+00
102	0.62740E-01	90.000	0.70000E-01	402	0.62740E-01	30.000	0.70000E-01
103	0.62740E-01	90.000	0.14000	403	0.62740E-01	30.000	0.14000
104	0.62740E-01	90.000	0.21000	404	0.62740E-01	30.000	0.21000
105	0.62740E-01	90.000	0.28000	405	0.62740E-01	30.000	0.28000
106	0.62740E-01	90.000	0.35000	406	0.62740E-01	30.000	0.35000
107	0.62740E-01	90.000	0.42000	407	0.62740E-01	30.000	0.42000
108	0.62740E-01	90.000	0.49000	408	0.62740E-01	30.000	0.49000
109	0.62740E-01	90.000	0.56000	409	0.62740E-01	30.000	0.56000
110	0.62740E-01	90.000	0.63000	410	0.62740E-01	30.000	0.63000
111	0.62740E-01	90.000	0.70000	411	0.62740E-01	30.000	0.70000
112	0.62740E-01	90.000	0.77000	412	0.62740E-01	30.000	0.77000
201	0.62740E-01	70.000	0.00000E+00	501	0.62740E-01	10.000	0.00000E+00
202	0.62740E-01	70.000	0.70000E-01	502	0.62740E-01	10.000	0.70000E-01
203	0.62740E-01	70.000	0.14000	503	0.62740E-01	10.000	0.14000
204	0.62740E-01	70.000	0.21000	504	0.62740E-01	10.000	0.21000
205	0.62740E-01	70.000	0.28000	505	0.62740E-01	10.000	0.28000
206	0.62740E-01	70.000	0.35000	506	0.62740E-01	10.000	0.35000
207	0.62740E-01	70.000	0.42000	507	0.62740E-01	10.000	0.42000
208	0.62740E-01	70.000	0.49000	508	0.62740E-01	10.000	0.49000
209	0.62740E-01	70.000	0.56000	509	0.62740E-01	10.000	0.56000
210	0.62740E-01	70.000	0.63000	510	0.62740E-01	10.000	0.63000
211	0.62740E-01	70.000	0.70000	511	0.62740E-01	10.000	0.70000
212	0.62740E-01	70.000	0.77000	512	0.62740E-01	10.000	0.77000
301	0.62740E-01	50.000	0.00000E+00	601	0.62740E-01	-10.000	0.00000E+00
302	0.62740E-01	50.000	0.70000E-01	602	0.62740E-01	-10.000	0.70000E-01
303	0.62740E-01	50.000	0.14000	603	0.62740E-01	-10.000	0.14000
304	0.62740E-01	50.000	0.21000	604	0.62740E-01	-10.000	0.21000
305	0.62740E-01	50.000	0.28000	605	0.62740E-01	-10.000	0.28000
306	0.62740E-01	50.000	0.35000	606	0.62740E-01	-10.000	0.35000
307	0.62740E-01	50.000	0.42000	607	0.62740E-01	-10.000	0.42000
308	0.62740E-01	50.000	0.49000	608	0.62740E-01	-10.000	0.49000
309	0.62740E-01	50.000	0.56000	609	0.62740E-01	-10.000	0.56000
310	0.62740E-01	50.000	0.63000	610	0.62740E-01	-10.000	0.63000
311	0.62740E-01	50.000	0.70000	611	0.62740E-01	-10.000	0.70000
312	0.62740E-01	50.000	0.77000	612	0.62740E-01	-10.000	0.77000

Table 5.1 Node position (cont'd)

NODE	r	θ	z	NODE	r	θ	z
701	0.62740E-01	-30.000	0.00000E+00	1001	0.62740E-01	-90.000	0.00000E+00
702	0.62740E-01	-30.000	0.70000E-01	1002	0.62740E-01	-90.000	0.70000E-01
703	0.62740E-01	-30.000	0.14000	1003	0.62740E-01	-90.000	0.14000
704	0.62740E-01	-30.000	0.21000	1004	0.62740E-01	-90.000	0.21000
705	0.62740E-01	-30.000	0.28000	1005	0.62740E-01	-90.000	0.28000
706	0.62740E-01	-30.000	0.35000	1006	0.62740E-01	-90.000	0.35000
707	0.62740E-01	-30.000	0.42000	1007	0.62740E-01	-90.000	0.42000
708	0.62740E-01	-30.000	0.49000	1008	0.62740E-01	-90.000	0.49000
709	0.62740E-01	-30.000	0.56000	1009	0.62740E-01	-90.000	0.56000
710	0.62740E-01	-30.000	0.63000	1010	0.62740E-01	-90.000	0.63000
711	0.62740E-01	-30.000	0.70000	1011	0.62740E-01	-90.000	0.70000
712	0.62740E-01	-30.000	0.77000	1012	0.62740E-01	-90.000	0.77000
801	0.62740E-01	-50.000	0.00000E+00				
802	0.62740E-01	-50.000	0.70000E-01				
803	0.62740E-01	-50.000	0.14000				
804	0.62740E-01	-50.000	0.21000				
805	0.62740E-01	-50.000	0.28000				
806	0.62740E-01	-50.000	0.35000				
807	0.62740E-01	-50.000	0.42000				
808	0.62740E-01	-50.000	0.49000				
809	0.62740E-01	-50.000	0.56000				
810	0.62740E-01	-50.000	0.63000				
811	0.62740E-01	-50.000	0.70000				
812	0.62740E-01	-50.000	0.77000				
901	0.62740E-01	-70.000	0.00000E+00				
902	0.62740E-01	-70.000	0.70000E-01				
903	0.62740E-01	-70.000	0.14000				
904	0.62740E-01	-70.000	0.21000				
905	0.62740E-01	-70.000	0.28000				
906	0.62740E-01	-70.000	0.35000				
907	0.62740E-01	-70.000	0.42000				
908	0.62740E-01	-70.000	0.49000				
909	0.62740E-01	-70.000	0.56000				
910	0.62740E-01	-70.000	0.63000				
911	0.62740E-01	-70.000	0.70000				
912	0.62740E-01	-70.000	0.77000				

Table 5.1 Node position (cont'd)

NODE	r	θ	z	NODE	r	θ	z
1101	0.23500E-01	90.000	0.00000E+00	1401	0.23500E-01	30.000	0.00000E+00
1102	0.23500E-01	90.000	0.70000E-01	1402	0.23500E-01	30.000	0.70000E-01
1103	0.23500E-01	90.000	0.14000	1403	0.23500E-01	30.000	0.14000
1104	0.23500E-01	90.000	0.21000	1404	0.23500E-01	30.000	0.21000
1105	0.23500E-01	90.000	0.28000	1405	0.23500E-01	30.000	0.28000
1106	0.23500E-01	90.000	0.35000	1406	0.23500E-01	30.000	0.35000
1107	0.23500E-01	90.000	0.42000	1407	0.23500E-01	30.000	0.42000
1108	0.23500E-01	90.000	0.49000	1408	0.23500E-01	30.000	0.49000
1109	0.23500E-01	90.000	0.56000	1409	0.23500E-01	30.000	0.56000
1110	0.23500E-01	90.000	0.63000	1410	0.23500E-01	30.000	0.63000
1111	0.23500E-01	90.000	0.70000	1411	0.23500E-01	30.000	0.70000
1112	0.23500E-01	90.000	0.77000	1412	0.23500E-01	30.000	0.77000
1201	0.23500E-01	70.000	0.00000E+00	1501	0.23500E-01	10.000	0.00000E+00
1202	0.23500E-01	70.000	0.70000E-01	1502	0.23500E-01	10.000	0.70000E-01
1203	0.23500E-01	70.000	0.14000	1503	0.23500E-01	10.000	0.14000
1204	0.23500E-01	70.000	0.21000	1504	0.23500E-01	10.000	0.21000
1205	0.23500E-01	70.000	0.28000	1505	0.23500E-01	10.000	0.28000
1206	0.23500E-01	70.000	0.35000	1506	0.23500E-01	10.000	0.35000
1207	0.23500E-01	70.000	0.42000	1507	0.23500E-01	10.000	0.42000
1208	0.23500E-01	70.000	0.49000	1508	0.23500E-01	10.000	0.49000
1209	0.23500E-01	70.000	0.56000	1509	0.23500E-01	10.000	0.56000
1210	0.23500E-01	70.000	0.63000	1510	0.23500E-01	10.000	0.63000
1211	0.23500E-01	70.000	0.70000	1511	0.23500E-01	10.000	0.70000
1212	0.23500E-01	70.000	0.77000	1512	0.23500E-01	10.000	0.77000
1301	0.23500E-01	50.000	0.00000E+00	1601	0.23500E-01	-10.000	0.00000E+00
1302	0.23500E-01	50.000	0.70000E-01	1602	0.23500E-01	-10.000	0.70000E-01
1303	0.23500E-01	50.000	0.14000	1603	0.23500E-01	-10.000	0.14000
1304	0.23500E-01	50.000	0.21000	1604	0.23500E-01	-10.000	0.21000
1305	0.23500E-01	50.000	0.28000	1605	0.23500E-01	-10.000	0.28000
1306	0.23500E-01	50.000	0.35000	1606	0.23500E-01	-10.000	0.35000
1307	0.23500E-01	50.000	0.42000	1607	0.23500E-01	-10.000	0.42000
1308	0.23500E-01	50.000	0.49000	1608	0.23500E-01	-10.000	0.49000
1309	0.23500E-01	50.000	0.56000	1609	0.23500E-01	-10.000	0.56000
1310	0.23500E-01	50.000	0.63000	1610	0.23500E-01	-10.000	0.63000
1311	0.23500E-01	50.000	0.70000	1611	0.23500E-01	-10.000	0.70000
1312	0.23500E-01	50.000	0.77000	1612	0.23500E-01	-10.000	0.77000

Table 5.1 Node position (cont'd)

NODE	r	θ	z	NODE	r	θ	z
1701	0.23500E-01	-30.000	0.00000E+00	2001	0.23500E-01	-90.000	0.00000E+00
1702	0.23500E-01	-30.000	0.70000E-01	2002	0.23500E-01	-90.000	0.70000E-01
1703	0.23500E-01	-30.000	0.14000	2003	0.23500E-01	-90.000	0.14000
1704	0.23500E-01	-30.000	0.21000	2004	0.23500E-01	-90.000	0.21000
1705	0.23500E-01	-30.000	0.28000	2005	0.23500E-01	-90.000	0.28000
1706	0.23500E-01	-30.000	0.35000	2006	0.23500E-01	-90.000	0.35000
1707	0.23500E-01	-30.000	0.42000	2007	0.23500E-01	-90.000	0.42000
1708	0.23500E-01	-30.000	0.49000	2008	0.23500E-01	-90.000	0.49000
1709	0.23500E-01	-30.000	0.56000	2009	0.23500E-01	-90.000	0.56000
1710	0.23500E-01	-30.000	0.63000	2010	0.23500E-01	-90.000	0.63000
1711	0.23500E-01	-30.000	0.70000	2011	0.23500E-01	-90.000	0.70000
1712	0.23500E-01	-30.000	0.77000	2012	0.23500E-01	-90.000	0.77000
1801	0.23500E-01	-50.000	0.00000E+00				
1802	0.23500E-01	-50.000	0.70000E-01				
1803	0.23500E-01	-50.000	0.14000				
1804	0.23500E-01	-50.000	0.21000				
1805	0.23500E-01	-50.000	0.28000				
1806	0.23500E-01	-50.000	0.35000				
1807	0.23500E-01	-50.000	0.42000				
1808	0.23500E-01	-50.000	0.49000				
1809	0.23500E-01	-50.000	0.56000				
1810	0.23500E-01	-50.000	0.63000				
1811	0.23500E-01	-50.000	0.70000				
1812	0.23500E-01	-50.000	0.77000				
1901	0.23500E-01	-70.000	0.00000E+00				
1902	0.23500E-01	-70.000	0.70000E-01				
1903	0.23500E-01	-70.000	0.14000				
1904	0.23500E-01	-70.000	0.21000				
1905	0.23500E-01	-70.000	0.28000				
1906	0.23500E-01	-70.000	0.35000				
1907	0.23500E-01	-70.000	0.42000				
1908	0.23500E-01	-70.000	0.49000				
1909	0.23500E-01	-70.000	0.56000				
1910	0.23500E-01	-70.000	0.63000				
1911	0.23500E-01	-70.000	0.70000				
1912	0.23500E-01	-70.000	0.77000				

TABLE 5.2 ELEMENT DEFINITIONS

EL #	NODE	NODE	NODE	NODE	NODE	NODE	NODE	NODE	MAT	TYPE
101	101	102	202	201					1	1
102	102	103	203	202					1	1
103	103	104	204	203					1	1
104	104	105	205	204					1	1
105	105	106	206	205					1	1
106	106	107	207	206					1	1
107	107	108	208	207					1	1
108	108	109	209	208					1	1
109	109	110	210	209					1	1
110	110	111	211	210					1	1
111	111	112	212	211					1	1
201	201	202	302	301					1	1
202	202	203	303	302					1	1
203	203	204	304	303					1	1
204	204	205	305	304					1	1
205	205	206	306	305					1	1
206	206	207	307	306					1	1
207	207	208	308	307					1	1
208	208	209	309	308					1	1
209	209	210	310	309					1	1
210	210	211	311	310					1	1
211	211	212	312	311					1	1
301	301	302	402	401					1	1
302	302	303	403	402					1	1
303	303	304	404	403					1	1
304	304	305	405	404					1	1
305	305	306	406	405					1	1
306	306	307	407	406					1	1
307	307	308	408	407					1	1
308	308	309	409	408					1	1
309	309	310	410	409					1	1
310	310	311	411	410					1	1
311	311	312	412	411					1	1
401	401	402	502	501					1	1
402	402	403	503	502					1	1
403	403	404	504	503					1	1
404	404	405	505	504					1	1
405	405	406	506	505					1	1
406	406	407	507	506					1	1
407	407	408	508	507					1	1
408	408	409	509	508					1	1
409	409	410	510	509					1	1
410	410	411	511	510					1	1
411	411	412	512	511					1	1
501	501	502	602	601					1	1
502	502	503	603	602					1	1
503	503	504	604	603					1	1
504	504	505	605	604					1	1
505	505	506	606	605					1	1
506	506	507	607	606					1	1
507	507	508	608	607					1	1
508	508	509	609	608					1	1
509	509	510	610	609					1	1
510	510	511	611	610					1	1
511	511	512	612	611					1	1

TABLE 5.2 ELEMENT DEFINITIONS (cont'd)

EL #	NODE	NODE	NODE	NODE	NODE	NODE	NODE	NODE	MAT	TYPE
601	601	602	702	701					1	1
602	602	603	703	702					1	1
603	603	604	704	703					1	1
604	604	605	705	704					1	1
605	605	606	706	705					1	1
606	606	607	707	706					1	1
607	607	608	708	707					1	1
608	608	609	709	708					1	1
609	609	610	710	709					1	1
610	610	611	711	710					1	1
611	611	612	712	711					1	1
701	701	702	802	801					1	1
702	702	703	803	802					1	1
703	703	704	804	803					1	1
704	704	705	805	804					1	1
705	705	706	806	805					1	1
706	706	707	807	806					1	1
707	707	708	808	807					1	1
708	708	709	809	808					1	1
709	709	710	810	809					1	1
710	710	711	811	810					1	1
711	711	712	812	811					1	1
801	801	802	902	901					1	1
802	802	803	903	902					1	1
803	803	804	904	903					1	1
804	804	805	905	904					1	1
805	805	806	906	905					1	1
806	806	807	907	906					1	1
807	807	808	908	907					1	1
808	808	809	909	908					1	1
809	809	810	910	909					1	1
810	810	811	911	910					1	1
811	811	812	912	911					1	1
901	901	902	1002	1001					1	1
902	902	903	1003	1002					1	1
903	903	904	1004	1003					1	1
904	904	905	1005	1004					1	1
905	905	906	1006	1005					1	1
906	906	907	1007	1006					1	1
907	907	908	1008	1007					1	1
908	908	909	1009	1008					1	1
909	909	910	1010	1009					1	1
910	910	911	1011	1010					1	1
911	911	912	1012	1011					1	1
1101	1101	1102	1202	1201	101	102	202	201	2	2
1102	1102	1103	1203	1202	102	103	203	202	2	2
1103	1103	1104	1204	1203	103	104	204	203	2	2
1104	1104	1105	1205	1204	104	105	205	204	2	2
1105	1105	1106	1206	1205	105	106	206	205	2	2
1106	1106	1107	1207	1206	106	107	207	206	2	2
1107	1107	1108	1208	1207	107	108	208	207	2	2
1108	1108	1109	1209	1208	108	109	209	208	2	2
1109	1109	1110	1210	1209	109	110	210	209	2	2
1110	1110	1111	1211	1210	110	111	211	210	2	2
1111	1111	1112	1212	1211	111	112	212	211	2	2

TABLE 5.2 ELEMENT DEFINITIONS (cont'd)

EL #	NODE	NODE	NODE	NODE	NODE	NODE	NODE	NODE	MAT	TYPE
1201	1201	1202	1302	1301	201	202	302	301	2	2
1202	1202	1203	1303	1302	202	203	303	302	2	2
1203	1203	1204	1304	1303	203	204	304	303	2	2
1204	1204	1205	1305	1304	204	205	305	304	2	2
1205	1205	1206	1306	1305	205	206	306	305	2	2
1206	1206	1207	1307	1306	206	207	307	306	2	2
1207	1207	1208	1308	1307	207	208	308	307	2	2
1208	1208	1209	1309	1308	208	209	309	308	2	2
1209	1209	1210	1310	1309	209	210	310	309	2	2
1210	1210	1211	1311	1310	210	211	311	310	2	2
1211	1211	1212	1312	1311	211	212	312	311	2	2
1301	1301	1302	1402	1401	301	302	402	401	2	2
1302	1302	1303	1403	1402	302	303	403	402	2	2
1303	1303	1304	1404	1403	303	304	404	403	2	2
1304	1304	1305	1405	1404	304	305	405	404	2	2
1305	1305	1306	1406	1405	305	306	406	405	2	2
1306	1306	1307	1407	1406	306	307	407	406	2	2
1307	1307	1308	1408	1407	307	308	408	407	2	2
1308	1308	1309	1409	1408	308	309	409	408	2	2
1309	1309	1310	1410	1409	309	310	410	409	2	2
1310	1310	1311	1411	1410	310	311	411	410	2	2
1311	1311	1312	1412	1411	311	312	412	411	2	2
1401	1401	1402	1502	1501	401	402	502	501	2	2
1402	1402	1403	1503	1502	402	403	503	502	2	2
1403	1403	1404	1504	1503	403	404	504	503	2	2
1404	1404	1405	1505	1504	404	405	505	504	2	2
1405	1405	1406	1506	1505	405	406	506	505	2	2
1406	1406	1407	1507	1506	406	407	507	506	2	2
1407	1407	1408	1508	1507	407	408	508	507	2	2
1408	1408	1409	1509	1508	408	409	509	508	2	2
1409	1409	1410	1510	1509	409	410	510	509	2	2
1410	1410	1411	1511	1510	410	411	511	510	2	2
1411	1411	1412	1512	1511	411	412	512	511	2	2
1501	1501	1502	1602	1601	501	502	602	601	2	2
1502	1502	1503	1603	1602	502	503	603	602	2	2
1503	1503	1504	1604	1603	503	504	604	603	2	2
1504	1504	1505	1605	1604	504	505	605	604	2	2
1505	1505	1506	1606	1605	505	506	606	605	2	2
1506	1506	1507	1607	1606	506	507	607	606	2	2
1507	1507	1508	1608	1607	507	508	608	607	2	2
1508	1508	1509	1609	1608	508	509	609	608	2	2
1509	1509	1510	1610	1609	509	510	610	609	2	2
1510	1510	1511	1611	1610	510	511	611	610	2	2
1511	1511	1512	1612	1611	511	512	612	611	2	2
1601	1601	1602	1702	1701	601	602	702	701	2	2
1602	1602	1603	1703	1702	602	603	703	702	2	2
1603	1603	1604	1704	1703	603	604	704	703	2	2
1604	1604	1605	1705	1704	604	605	705	704	2	2
1605	1605	1606	1706	1705	605	606	706	705	2	2
1606	1606	1607	1707	1706	606	607	707	706	2	2
1607	1607	1608	1708	1707	607	608	708	707	2	2
1608	1608	1609	1709	1708	608	609	709	708	2	2
1609	1609	1610	1710	1709	609	610	710	709	2	2
1610	1610	1611	1711	1710	610	611	711	710	2	2
1611	1611	1612	1712	1711	611	612	712	711	2	2

TABLE 5.2 ELEMENT DEFINITIONS (cont'd)

EL #	NODE	NODE	NODE	NODE	NODE	NODE	NODE	NODE	MAT	TYPE
1701	1701	1702	1802	1801	701	702	802	801	2	2
1702	1702	1703	1803	1802	702	703	803	802	2	2
1703	1703	1704	1804	1803	703	704	804	803	2	2
1704	1704	1705	1805	1804	704	705	805	804	2	2
1705	1705	1706	1806	1805	705	706	806	805	2	2
1706	1706	1707	1807	1806	706	707	807	806	2	2
1707	1707	1708	1808	1807	707	708	808	807	2	2
1708	1708	1709	1809	1808	708	709	809	808	2	2
1709	1709	1710	1810	1809	709	710	810	809	2	2
1710	1710	1711	1811	1810	710	711	811	810	2	2
1711	1711	1712	1812	1811	711	712	812	811	2	2
1801	1801	1802	1902	1901	801	802	902	901	2	2
1802	1802	1803	1903	1902	802	803	903	902	2	2
1803	1803	1804	1904	1903	803	804	904	903	2	2
1804	1804	1805	1905	1904	804	805	905	904	2	2
1805	1805	1806	1906	1905	805	806	906	905	2	2
1806	1806	1807	1907	1906	806	807	907	906	2	2
1807	1807	1808	1908	1907	807	808	908	907	2	2
1808	1808	1809	1909	1908	808	809	909	908	2	2
1809	1809	1810	1910	1909	809	810	910	909	2	2
1810	1810	1811	1911	1910	810	811	911	910	2	2
1811	1811	1812	1912	1911	811	812	912	911	2	2
1901	1901	1902	2002	2001	901	902	1002	1001	2	2
1902	1902	1903	2003	2002	902	903	1003	1002	2	2
1903	1903	1904	2004	2003	903	904	1004	1003	2	2
1904	1904	1905	2005	2004	904	905	1005	1004	2	2
1905	1905	1906	2006	2005	905	906	1006	1005	2	2
1906	1906	1907	2007	2006	906	907	1007	1006	2	2
1907	1907	1908	2008	2007	907	908	1008	1007	2	2
1908	1908	1909	2009	2008	908	909	1009	1008	2	2
1909	1909	1910	2010	2009	909	910	1010	1009	2	2
1910	1910	1911	2011	2010	910	911	1011	1010	2	2
1911	1911	1912	2012	2011	911	912	1012	1011	2	2

Table 5.3 SPECIFIED DISPLACEMENTS

NODE	UX	UY	UZ	ROTX	ROTY	ROTZ
101	0.000000E+00	0.000000E+00	0.000000E+00	0.000000E+00	0.000000E+00	0.000000E+00
102	0.000000E+00				0.000000E+00	0.000000E+00
103	0.000000E+00				0.000000E+00	0.000000E+00
104	0.000000E+00				0.000000E+00	0.000000E+00
105	0.000000E+00				0.000000E+00	0.000000E+00
106	0.000000E+00				0.000000E+00	0.000000E+00
107	0.000000E+00				0.000000E+00	0.000000E+00
108	0.000000E+00				0.000000E+00	0.000000E+00
109	0.000000E+00				0.000000E+00	0.000000E+00
110	0.000000E+00				0.000000E+00	0.000000E+00
111	0.000000E+00				0.000000E+00	0.000000E+00
112	0.000000E+00				0.000000E+00	0.000000E+00
201	0.000000E+00	0.000000E+00	0.000000E+00	0.000000E+00	0.000000E+00	0.000000E+00
301	0.000000E+00	0.000000E+00	0.000000E+00	0.000000E+00	0.000000E+00	0.000000E+00
401	0.000000E+00	0.000000E+00	0.000000E+00	0.000000E+00	0.000000E+00	0.000000E+00
501	0.000000E+00	0.000000E+00	0.000000E+00	0.000000E+00	0.000000E+00	0.000000E+00
601	0.000000E+00	0.000000E+00	0.000000E+00	0.000000E+00	0.000000E+00	0.000000E+00
701	0.000000E+00	0.000000E+00	0.000000E+00	0.000000E+00	0.000000E+00	0.000000E+00
801	0.000000E+00	0.000000E+00	0.000000E+00	0.000000E+00	0.000000E+00	0.000000E+00
901	0.000000E+00	0.000000E+00	0.000000E+00	0.000000E+00	0.000000E+00	0.000000E+00
1001	0.000000E+00	0.000000E+00	0.000000E+00	0.000000E+00	0.000000E+00	0.000000E+00
1002	0.000000E+00				0.000000E+00	0.000000E+00
1003	0.000000E+00				0.000000E+00	0.000000E+00
1004	0.000000E+00				0.000000E+00	0.000000E+00
1005	0.000000E+00				0.000000E+00	0.000000E+00
1006	0.000000E+00				0.000000E+00	0.000000E+00
1007	0.000000E+00				0.000000E+00	0.000000E+00
1008	0.000000E+00				0.000000E+00	0.000000E+00
1009	0.000000E+00				0.000000E+00	0.000000E+00
1010	0.000000E+00				0.000000E+00	0.000000E+00
1011	0.000000E+00				0.000000E+00	0.000000E+00
1012	0.000000E+00				0.000000E+00	0.000000E+00

Table 5.3 SPECIFIED DISPLACEMENTS (cont'd)

NODE	UX	UY	UZ	ROTX	ROTY	ROTZ
1101	0.000000E+00	0.000000E+00	0.000000E+00	0.000000E+00	0.000000E+00	0.000000E+00
1102	0.000000E+00					
1103	0.000000E+00					
1104	0.000000E+00					
1105	0.000000E+00					
1106	0.000000E+00					
1107	0.000000E+00					
1108	0.000000E+00					
1109	0.000000E+00					
1110	0.000000E+00					
1111	0.000000E+00					
1112	0.000000E+00					
1201	0.000000E+00	0.000000E+00	0.000000E+00	0.000000E+00	0.000000E+00	0.000000E+00
1301	0.000000E+00	0.000000E+00	0.000000E+00	0.000000E+00	0.000000E+00	0.000000E+00
1401	0.000000E+00	0.000000E+00	0.000000E+00	0.000000E+00	0.000000E+00	0.000000E+00
1501	0.000000E+00	0.000000E+00	0.000000E+00	0.000000E+00	0.000000E+00	0.000000E+00
1601	0.000000E+00	0.000000E+00	0.000000E+00	0.000000E+00	0.000000E+00	0.000000E+00
1701	0.000000E+00	0.000000E+00	0.000000E+00	0.000000E+00	0.000000E+00	0.000000E+00
1801	0.000000E+00	0.000000E+00	0.000000E+00	0.000000E+00	0.000000E+00	0.000000E+00
1901	0.000000E+00	0.000000E+00	0.000000E+00	0.000000E+00	0.000000E+00	0.000000E+00
2001	0.000000E+00	0.000000E+00	0.000000E+00	0.000000E+00	0.000000E+00	0.000000E+00
2002	0.000000E+00					
2003	0.000000E+00					
2004	0.000000E+00					
2005	0.000000E+00					
2006	0.000000E+00					
2007	0.000000E+00					
2008	0.000000E+00					
2009	0.000000E+00					
2010	0.000000E+00					
2011	0.000000E+00					
2012	0.000000E+00					

6.0 RANDOM VIBRATION ANALYSIS OF SOLID ROCKET MOTOR SUBJECTED TO SUPPORT EXCITATION WITH FINITE ELEMENT METHOD

In Chapter 5, a solid rocket motor has been modeled as a layered cylinder by finite shell elements and solid elements. The equation of motion of such a viscoelastic structure with frequency dependent stiffness and damping material properties at a constant temperature can be expressed as

$$[M]\{\ddot{q}\} + (\beta_e + \frac{\eta_e(\omega)}{\omega})[K(\omega)]\{\dot{q}\} + [K(\omega)]\{q\} = \{f(t)\} \qquad [6.1]$$

where

$[K(\omega)]$	Frequency dependent stiffness matrix
β_e	Equivalent viscous damping coefficient
η_e	Equivalent viscoelastic damping coefficient
$\{q\}$	Nodal displacement vector of finite element model
$\{f(t)\}$	External exciting force vector

For the case of support excitation in the vertical direction, the equation of motion becomes

$$[M]\{_r\ddot{q}\} + (\beta_e + \frac{\eta_e(\omega)}{\omega})[K(\omega)]\{_r\dot{q}\} + [K(\omega)]\{_rq\} = -[M]\{\alpha\}\ddot{u}_y(t) \qquad [6.2]$$

where $\{\alpha\}$ is the direction participation column vector consisting of one for y component and zero for other components in the vector. u_y represents the support displacement. The

subcript r for q indicates it is a relative displacement with respect to the support motion. Note that

$$
\begin{aligned}
{}_rq_y &= q_y - u_y \\
{}_rq_x &= q_x - u_x \\
{}_rq_z &= q_z - u_z
\end{aligned}
\qquad [6.3]
$$

For harmonic support motion, the equation becomes

$$
\begin{aligned}
&-\omega^2[M]\{{}_rQ\}e^{i\omega t} + i\,(\beta_e + \frac{\eta_e(\omega)}{\omega})\omega[K(\omega)]\{{}_rQ\}e^{i\omega t} + [K(\omega)]\{{}_rQ\}e^{i\omega t} \\
&= [M]\{\alpha\}\omega^2\, U_y\, e^{i\omega t}
\end{aligned}
\qquad [6.4]
$$

where $q = Q\, e^{i\omega t}$ relates Q and q, they in general are complex values with a phase shift φ with respect to U_y . The above equation can be further simplified by clearing the $e^{i\omega t}$ term

$$
[\, -\omega^2[M] + i\,(\beta_e\omega + \eta_e(\omega))[K(\omega)] + [K(\omega)]\ ]\ \{{}_rQ\} = [M]\{\alpha\}\omega^2 U_y \qquad [6.5]
$$

For a unit harmonic support motion, the frequency reponse Q at any frequency can be readily calculated by the above equation, even for rather complicated structures, since stiffness and damping matrices can be obtained by the finite element method. The harmonic reponse method is especially useful for the current case of structures with frequency dependent viscoelastic material properties.

The strain energy approach [19,18] has been used to calculate the equivalent damping coefficients. The basic idea can

be explained by the example of a viscoelastic spring in sinusoidal motion, $x = X \sin \omega t$, the dissipated energy per cycle [19,18,27] is equal to $[2\pi\eta(\frac{1}{2}kX^2)]$ which is proportional to the strain energy. In that sense, the overall equivalent damping ratio of a layered cylinder can be obtained in terms of weighted damping ratios of constituent materials as

$$\eta'_e = (\eta_p)_e + (\eta_s)_e = \eta_p \frac{(SE)p}{(SE)p + (SE)s} + \eta_s \frac{(SE)s}{(SE)p + (SE)s} \qquad [6.6]$$

where (SE) means strain energy. Subcripts p and s indicate propellant core and steel casing of rocket motor respectively. The strain energy can be readily calculated after the stiffness matrix and displacement matrix are obtained [Table 6.5, 6.6]. For frequencies near the first and second natural frequencies, the strain energy ratios of steel casing over propellant core are 113 and 25 respectively, and the equivalent damping ratios are 0.0047 and 0.016 respectively, more than 75% of these damping effects are due to the propellant core. The frequency dependent equivalent viscoelastic damping can in turn be represented by a combination of linearly varying $\beta_e\omega$ part and an η_e part which may be kept constant within each appropriate segmented frequency range. Alternately, the equivalent damping can be roughly estimated for the layered cylinder assuming that it behaves like an Euler beam. The bending strain energy can be expressed as

$$(SE) = \frac{1}{2}EI(\frac{d^2y}{dz^2})^2 \qquad [6.7]$$

After clearing the common differential terms, the approximate equivalent damping can be estimated as

$$\eta_e' = \frac{E_{2p}}{E_{1p}}(\frac{E_{1p}I_p}{E_{1s}I_s + E_{1p}I_p}) + \eta_s(\frac{E_{1s}I_s}{E_{1s}I_s + E_{1p}I_p}) \qquad [6.8]$$

where E_1 and E_2 are storage modulus and loss modulus respectively. I_s is the area moment of inertia for the steel casing, I_p is that for the propellant correspondingly. The estimate of strain energy under the Euler beam's somewhat rough assumptions of planes remaining plane and normals remaining normal gives a higher strain energy ratio of 180 near the first natural frequency.

A typical acceleration power spectral density (PSD) input curve with a frequency range of 20 Hz to 750 Hz and a rms acceleration of 9.55 g as shown in Fig. 6.1 can be used together with the discrete frequency reponse function H(f) to calculate the displacement response power spectrum density

$$S_{qq}(f) = |H_q(f)|^2 S_{uu}(f) \qquad [6.9]$$

The following well-known equation is derived from the relation of autocorrelation function and power spectral density

function by setting time interval $\tau = 0$. The standard deviation of displacement response is the same as its root mean square value for a stationary random process with a zero mean value as assumed in this study. The mean square value of displacement reponse at any nodal point can be calculated by

$$\bar{q}^2 = \int_{f_1}^{f_2} |H_q(f)|^2 S_{uu}(f) df \qquad [6.10]$$

where $S_{uu}(f)$ is the input displacement power spectrum density which can be obtained by dividing the acceleration power spectrum with $((2\pi f)^4)$ at each frequency station. The root mean square value is the square root of the mean square value. For node 112 at the free end and node 106 near the middle point of the rocket motor, the displacement frequency reponse functions (FRF), acceleration FRF and associated power spectral density curves are shown in Fig. 6.2-6.9. The real and imaginary components of these curves are shown in and Table 6.1 & 6.2 respectively. It is obvious that these response curves are highly amplified at the first two bending natural frequencies. On the other hand, ring modes and axial mode have little participation factors in this case of vertical excitation, although the 20-750 hz frequency range covers a ring mode also. The rms displacement at the free end tip of the rocket motor is 3.35 mm, the rms acceleration is about 142 g. At node 106, the rms displacement is 1.15 mm, and rms acceleration is about 59 g [Fig. 6.2-6.9].

Once the displacement field of the structure is known, the strain field and then stress field can be readily calculated by a similar procedure as that used for displacement response

$$S_{\sigma\sigma}(f) = |H_{\sigma}(f)|^2 S_{uu}(f) \qquad [6.11]$$

$$\bar{\sigma}^2 = \int_{f_1}^{f_2} |H_{\sigma}(f)|^2 S_{uu}(f) df \qquad [6.12]$$

therefore their corresponding stress frequency response functions and stress power spectral densities can be calculated also. Fig. 6.10 & 6.11 show the longitudinal stress FRF and PSD of node 101 at the supported end of the steel casing. This is in general one of critical points for many loading case, through numerical integration, the rms stress due to the random support vibration is obtained as 235.4 MPa. This level of stress intensity may be comparable to stress induced by the rocket motor internal pressure in flight, and may be the critical stress considered in structural design. Fig. 6.12 & 6.13 show the circumferential stress FRF and PSD at node 102 of the steel casing. The rms stress is 16.3 MPa, which is much smaller than the above-mentioned stress at node 101. The real and imaginary components of the FRF and PSD functions [Fig. 6.10-6.13] are also listed in Table 6.3 & 6.4. Shear stress responses at elements 501 and 511 are

shown in Fig. 6.14-6.17. The output rms shear stresses of 27.5 MPa and 3.62 MPa are not serious compared with 235.4 MPa of node 101. Due to the high rigidity of the steel casing, the soft propellant core is subjected to much less severe stresses; the axial rms stress at the node 101 of the propellant element 1101 is 179 KPa, shear stress at the centroids of element 1501 and 1511 are 19.1 KPa and 8.7 KPa respectively. These stresses, although small, may still become significant when combined with the effects of aging degradation, thermal and other environmental conditions. The associated computer programs "SHPSD11 OUT2" and "SHPSD16 OUT" for this random vibration analysis with finite element method have been written in the language of ANSYS engineering analysis system [51,52] to compute the discrete frequency response function and response power spectral density function in the form of real and imaginary components. These response data are then further processed with other programs to obtain the data presented in this chapter. The above programs are listed in appendix A.9 and A.10.

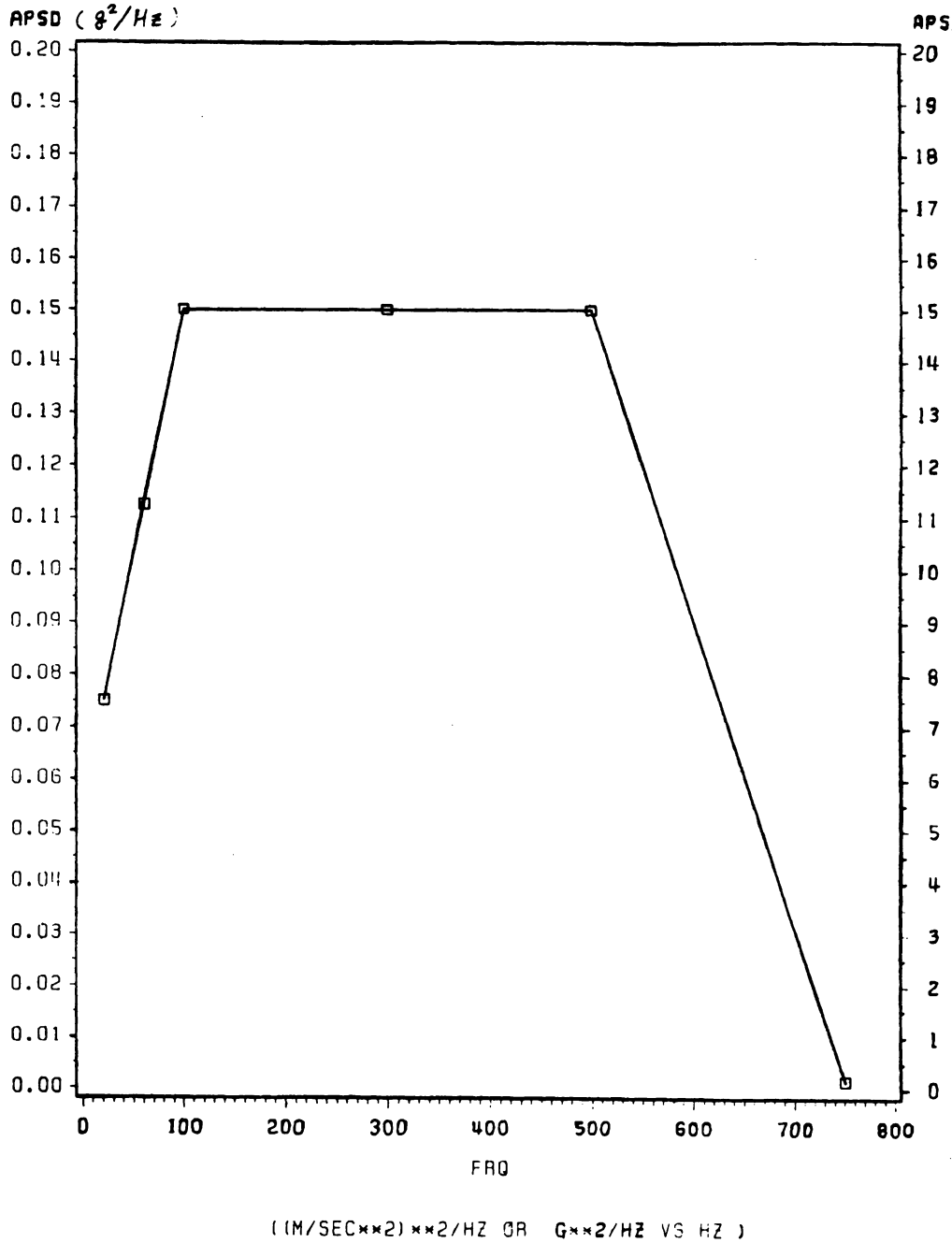

Figure 6.1 Vertical Acceleration PSD Input of Support

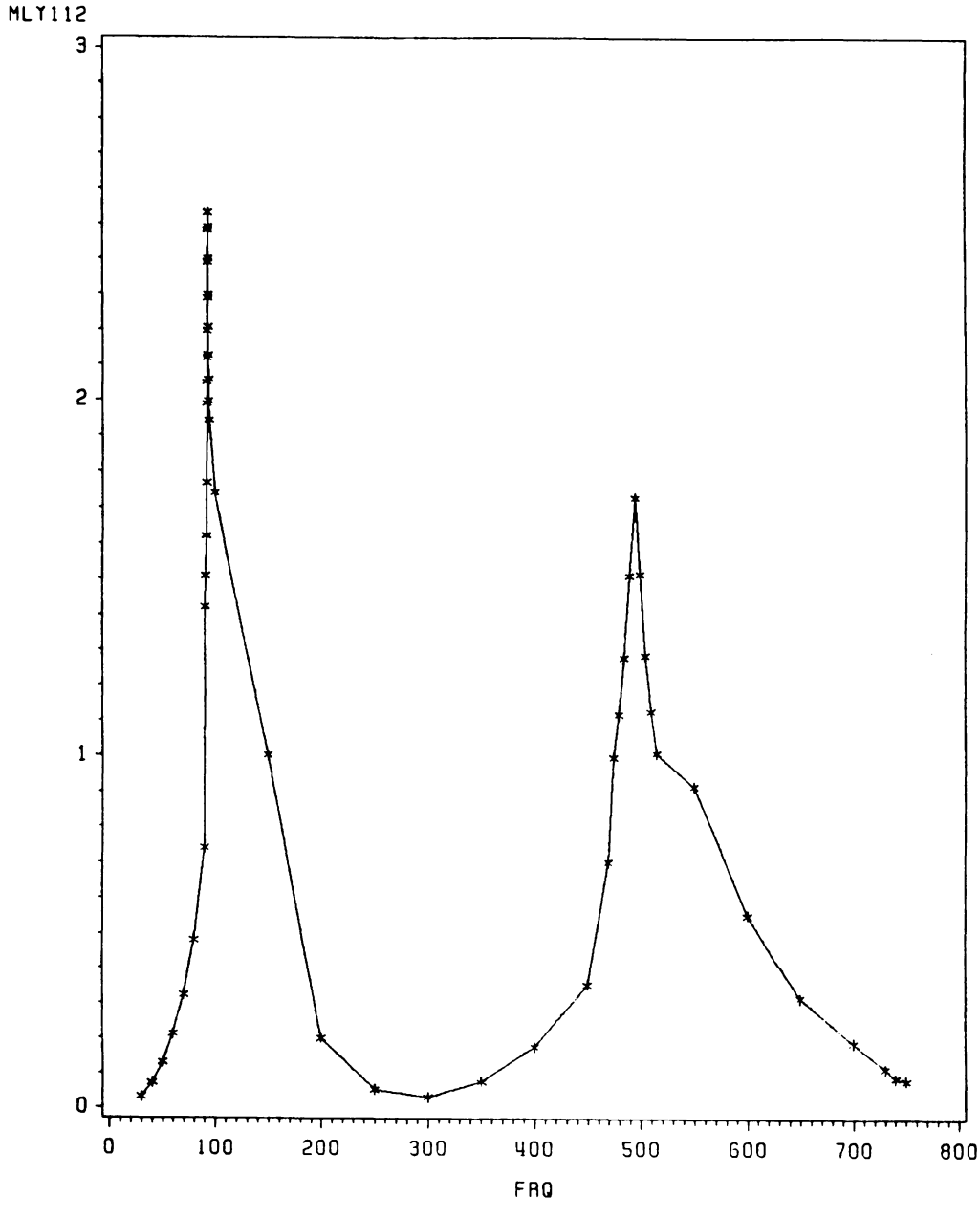

Figure 6.2 Log Vertical Displacement FRF of Node #112

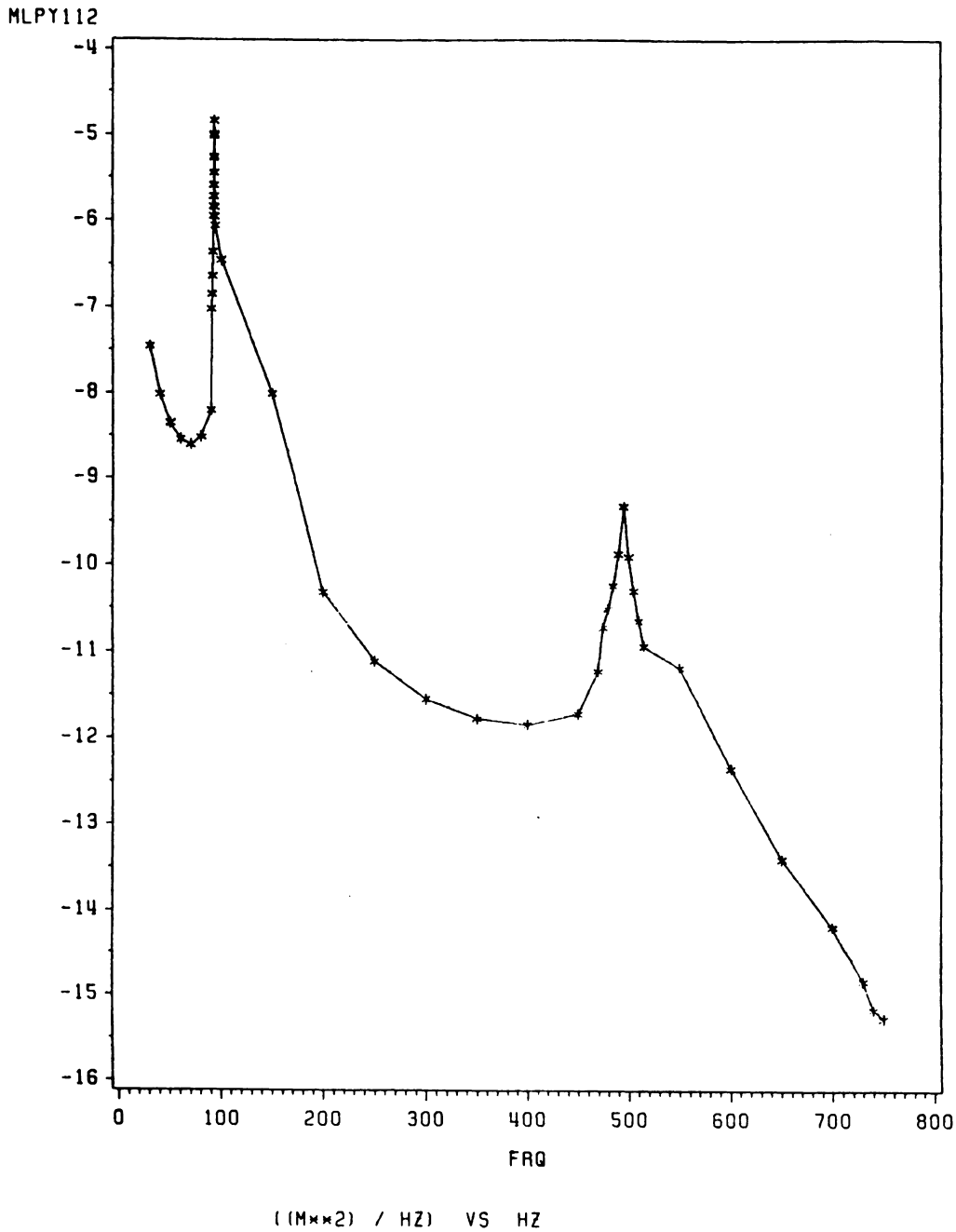

Figure 6.3 Log Vertical Displacement PSD of Node #112

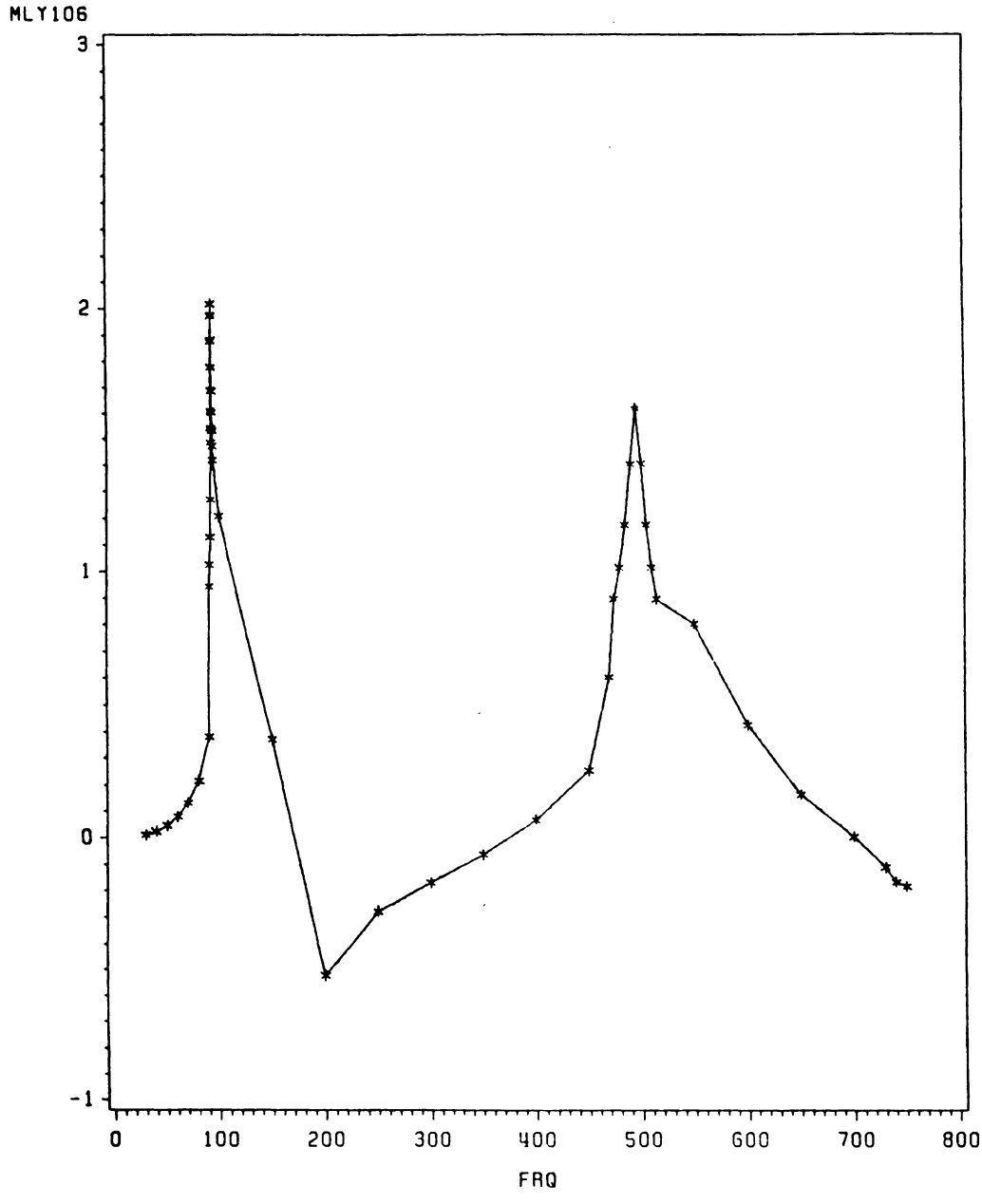

Figure 6.4 Log Vertical Displacement FRF of Node #106

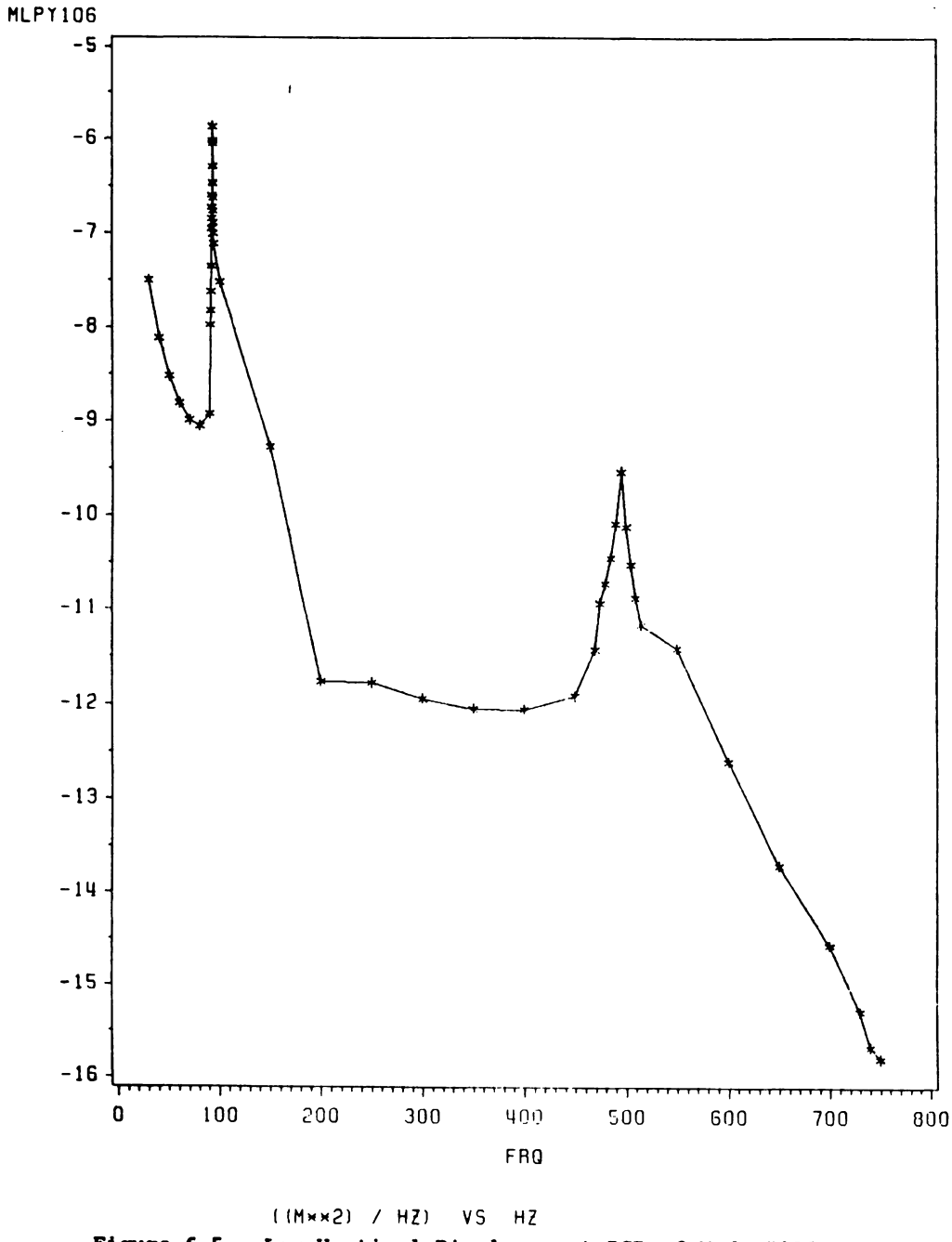

Figure 6.5 Log Vertical Displacement PSD of Node #106

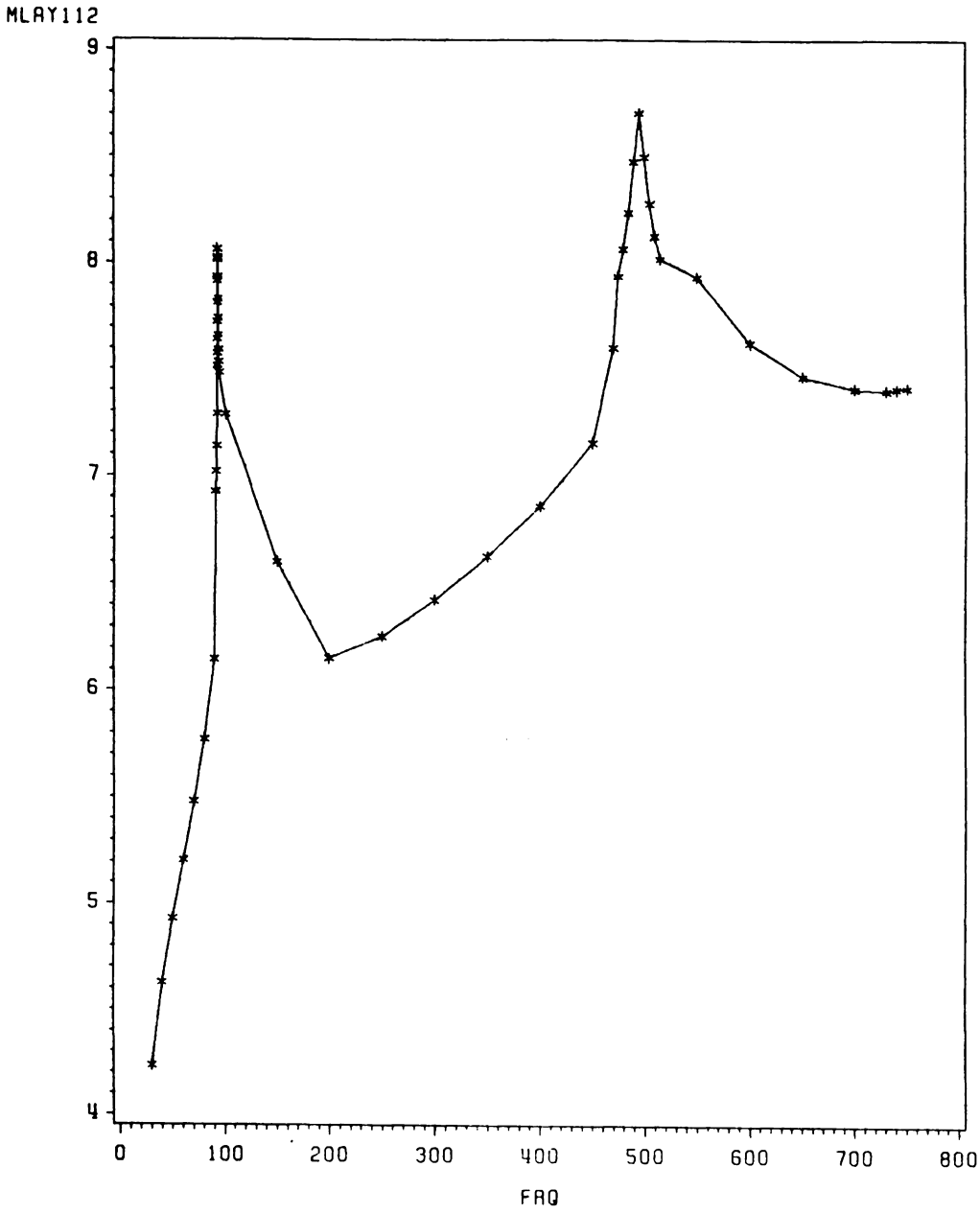

Figure 6.6 Log Vertical Acceleration FRF of Node #112

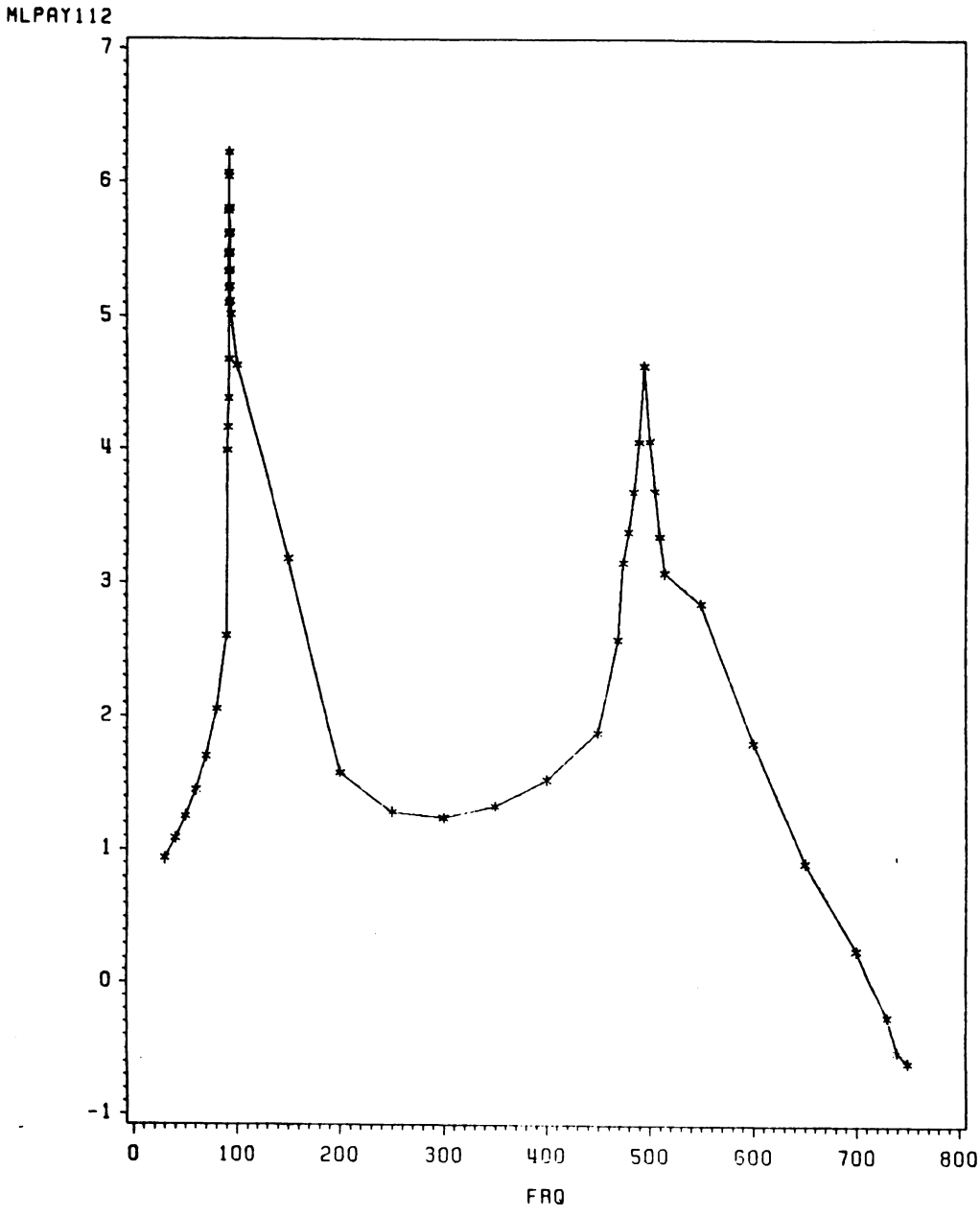

Figure 6.7 Log Vertical Acceleration PSD of Node #112

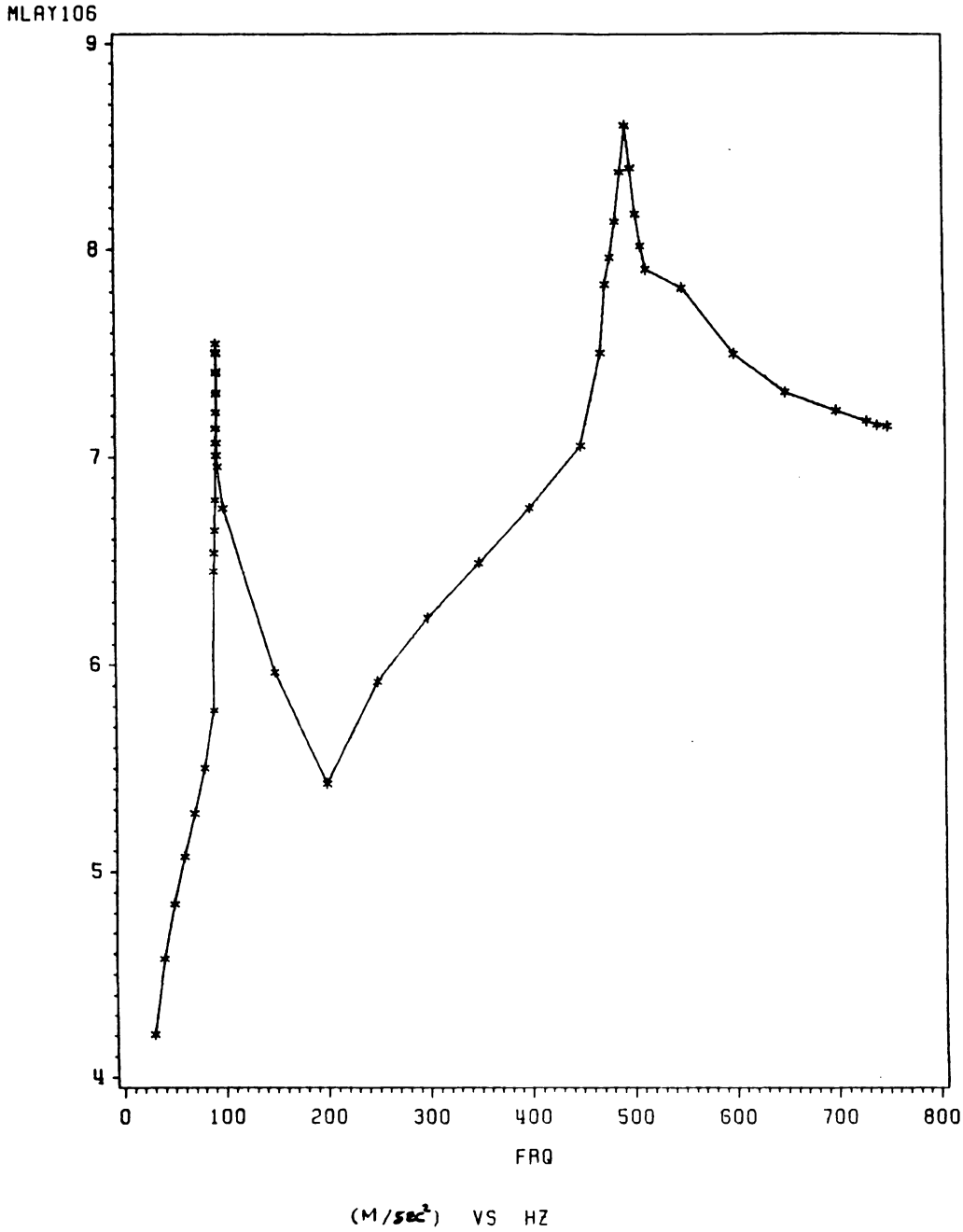

Figure 6.8 Log Vertical Acceleration FRF of Node #106

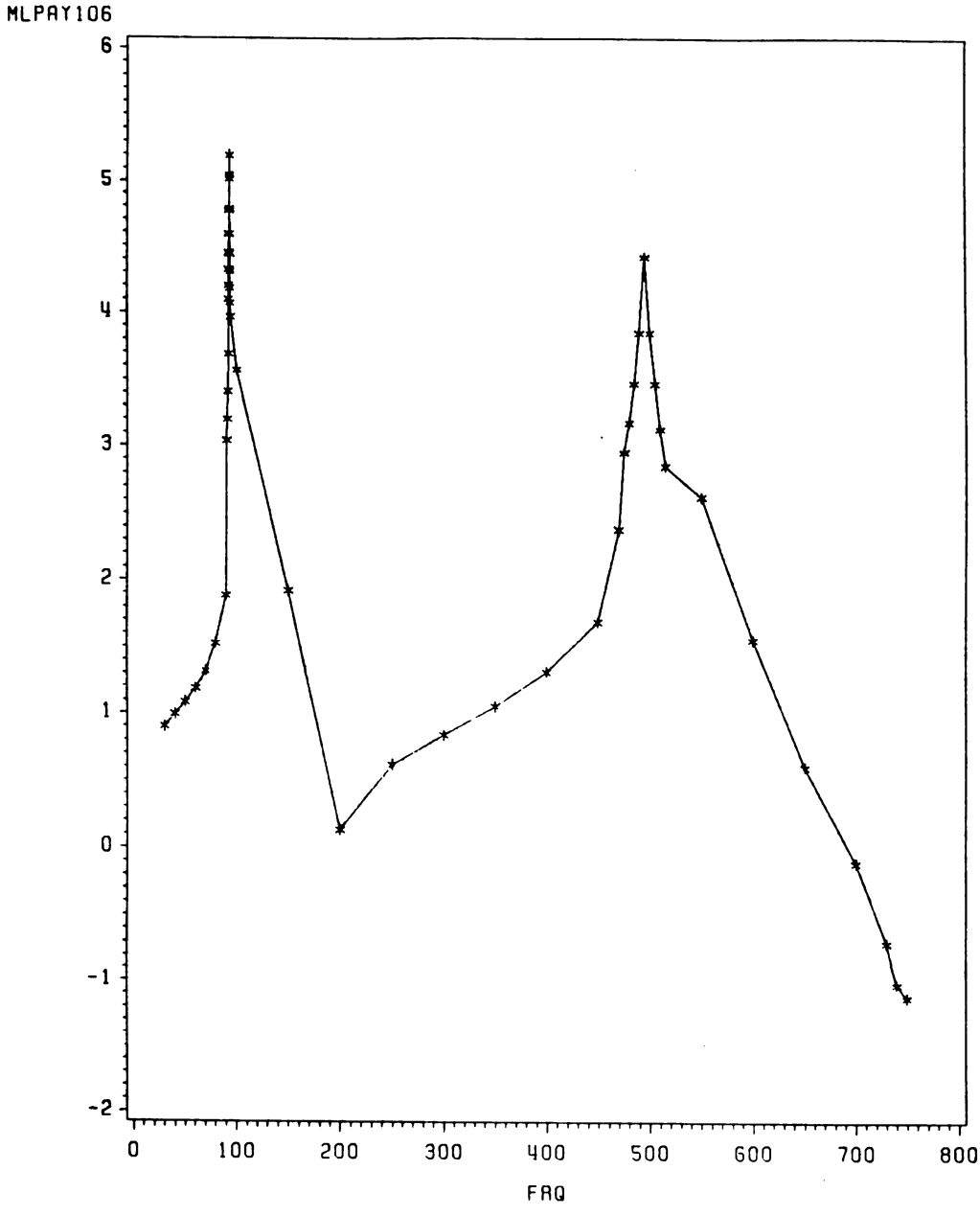

Figure 6.9 **Log Vertical Acceleration PSD of Node #106**

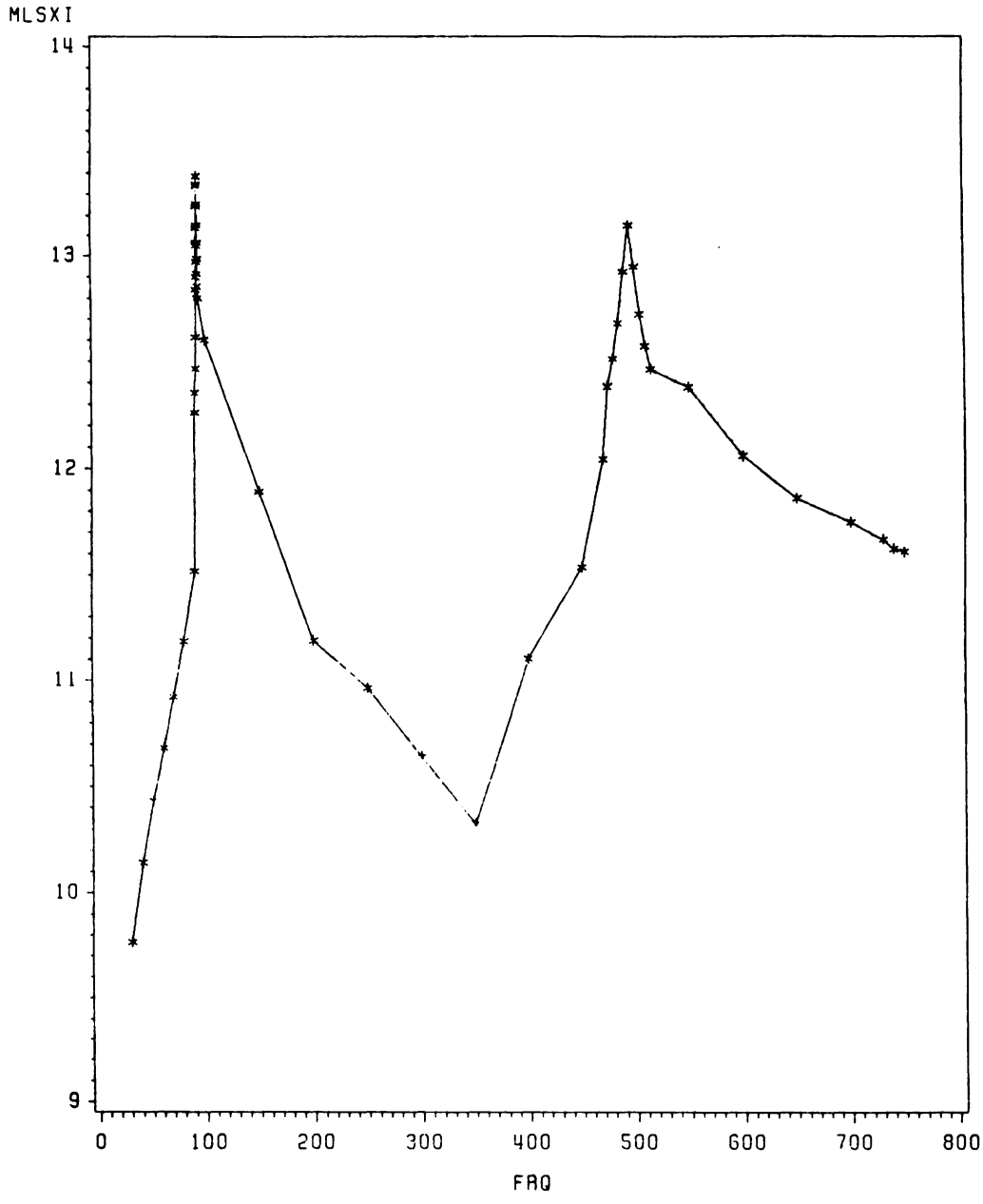

Figure 6.10 Log Longitudinal stress FRF of Node #101

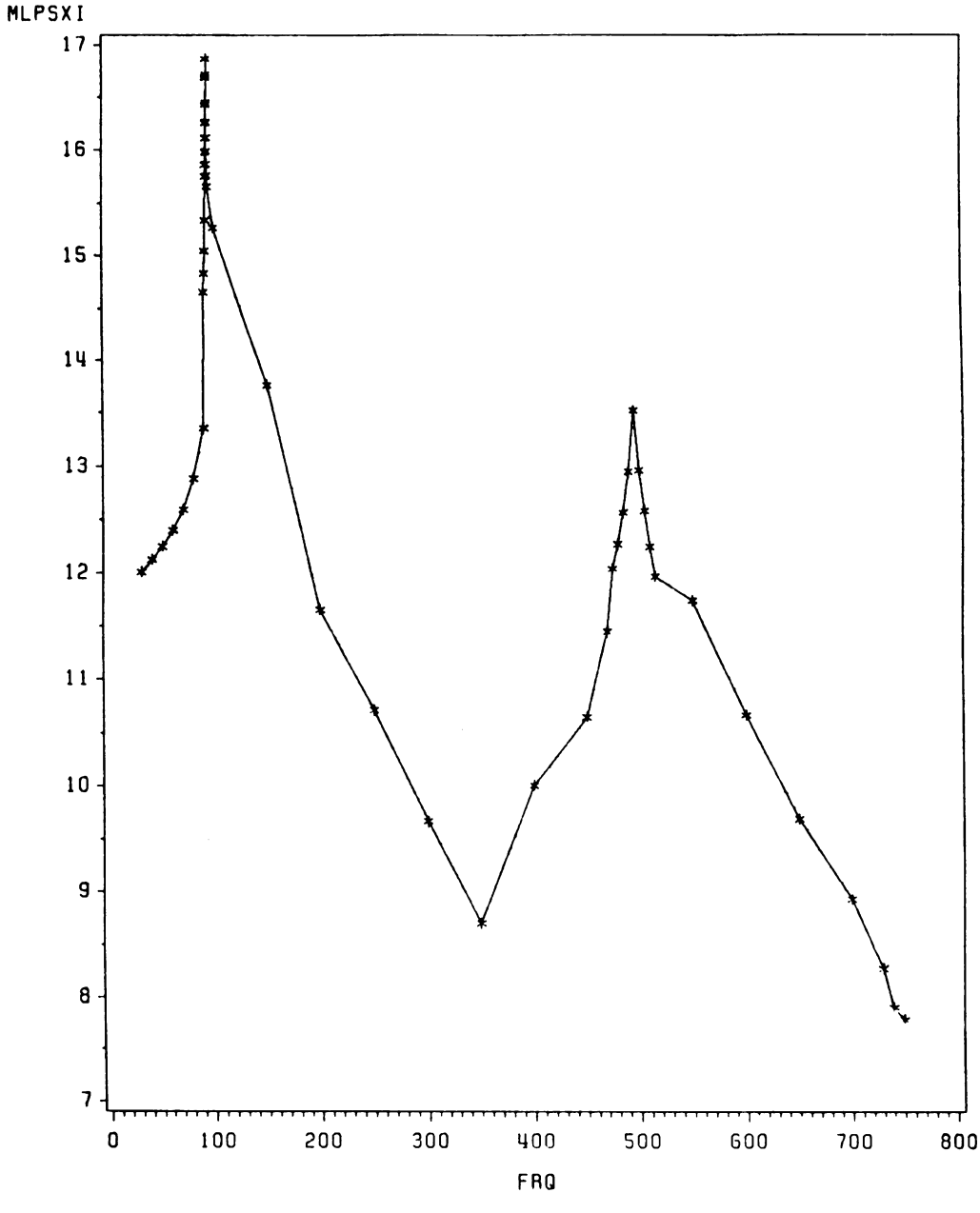

Figure 6.11 Log Longitudinal stress PSD of Node #101

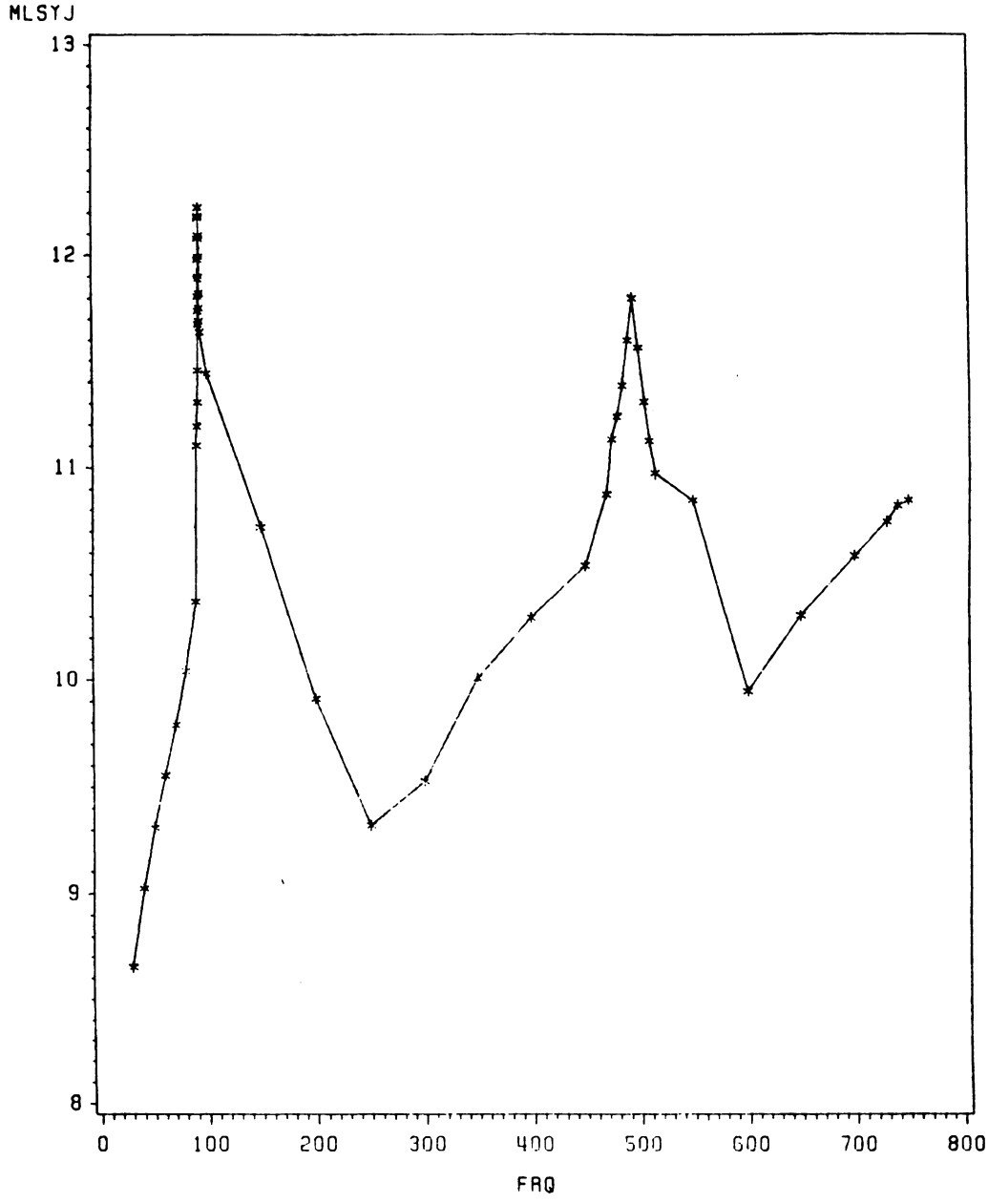

Figure 6.12 Log Circumferential stress FRF of Node #102

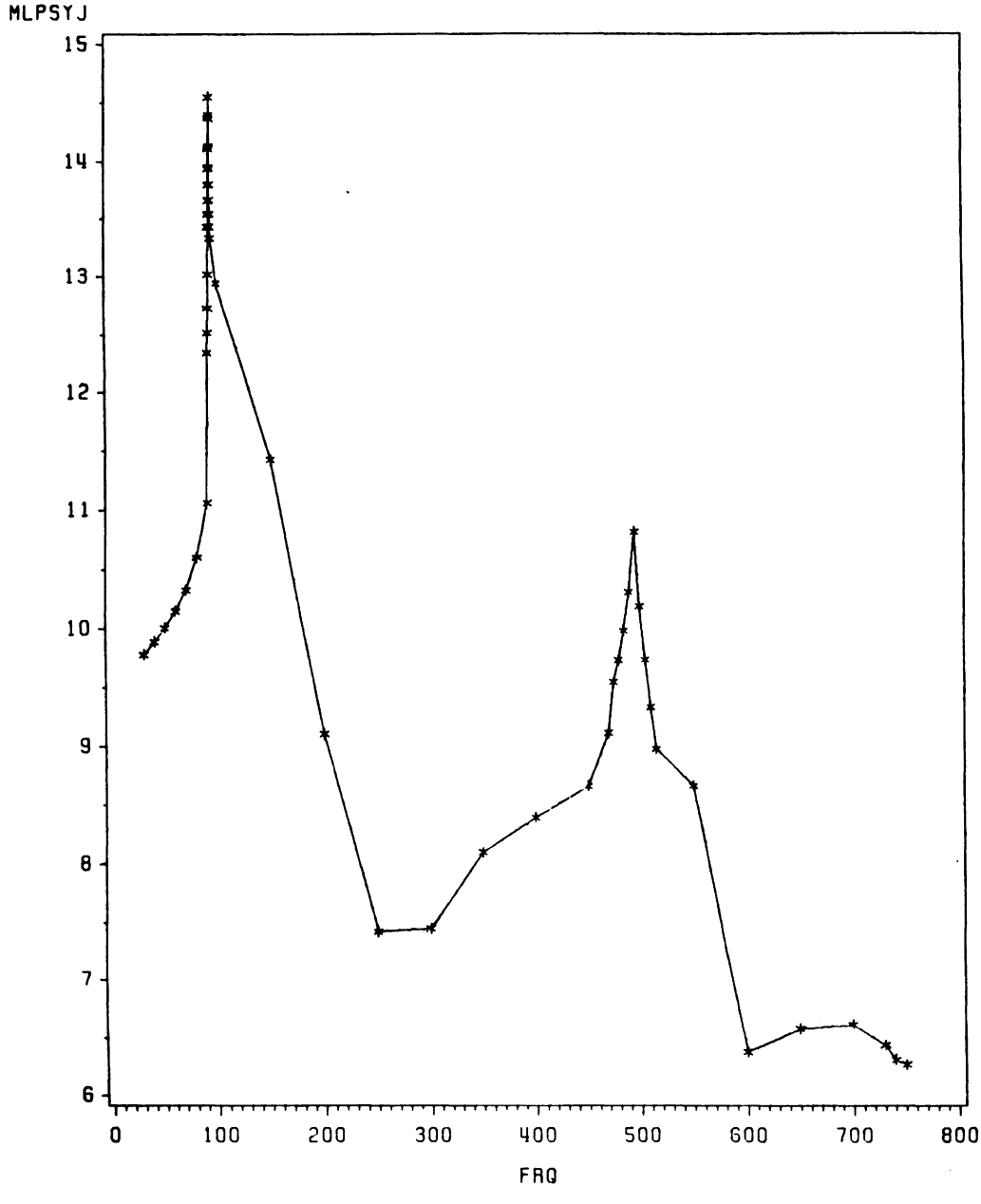

Figure 6.13 Log Circumferential stress PSD of Node #102

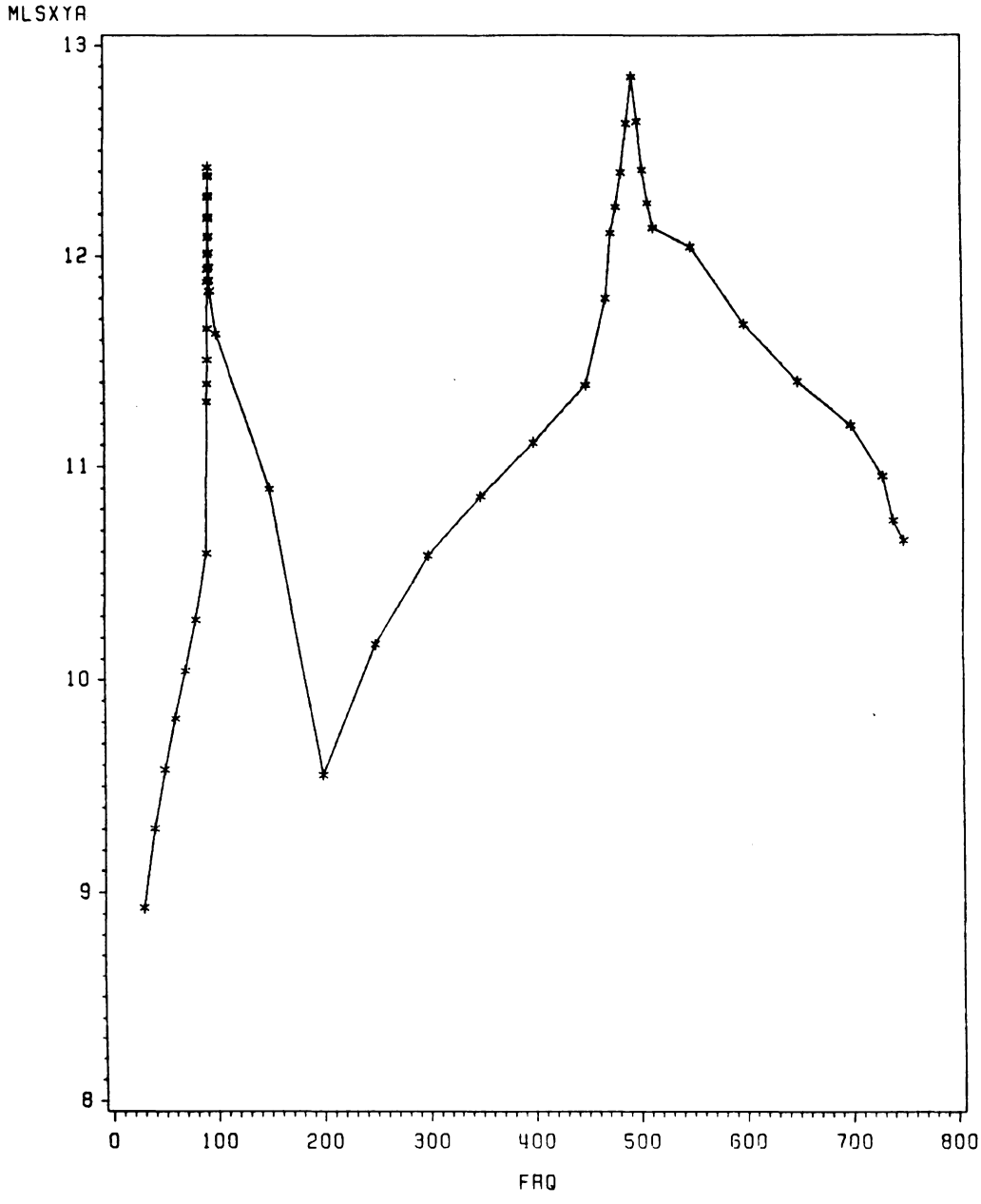

Figure 6.14 Log Shear stress FRF of Element #501

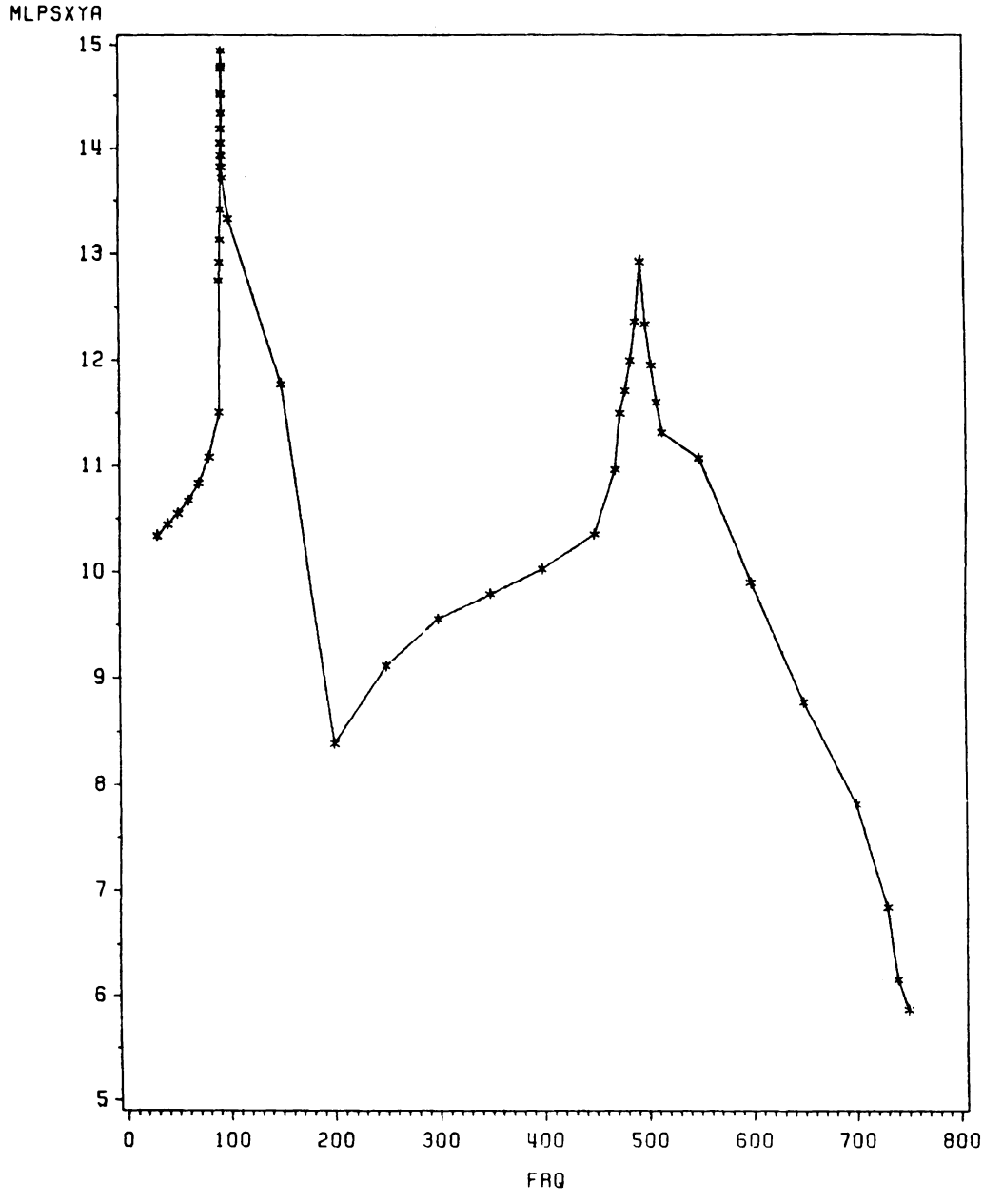

Figure 6.15 Log Shear stress PSD of Element #501

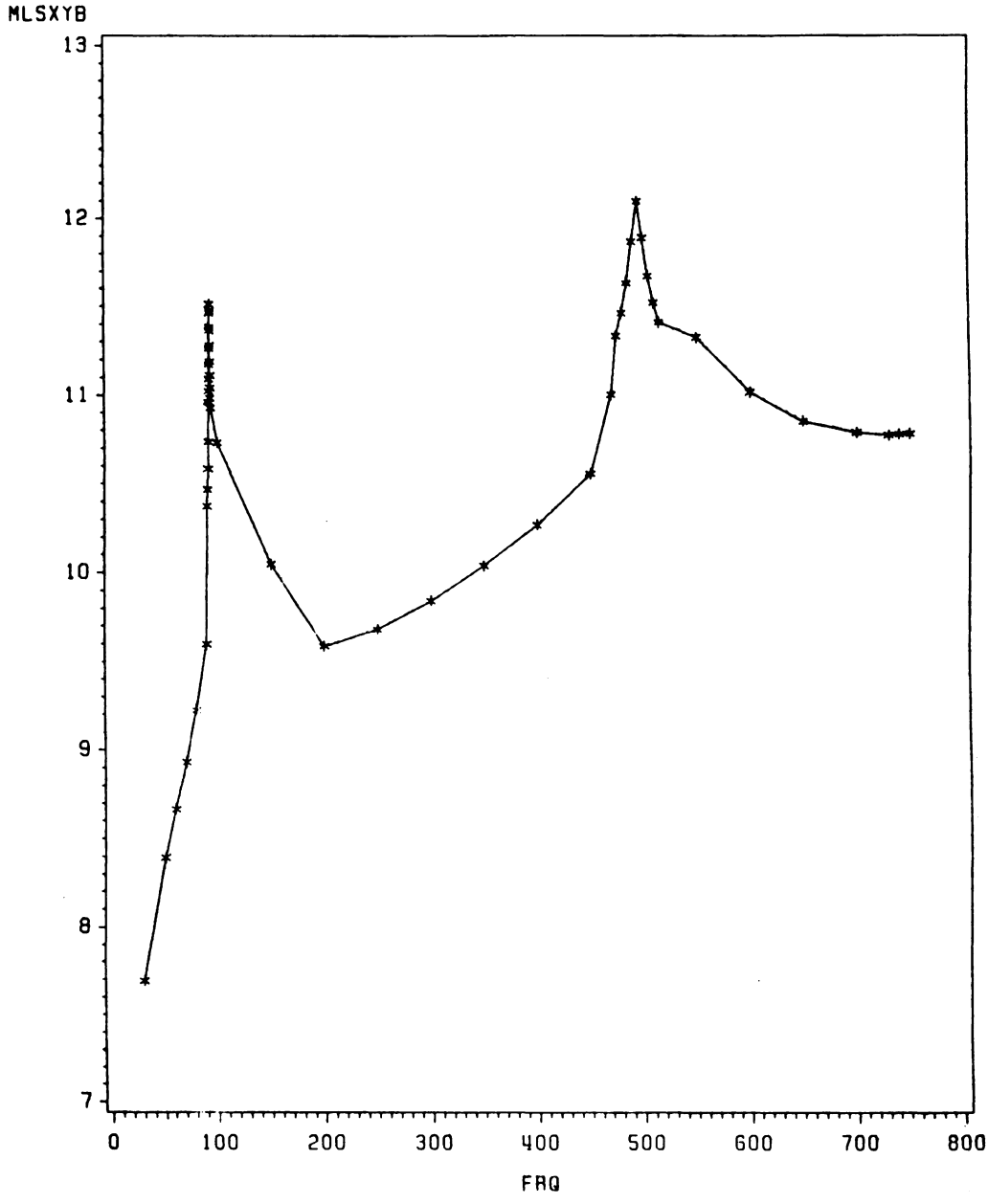

Figure 6.16 Log Shear stress FRF of Element #511

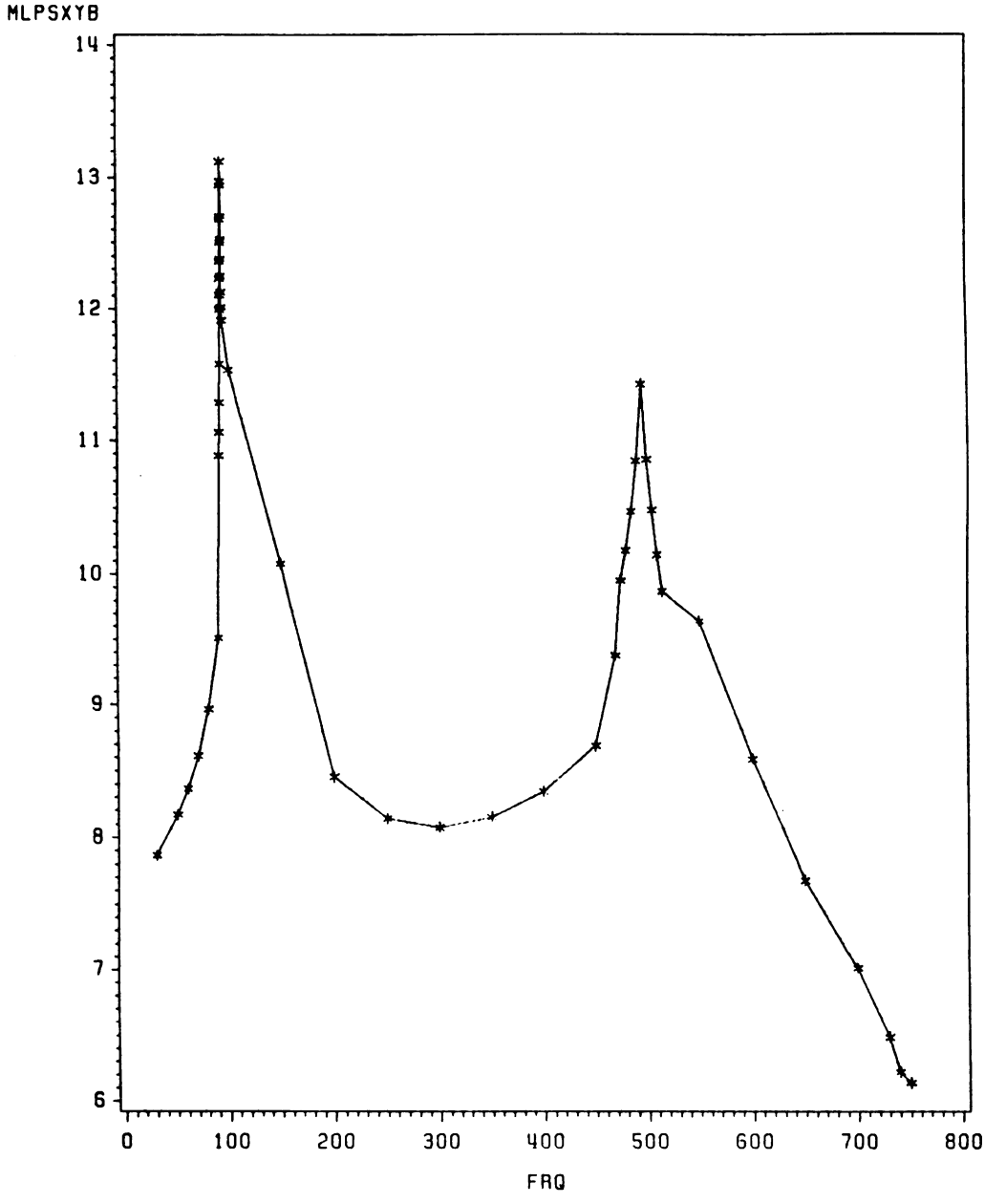

Figure 6.17 Log Shear stress PSD of Element #511

Table 6.1 FRF & PSD of Y112 & Y106 at Zero Phase Angle

Frequency (Hz)	Disp. PSD Input ((m**2)/Hz)	FRF(Y112) (m)	PSD(Y112) ((m**2)/Hz)	FRF(Y106) (m)	PSD(106) ((m**2)/Hz)
20.000	0.300761E-07	1.07442	0.347193E-07	1.02427	0.315539E-07
30.000	0.689996E-08	1.17843	0.958195E-08	1.05798	0.772331E-08
40.000	0.242774E-08	1.34940	0.442062E-08	1.11295	0.300716E-08
50.000	0.107977E-08	1.62767	0.286063E-08	1.20155	0.155889E-08
60.000	0.556965E-09	2.10538	0.246881E-08	1.35201	0.101810E-08
70.000	0.327901E-09	3.03939	0.302912E-08	1.64301	0.885164E-09
80.000	0.207222E-09	5.49795	0.626379E-08	2.40168	0.119526E-08
90.000	0.138240E-09	26.2193	0.950332E-07	8.75346	0.105924E-07
90.500	0.135632E-09	32.1081	0.139828E-06	10.5570	0.151163E-07
91.000	0.133088E-09	41.3269	0.227303E-06	13.3803	0.238271E-07
91.500	0.130605E-09	57.6845	0.434589E-06	18.3895	0.441672E-07
92.000	0.128182E-09	93.4052	0.111833E-05	29.3279	0.110252E-06
92.100	0.127704E-09	105.767	0.142860E-05	33.1134	0.140027E-06
92.200	0.127229E-09	121.041	0.186401E-05	37.7903	0.181696E-06
92.300	0.126756E-09	139.477	0.246590E-05	43.4359	0.239147E-06
92.400	0.126285E-09	159.312	0.320514E-05	49.5094	0.309547E-06
92.500	0.125816E-09	170.234	0.364610E-05	52.8539	0.351473E-06
92.600	0.125350E-09	135.955	0.231694E-05	42.3575	0.224898E-06
92.700	0.124886E-09	8.48614	0.899359E-08	3.32535	0.138099E-08
92.800	0.124424E-09	-126.805	0.200067E-05	-38.1020	0.180634E-06
92.900	0.123964E-09	-169.212	0.354945E-05	-51.0875	0.323539E-06
93.000	0.123507E-09	-160.832	0.319473E-05	-48.5212	0.290773E-06
93.100	0.123051E-09	-141.378	0.245951E-05	-42.5642	0.222933E-06
93.200	0.122598E-09	-122.791	0.184850E-05	-36.8727	0.166684E-06
93.300	0.122147E-09	-107.287	0.140598E-05	-32.1251	0.126059E-06
93.400	0.121698E-09	-94.7179	0.109181E-05	-28.2762	0.973033E-07
93.500	0.121252E-09	-84.5192	0.866161E-06	-25.1532	0.767139E-07
94.000	0.119049E-09	-54.1986	0.349706E-06	-15.8684	0.299772E-07
100.00	0.962436E-10	-10.0487	0.971825E-08	-2.34453	0.529035E-09
150.00	0.190111E-10	-1.58790	0.479351E-10	0.299723	0.170784E-11
200.00	0.601522E-11	-1.13014	0.768270E-11	0.526317	0.166627E-11

Table 6.1 FRF & PSD of Y112 & Y106 at Zero Phase Angle (cont'd)

Frequency (Hz)	Disp. PSD Input ((m**2)/Hz)	FRF(Y112) (m)	PSD(Y112) ((m**2)/Hz)	FRF(Y106) (m)	PSD(106) ((m**2)/Hz)
250.00	0.246384E-11	-1.07367	0.284020E-11	0.678839	0.113539E-11
300.00	0.118819E-11	-1.18865	0.167879E-11	0.866184	0.891470E-12
350.00	0.641357E-12	-1.50136	0.144568E-11	1.16953	0.877255E-12
400.00	0.375951E-12	-2.25959	0.191952E-11	1.80367	0.122305E-11
450.00	0.234705E-12	-5.04160	0.596566E-11	4.01117	0.377629E-11
469.80	0.197570E-12	-9.82071	0.190549E-10	7.75810	0.118914E-10
474.80	0.189378E-12	-12.7707	0.308857E-10	10.0665	0.191904E-10
479.80	0.181607E-12	-17.8450	0.578314E-10	14.0350	0.357730E-10
484.80	0.174230E-12	-25.9513	0.117339E-09	20.3730	0.723155E-10
489.80	0.167224E-12	-0.604351	0.610768E-13	0.567531	0.538613E-13
494.80	0.160566E-12	25.9149	0.107833E-09	-20.1540	0.652195E-10
499.80	0.154237E-12	18.0096	0.500262E-10	-13.9732	0.301148E-10
504.80	0.132975E-12	12.9667	0.223579E-10	-10.0293	0.133755E-10
509.80	0.114296E-12	10.0261	0.114894E-10	-7.72826	0.682645E-11
514.80	0.983862E-13	8.15322	0.654022E-11	-6.26167	0.385758E-11
550.00	0.356282E-13	3.55906	0.451298E-12	-2.65034	0.250263E-12
600.00	0.936367E-14	2.07108	0.401643E-13	-1.45559	0.198393E-13
650.00	0.273892E-14	1.54410	0.653025E-14	-1.00736	0.277939E-14
700.00	0.877595E-15	1.30096	0.148533E-14	-0.773653	0.525276E-15
730.00	0.460683E-15	1.22155	0.687426E-15	-0.680367	0.213250E-15
740.00	0.373814E-15	1.20278	0.540784E-15	-0.654222	0.159995E-15
750.00	0.304177E-15	1.18731	0.428798E-15	-0.630055	0.120749E-15

Table 6.2 FRF & PSD of Y112 & Y106 at 90 Deg. Phase Angle

Frequency (Hz)	Disp. PSD Input ((m**2)/Hz)	FRF(Y112) (m)	PSD(Y112) ((m**2)/Hz)	FRF(Y106) (m)	PSD(106) ((m**2)/Hz)
20.000	0.300761E-07	-0.309190E-03	0.287524E-14	-0.100565E-03	0.304170E-15
30.000	0.689996E-08	-0.807061E-03	0.449428E-14	-0.260710E-03	0.468990E-15
40.000	0.242774E-08	-0.177594E-02	0.765704E-14	-0.568591E-03	0.784880E-15
50.000	0.107977E-08	-0.373813E-02	0.150883E-13	-0.118445E-02	0.151482E-14
60.000	0.556965E-09	-0.819525E-02	0.374070E-13	-0.256844E-02	0.367424E-14
70.000	0.327901E-09	-0.208323E-01	0.142304E-12	-0.646179E-02	0.136915E-13
80.000	0.207222E-09	-0.787292E-01	0.128442E-11	-0.242192E-01	0.121550E-12
90.000	0.138240E-09	-1.99109	0.548041E-09	-0.609837	0.514114E-10
90.500	0.135632E-09	-3.00698	0.122638E-08	-0.920916	0.115028E-09
91.000	0.133088E-09	-5.03138	0.336910E-08	-1.54081	0.315963E-09
91.500	0.130605E-09	-9.98757	0.130281E-07	-3.05844	0.122169E-08
92.000	0.128182E-09	-27.7786	0.989113E-07	-8.50622	0.927470E-08
92.100	0.127704E-09	-36.6889	0.171900E-06	-11.2347	0.161185E-07
92.200	0.127229E-09	-50.3474	0.322507E-06	-15.4170	0.302403E-07
92.300	0.126756E-09	-72.4042	0.664500E-06	-22.1710	0.623074E-07
92.400	0.126285E-09	-109.901	0.152529E-05	-33.6529	0.143020E-06
92.500	0.125816E-09	-174.819	0.384517E-05	-53.5315	0.360542E-06
92.600	0.125350E-09	-272.511	0.930879E-05	-83.4458	0.872837E-06
92.700	0.124886E-09	-339.879	0.144265E-04	-104.075	0.135270E-05
92.800	0.124424E-09	-283.033	0.996734E-05	-86.6678	0.934586E-06
92.900	0.123964E-09	-183.911	0.419289E-05	-56.3156	0.393146E-06
93.000	0.123507E-09	-115.606	0.165065E-05	-35.4000	0.154774E-06
93.100	0.123051E-09	-75.9523	0.709853E-06	-23.2575	0.665599E-07
93.200	0.122598E-09	-52.6846	0.340292E-06	-16.1327	0.319079E-07
93.300	0.122147E-09	-38.3298	0.179456E-06	-11.7371	0.168270E-07
93.400	0.121698E-09	-28.9967	0.102325E-06	-8.87922	0.959476E-08
93.500	0.121252E-09	-22.6407	0.621537E-07	-6.93296	0.582808E-08
94.000	0.119049E-09	-8.95481	0.954640E-08	-2.74221	0.895219E-09
100.00	0.962436E-10	-0.310714	0.929168E-11	-0.953303E-01	0.874649E-12
150.00	0.190111E-10	-0.733896E-02	0.102394E-14	-0.275964E-02	0.144781E-15
200.00	0.601522E-11	-0.190447E-02	0.218173E-16	-0.175273E-02	0.184792E-16

Table 6.2 FRF & PSD of Y112 & Y106 at 90 Deg. Phase Angle (cont'd)

Frequency (Hz)	Disp. PSD Input ((m**2)/Hz)	FRF(Y112) (m)	PSD(Y112) ((m**2)/Hz)	FRF(Y106) (m)	PSD(106) ((m**2)/Hz)
250.00	0.246384E-11	0.142881E-02	0.502994E-17	-0.621568E-02	0.951895E-16
300.00	0.118819E-11	0.925350E-02	0.101742E-15	-0.106464E-01	0.134676E-15
350.00	0.641357E-12	0.252041E-01	0.407419E-15	-0.223260E-01	0.319684E-15
400.00	0.375951E-12	0.760386E-01	0.217370E-14	-0.616981E-01	0.143112E-14
450.00	0.234705E-12	0.447093	0.469157E-13	-0.351583	0.290121E-13
469.80	0.197570E-12	1.80781	0.645694E-12	-1.41499	0.395576E-12
474.80	0.189378E-12	3.16210	0.189357E-11	-2.47337	0.115853E-11
479.80	0.181607E-12	6.67778	0.809833E-11	-5.22085	0.495010E-11
484.80	0.174230E-12	19.5028	0.662696E-10	-15.2435	0.404845E-10
489.80	0.167224E-12	53.7407	0.482953E-09	-42.0001	0.294984E-09
494.80	0.160566E-12	20.1156	0.649713E-10	-15.7225	0.396912E-10
499.80	0.154237E-12	7.00695	0.757260E-11	-5.47816	0.462867E-11
504.80	0.132975E-12	3.37953	0.151874E-11	-2.64339	0.929164E-12
509.80	0.114296E-12	1.96969	0.443432E-12	-1.54164	0.271641E-12
514.80	0.983862E-13	1.28754	0.163100E-12	-1.00857	0.100080E-12
550.00	0.356282E-13	0.238290	0.202304E-14	-0.188834	0.127044E-14
600.00	0.936367E-14	0.743867E-01	0.518127E-16	-0.612913E-01	0.351758E-16
650.00	0.273892E-14	0.348135E-01	0.331950E-17	-0.312153E-01	0.266879E-17
700.00	0.877595E-15	0.180764E-01	0.286758E-18	-0.194237E-01	0.331098E-18
730.00	0.460683E-15	0.116950E-01	0.630095E-19	-0.155116E-01	0.110844E-18
740.00	0.373814E-15	0.986543E-02	0.363821E-19	-0.145059E-01	0.786587E-19
750.00	0.304177E-15	0.813337E-02	0.201219E-19	-0.136153E-01	0.563870E-19

Table 6.3
FRF & PSD of Longitudinal Stress (SX(I)) at Node #101 & Circumferential Stress (SY(J)) at Node #102 (SY(J) at Zero Phase Angle

Frequency (Hz)	Disp. PSD Input ((m**2)/Hz)	FRF(SX(I)) (m)	PSD(SX(I)) ((pascal**2)/Hz)	FRF(SY(J)) (m)	PSD(SY(J)) ((pascal**2)/Hz)
20.000	0.300761E-07	-0.582003E+10	0.101876E+13	0.446674E+09	0.600072E+10
30.000	0.689996E-08	-0.138813E+11	0.132956E+13	0.105933E+10	0.774304E+10
40.000	0.242774E-08	-0.269827E+11	0.176755E+13	0.204258E+10	0.101289E+11
50.000	0.107977E-08	-0.480102E+11	0.248884E+13	0.359600E+10	0.139627E+11
60.000	0.556965E-09	-0.835509E+11	0.388803E+13	0.617510E+10	0.212381E+11
70.000	0.327901E-09	-0.151961E+12	0.757192E+13	0.110494E+11	0.400333E+11
80.000	0.207222E-09	-0.329556E+12	0.225057E+14	0.234972E+11	0.114411E+12
90.000	0.138240E-09	-0.181201E+13	0.453895E+15	0.126218E+12	0.220228E+13
90.500	0.135632E-09	-0.223279E+13	0.676175E+15	0.155330E+12	0.327248E+13
91.000	0.133088E-09	-0.289144E+13	0.111268E+16	0.200896E+12	0.537134E+13
91.500	0.130605E-09	-0.406003E+13	0.215288E+16	0.281732E+12	0.103665E+14
92.000	0.128182E-09	-0.661180E+13	0.560359E+16	0.458235E+12	0.269156E+14
92.100	0.127704E-09	-0.749490E+13	0.717361E+16	0.519317E+12	0.344406E+14
92.200	0.127229E-09	-0.858594E+13	0.937911E+16	0.594781E+12	0.450090E+14
92.300	0.126756E-09	-0.990297E+13	0.124308E+17	0.685875E+12	0.596290E+14
92.400	0.126285E-09	-0.113198E+14	0.161819E+17	0.783873E+12	0.775966E+14
92.500	0.125816E-09	-0.121000E+14	0.184209E+17	0.837839E+12	0.883199E+14
92.600	0.125350E-09	-0.965142E+13	0.116763E+17	0.668483E+12	0.560151E+14
92.700	0.124886E-09	-0.545939E+12	0.372222E+14	0.387034E+11	0.187073E+12
92.800	0.124424E-09	0.911831E+13	0.103451E+17	-0.629723E+12	0.493405E+14
92.900	0.123964E-09	0.121476E+14	0.182926E+17	-0.839241E+12	0.873112E+14
93.000	0.123507E-09	0.115489E+14	0.164730E+17	-0.797832E+12	0.786164E+14
93.100	0.123051E-09	0.101592E+14	0.127001E+17	-0.701712E+12	0.605905E+14
93.200	0.122598E-09	0.883150E+13	0.956209E+16	-0.609878E+12	0.456005E+14
93.300	0.122147E-09	0.772397E+13	0.728727E+16	-0.533273E+12	0.347363E+14
93.400	0.121698E-09	0.682608E+13	0.567058E+16	-0.471169E+12	0.270170E+14
93.500	0.121252E-09	0.609753E+13	0.450812E+16	-0.420776E+12	0.214679E+14
94.000	0.119049E-09	0.393150E+13	0.184011E+16	-0.270953E+12	0.874005E+13
100.00	0.962436E-10	0.776154E+12	0.579787E+14	-0.525858E+11	0.266139E+12
150.00	0.190111E-10	0.153813E+12	0.449771E+12	-0.818901E+10	0.127488E+10

Table 6.3
FRF & PSD of Longitudinal Stress (SX(I)) at Node #101 & Circumferential Stress (SY(J)) at Node #102 (SY(J) at Zero Phase Angle (cont'd)

Frequency (Hz)	Disp. PSD Input ((m**2)/Hz)	FRF(SX(I)) (m)	PSD(SX(I)) ((pascal**2)/Hz)	FRF(SY(J)) (m)	PSD(SY(J)) ((pascal**2)/Hz)
200.00	0.601522E-11	0.924101E+11	0.513678E+11	-0.228658E+10	0.314504E+08
250.00	0.246384E-11	0.434922E+11	0.466051E+10	0.336334E+10	0.278710E+08
300.00	0.118819E-11	-0.205988E+11	0.504165E+09	0.102714E+11	0.125356E+09
350.00	0.641357E-12	-0.125857E+12	0.101591E+11	0.197379E+11	0.249862E+09
400.00	0.375951E-12	-0.344262E+12	0.445564E+11	0.350465E+11	0.461764E+09
450.00	0.234705E-12	-0.109499E+13	0.281411E+12	0.748950E+11	0.131652E+10
469.80	0.197570E-12	-0.236201E+13	0.110226E+13	0.134012E+12	0.354822E+10
474.80	0.189378E-12	-0.314162E+13	0.186912E+13	0.169382E+12	0.543330E+10
479.80	0.181607E-12	-0.448142E+13	0.364722E+13	0.229642E+12	0.957708E+10
484.80	0.174230E-12	-0.662074E+13	0.763721E+13	0.325423E+12	0.184509E+11
489.80	0.167224E-12	0.612007E+11	0.626340E+09	0.294230E+11	0.144767E+09
494.80	0.160566E-12	0.705223E+13	0.798558E+13	-0.280294E+12	0.126148E+11
499.80	0.154237E-12	0.496590E+13	0.380350E+13	-0.186835E+12	0.538396E+10
504.80	0.132975E-12	0.363431E+13	0.175636E+13	-0.126886E+12	0.214089E+10
509.80	0.114296E-12	0.285706E+13	0.932977E+12	-0.915462E+11	0.957881E+09
514.80	0.983862E-13	0.236134E+13	0.548596E+12	-0.686995E+11	0.464345E+09
550.00	0.356282E-13	0.113619E+13	0.459934E+11	-0.811488E+10	0.234616E+07
600.00	0.936367E-14	0.721842E+12	0.487900E+10	0.201251E+11	0.379245E+07
650.00	0.273892E-14	0.556792E+12	0.849112E+09	0.387267E+11	0.410770E+07
700.00	0.877595E-15	0.460795E+12	0.186341E+09	0.559562E+11	0.274783E+07
730.00	0.460683E-15	0.416996E+12	0.801060E+08	0.666423E+11	0.204598E+07
740.00	0.373814E-15	0.403659E+12	0.609095E+08	0.703305E+11	0.184903E+07
750.00	0.304177E-15	0.390763E+12	0.464466E+08	0.740978E+11	0.167008E+07

Table 6.4
FRF & PSD of Longitudinal Stress (SX(I)) at Node #101 & Circumferential Stress (SY(J)) at Node #102 (SY(J) at 90 Deg. Phase Angle

Frequency (Hz)	Disp. PSD Input ((m**2)/Hz)	FRF(SX(I)) (m)	PSD(SX(I)) ((pascal**2)/Hz)	FRF(SY(J)) (m)	PSD(SY(J)) ((pascal**2)/Hz)
20.000	0.300761E-07	0.240848E+08	0.174465E+08	-0.184077E+07	101910.
30.000	0.689996E-08	0.622588E+08	0.267453E+08	-0.470742E+07	152902.
40.000	0.242774E-08	0.135265E+09	0.444197E+08	-0.100828E+08	246810.
50.000	0.107977E-08	0.280515E+09	0.849652E+08	-0.205593E+08	456401.
60.000	0.556965E-09	0.605388E+09	0.204125E+09	-0.435688E+08	0.105725E+07
70.000	0.327901E-09	0.151612E+10	0.753717E+09	-0.107213E+09	0.376910E+07
80.000	0.207222E-09	0.566159E+10	0.664219E+10	-0.394707E+09	0.322837E+08
90.000	0.138240E-09	0.142279E+12	0.279843E+13	-0.984476E+10	0.133981E+11
90.500	0.135632E-09	0.214848E+12	0.626077E+13	-0.148641E+11	0.299667E+11
91.000	0.133088E-09	0.359458E+12	0.171963E+14	-0.248660E+11	0.822911E+11
91.500	0.130605E-09	0.713495E+12	0.664880E+14	-0.493531E+11	0.318120E+12
92.000	0.128182E-09	0.198436E+13	0.504741E+15	-0.137253E+12	0.241473E+13
92.100	0.127704E-09	0.262086E+13	0.877188E+15	-0.181276E+12	0.419650E+13
92.200	0.127229E-09	0.359652E+13	0.164570E+16	-0.248758E+12	0.787300E+13
92.300	0.126756E-09	0.517211E+13	0.339081E+16	-0.357734E+12	0.162214E+14
92.400	0.126285E-09	0.785062E+13	0.778322E+16	-0.542993E+12	0.372340E+14
92.500	0.125816E-09	0.124879E+14	0.196209E+17	-0.863734E+12	0.938636E+14
92.600	0.125350E-09	0.194664E+14	0.475002E+17	-0.134640E+13	0.227233E+15
92.700	0.124886E-09	0.242787E+14	0.736146E+17	-0.167924E+13	0.352160E+15
92.800	0.124424E-09	0.202180E+14	0.508606E+17	-0.139839E+13	0.243309E+15
92.900	0.123964E-09	0.131374E+14	0.213952E+17	-0.908656E+12	0.102352E+15
93.000	0.123507E-09	0.825819E+13	0.842287E+16	-0.571183E+12	0.402940E+14
93.100	0.123051E-09	0.542557E+13	0.362224E+16	-0.375264E+12	0.173285E+14
93.200	0.122598E-09	0.376348E+13	0.173646E+16	-0.260306E+12	0.830716E+13
93.300	0.122147E-09	0.273808E+13	0.915745E+15	-0.189384E+12	0.438095E+13
93.400	0.121698E-09	0.207138E+13	0.522159E+15	-0.143271E+12	0.249806E+13
93.500	0.121252E-09	0.161735E+13	0.317173E+15	-0.111869E+12	0.151741E+13
94.000	0.119049E-09	0.639725E+12	0.487207E+14	-0.442511E+11	0.233117E+12
100.00	0.962436E-10	0.222582E+11	0.476818E+11	-0.154453E+10	0.229596E+09
150.00	0.190111E-10	0.695623E+09	0.919930E+07	-0.602372E+08	68982.1
200.00	0.601522E-11	0.522863E+09	0.164448E+07	-0.587065E+08	20731.2

Table 6.4
FRF & PSD of Longitudinal Stress (SX(I)) at Node #101 & Circumferential Stress (SY(J)) at Node #102 (SY(J) at 90 Deg. Phase Angle (cont'd)

Frequency (Hz)	Disp. PSD Input ((m**2)/Hz)	FRF(SX(I)) (m)	PSD(SX(I)) ((pascal**2)/Hz)	FRF(SY(J)) (m)	PSD(SY(J)) ((pascal**2)/Hz)
250.00	0.246384E-11	0.207738E+10	0.106327E+08	-0.237902E+09	139446.
300.00	0.118819E-11	0.368707E+10	0.161528E+08	-0.370149E+09	162794.
350.00	0.641357E-12	0.773562E+10	0.383786E+08	-0.626771E+09	251952.
400.00	0.375951E-12	0.211397E+11	0.168007E+09	-0.131599E+10	651083.
450.00	0.234705E-12	0.119095E+12	0.332894E+10	-0.577972E+10	0.784036E+07
469.80	0.197570E-12	0.477974E+12	0.451366E+11	-0.217699E+11	0.936340E+08
474.80	0.189378E-12	0.835106E+12	0.132073E+12	-0.376451E+11	0.268378E+09
479.80	0.181607E-12	0.176217E+13	0.563934E+12	-0.788339E+11	0.112865E+10
484.80	0.174230E-12	0.514400E+13	0.461024E+13	-0.229050E+12	0.914074E+10
489.80	0.167224E-12	0.141722E+14	0.335870E+14	-0.630046E+12	0.663807E+11
494.80	0.160566E-12	0.530566E+13	0.451993E+13	-0.236258E+12	0.896247E+10
499.80	0.154237E-12	0.184907E+13	0.527343E+12	-0.827505E+11	0.105616E+10
504.80	0.132975E-12	0.892588E+12	0.105943E+12	-0.402839E+11	0.215791E+09
509.80	0.114296E-12	0.520857E+12	0.310076E+11	-0.237889E+11	0.646816E+08
514.80	0.983862E-13	0.341012E+12	0.114412E+11	-0.158167E+11	0.246130E+08
550.00	0.356282E-13	0.645836E+11	0.148606E+09	-0.365682E+10	476431.
600.00	0.936367E-14	0.218429E+11	0.446751E+07	-0.195466E+10	35775.7
650.00	0.273892E-14	0.120871E+11	400153.	-0.176065E+10	8490.35
700.00	0.877595E-15	0.864432E+10	65577.7	-0.190480E+10	3184.16
730.00	0.460683E-15	0.774406E+10	27627.3	-0.207997E+10	1993.05
740.00	0.373814E-15	0.756586E+10	21397.9	-0.215142E+10	1730.24
750.00	0.304177E-15	0.743883E+10	16832.0	-0.222950E+10	1511.97

Table 6.5 Element Strain Energy at 92.7 Hz

FREQ= 92.700

ELEM	SENE	ELEM	SENE
101	0.27438570E+10	601	0.44908641E+09
102	0.22180856E+10	602	0.38217625E+09
103	0.15437843E+10	603	0.29018490E+09
104	0.10610063E+10	604	0.22204794E+09
105	0.66449536E+09	605	0.16378637E+09
106	0.38202201E+09	606	0.11407774E+09
107	0.19615576E+09	607	75759776.
108	79925565.	608	47661719.
109	24896361.	609	24059206.
110	6316149.8	610	9511527.3
111	1304906.3	611	2071133.1
201	0.21508773E+10	701	0.12449723E+10
202	0.17498046E+10	702	0.10229703E+10
203	0.12172784E+10	703	0.72153123E+09
204	0.84336511E+09	704	0.51219195E+09
205	0.54200672E+09	705	0.34237687E+09
206	0.30968561E+09	706	0.20287275E+09
207	0.16430945E+09	707	0.11691505E+09
208	75732028.	708	61959809.
209	23576036.	709	22727510.
210	7031766.0	710	8528666.6
211	2031765.0	711	2511300.0
301	0.12449723E+10	801	0.21508773E+10
302	0.10229703E+10	802	0.17498046E+10
303	0.72153123E+09	803	0.12172784E+10
304	0.51219195E+09	804	0.84336511E+09
305	0.34237687E+09	805	0.54200672E+09
306	0.20287275E+09	806	0.30968561E+09
307	0.11691505E+09	807	0.16430945E+09
308	61959809.	808	75732028.
309	22727510.	809	23576036.
310	8528666.6	810	7031766.0
311	2511300.0	811	2031765.0
401	0.44908641E+09	901	0.27438570E+10
402	0.38217625E+09	902	0.22180856E+10
403	0.29018490E+09	903	0.15437843E+10
404	0.22204794E+09	904	0.10610063E+10
405	0.16378637E+09	905	0.66449536E+09
406	0.11407774E+09	906	0.38202201E+09
407	75759776.	907	0.19615576E+09
408	47661719.	908	79925565.
409	24059206.	909	24896361.
410	9511527.3	910	6316149.8
411	2071133.1	911	1304906.3
501	0.13517873E+09		
502	0.13031161E+09		
503	0.11914290E+09		
504	0.10794532E+09		
505	93898252.		
506	78038461.		
507	60238084.		
508	41495512.		
509	24143375.		
510	9835193.9		
511	1404949.3		

Table 6.5 Element Strain Energy at 92.7 Hz (cont'd)

FREQ= 92.700

ELEM	SENE	ELEM	SENE
1101	16466161.	1509	800592.28
1102	17660710.	1510	958403.84
1103	9219084.6	1511	2292044.0
1104	6791776.1	1601	4697015.0
1105	4408717.3	1602	5533713.7
1106	2749825.7	1603	2724759.7
1107	1694234.3	1604	2311094.1
1108	1012369.9	1605	1793937.7
1109	818024.68	1606	1445173.9
1110	996687.52	1607	1208601.9
1111	1562312.1	1608	1175797.7
1201	13415452.	1609	1168531.8
1202	14624335.	1610	1324977.0
1203	7474490.4	1611	2456581.6
1204	5569483.6	1701	8821638.0
1205	3829761.7	1702	9864459.3
1206	2306576.1	1703	5027427.9
1207	1487796.6	1704	4141327.1
1208	1075880.2	1705	3140924.3
1209	763495.79	1706	2354942.5
1210	1215218.6	1707	2200864.4
1211	1891134.6	1708	2374357.5
1301	8821638.0	1709	2541642.0
1302	9864459.3	1710	2772207.6
1303	5027427.9	1711	4215093.2
1304	4141327.1	1801	13415452.
1305	3140924.3	1802	14624335.
1306	2354942.5	1803	7474490.4
1307	2200864.4	1804	5569483.6
1308	2374357.5	1805	3829761.7
1309	2541642.0	1806	2306576.1
1310	2772207.6	1807	1487796.6
1311	4215093.2	1808	1075880.2
1401	4697015.0	1809	763495.79
1402	5533713.7	1810	1215218.6
1403	2724759.7	1811	1891134.6
1404	2311094.1	1901	16466161.
1405	1793937.7	1902	17660710.
1406	1445173.9	1903	9219084.6
1407	1208601.9	1904	6791776.1
1408	1175797.7	1905	4408717.3
1409	1168531.8	1906	2749825.7
1410	1324977.0	1907	1694234.3
1411	2456581.6	1908	1012369.9
1501	3075832.8	1909	818024.68
1502	3833505.5	1910	996687.52
1503	1778729.7	1911	1562312.1
1504	1581093.2		
1505	1275456.5		
1506	1069971.5		
1507	857062.57		
1508	815972.63		

Table 6.6 Element Strain Energy at 489.8 Hz

FREQ= 489.80

ELEM	SENE
101	0.87892694E+09
102	0.16274209E+09
103	50530224.
104	0.36303777E+09
105	0.79370255E+09
106	0.10019802E+10
107	0.88152049E+09
108	0.58327277E+09
109	0.26448111E+09
110	74989066.
111	16790159.
201	0.83391395E+09
202	0.31112016E+09
203	0.14829326E+09
204	0.33960818E+09
205	0.64508411E+09
206	0.76229950E+09
207	0.68384480E+09
208	0.52410632E+09
209	0.22150172E+09
210	71188830.
211	33796329.
301	0.80248516E+09
302	0.45699326E+09
303	0.27323550E+09
304	0.32205538E+09
305	0.39737389E+09
306	0.41150157E+09
307	0.40965607E+09
308	0.32554847E+09
309	0.14873681E+09
310	92637412.
311	28141309.
401	0.75421191E+09
402	0.59957976E+09
403	0.41403468E+09
404	0.28558556E+09
405	0.17527996E+09
406	0.12178699E+09
407	0.14781542E+09
408	0.15176708E+09
409	0.14120217E+09
410	90190941.
411	23159574.
501	0.74173705E+09
502	0.65119055E+09
503	0.47354394E+09
504	0.26585673E+09
505	88811555.
506	12336907.
507	35973386.
508	98512774.
509	0.12885195E+09
510	94018135.
511	19156699.
601	0.75421191E+09
602	0.59957976E+09
603	0.41403468E+09
604	0.28558556E+09
605	0.17527996E+09
606	0.12178699E+09
607	0.14781542E+09
608	0.15176708E+09
609	0.14120217E+09
610	90190941.
611	23159574.
701	0.80248516E+09
702	0.45699326E+09
703	0.27323550E+09
704	0.32205538E+09
705	0.39737389E+09
706	0.41150157E+09
707	0.40965607E+09
708	0.32554847E+09
709	0.14873681E+09
710	92637412.
711	28141309.
801	0.83391395E+09
802	0.31112016E+09
803	0.14829326E+09
804	0.33960818E+09
805	0.64508411E+09
806	0.76229950E+09
807	0.68384480E+09
808	0.52410632E+09
809	0.22150172E+09
810	71188830.
811	33796329.
901	0.87892694E+09
902	0.16274209E+09
903	50530224.
904	0.36303777E+09
905	0.79370255E+09
906	0.10019802E+10
907	0.88152049E+09
908	0.58327277E+09
909	0.26448111E+09
910	74989066.
911	16790159.

Table 6.6 Element Strain Energy at 489.8 Hz (cont'd)

FREQ= 489.80

ELEM	SENE
1101	13565721.
1102	7606092.3
1103	8705640.6
1104	13838010.
1105	16098532.
1106	17010219.
1107	16398053.
1108	11078942.
1109	7799342.7
1110	8903461.4
1111	14878805.
1201	12908484.
1202	9640235.2
1203	9705129.3
1204	15580193.
1205	15956155.
1206	16527498.
1207	17049242.
1208	11633178.
1209	7019841.0
1210	8299627.9
1211	20090587.
1301	13935445.
1302	15962779.
1303	20561480.
1304	30121199.
1305	39568398.
1306	37177364.
1307	23985518.
1308	11466070.
1309	4521408.0
1401	12194359.
1402	14021203.
1403	13663064.
1404	15756389.
1405	19414811.
1406	17469352.
1407	10962291.
1408	5935371.4
1409	3148975.8
1410	6122225.3
1411	22888458.
1501	11517001.
1502	12884900.
1503	12251678.
1504	12977347.
1505	16775354.
1506	15349276.
1507	8619943.4
1508	4557642.7
1509	1693652.3
1510	4148872.8
1511	26686013.

ELEM	SENE
1601	12194359.
1602	14021203.
1603	13663064.
1604	15756389.
1605	19414811.
1606	17469352.
1607	10962291.
1608	5935371.4
1609	3148975.8
1610	6122225.3
1611	22888458.
1701	13935445.
1702	15962779.
1703	20561480.
1704	30121199.
1705	39568398.
1706	37177364.
1707	23985518.
1708	11466070.
1709	4521408.0
1710	11904620.
1711	36582893.
1801	12908484.
1802	9640235.2
1803	9705129.3
1804	15580193.
1805	15956155.
1806	16527498.
1807	17049242.
1808	11633178.
1809	7019841.0
1810	8299627.9
1811	20090587.
1901	13565721.
1902	7606092.3
1903	8705640.6
1904	13838010.
1905	16098532.
1906	17010219.
1907	16398053.
1908	11078942.
1909	7799342.7
1910	8903461.4
1911	14878805.

7.0 Summary and Conclusions

In the study, a methodology has been developed to deal with the random vibration of a general class of composite viscoelastic structures with frequency-dependent material properties as represented by the example of solid rocket motors. The method combines the finite element method, structural dynamics, strain energy approach , random vibration analysis concepts, and computing power. This combination is a powerful tool capable of treating more sophisticated structural dynamics problems with complicated geometry, nonhomogeneous materials, and frequency-dependent stiffness and damping properties. Most researchers in the area of random vibration analysis and experiments are not aware of the importance of finite element methods for random structural vibration analysis, thus are not prepared to tap the power of this method effectively. Most research has been concerned with simple discrete systems with small numbers of degrees of freedom or continuous random sturctural dynamics problems with simple geometry, homogeneous elastic material, and simple viscous damping mechanism.

The strain energy ratio between different materials of the rocket model has been obtained around natural frequencies, and then the strain energy approach has been used to calculate the frequency-dependent equivalent viscoelastic damping which is in turn judiciously represented by a combination of viscous damping and stuctural damping to accommodate this frequency dependent viscoelastic property. In this study, due to the more realistic 3-D rocket motor modeling, the vibration mode shapes include ring mode and axial modes in addition to the usual bending modes. As discussed in Chapter 6, the damping effect of 3-D finite element rocket model is higher than that of the Euler beam model, especially for higher modes, due to the higher propellant/steel casing strain energy ratio than the beam model can predict. The frequency-dependent stiffness matrix can be updated as deemed necessary. Usually good results can be obtained by updating this matrix at each significant natural frequency for a given structural configuration and excitation condition.

Modal analysis data together with half power band width calculated at each natural frequency are useful guides in the harmonic analysis in order to achieve computational efficiency. On one hand, the technique used in this investigation has a hybrid sense in that it makes use of the best features and capabilities of both modal analysis and harmonic analysis to achieve the goals of random vibration analysis

in addition to the finite element technique. On the other hand, vibration experiments and computational power are merged in this study to establish a useful tool for analysis.

The experimental part of this study makes use of a computer-aided dynamic mechanical analysis system and the time-temperature superposition principle to obtain the dynamic properties of viscoelastic materials for a wider range of temperatures and frequencies. This microcomputer-based testing system together with the data processing capability of mainframe computers, is a useful combination for sophisticated dynamic testing. Microcomputer systems will play an even more prominent role in future engineering analyses and experiments, as more dramatic improvements in its power are to be achieved [62,63,64].

Like many other testing techniques, the dynamic mechanical analyzer does not measure the desired dynamic viscoelastic properties directly. Rather, through the simulated mathematical model, system characteristics, frequency and energy signals, it obtains the dynamic properties through sophisticated calculations.

The experiments require special attention. When carrying out a temperature sweep, the rate should be slow enough to allow time for a reasonably consistent temperature to develop be-

tween the sample surface and internal points. Prolonged vibration testing with relatively large displacements may result some fatigue effect, and hurt data consistency. For some materials, moisture content in the sample may play a siginicant role, thus another parameter may have to be considered. In order to maintain data quality, test data from the DMA should not be extended too far beyond the test frequency by time-temperature superposition principle. On the other hand, a methodology combining the sandwich beam technique [17,65], support excitation technique, strain energy approach, finite element procedure, and computing power has been devised to obtain viscoelastic material data at relatively higher frequencies. The results agree reasonably with the data from the dynamic mechanical analyzer and time-temperature superposition principle.

Displacement power spectra have been calculated for several significant points of the rocket model as discussed in Chapter 6. Additionally, the associated acceleration power spectra were also calculated. The stress power spectra at several significant points have been obtained together with their root mean square stress levels. The stress power spectra can later be used for structural fatigue failure analysis, first passage analysis, and design modification [66] to redistribute the critical stresses induced. Some of the calculated stresses may be comparable to stress levels

due to the rocket motor internal pressure in flight. Similar response acceleration PSD near the electronic, control, or detection compartment of a missile can also be calculated before a real physical rocket model is constructed and tested. The reponse data can be used as random vibration criteria for selecting or designing these sensitive and critical parts, or used as random vibration input on a laboratory shaker to test these parts independently, thus to accelerate the interactive design cycle, and to enhance and economize the whole test strategy.

References

1. Du Pont Co., "Du Pont 982 Dynamic Mechanical Analyzer, Operator's Manual", 1983.

2. Heller, R. A., Thakker, A. B and Arthur, C. E., "Temperature Dependence of the Complex Modulus for Fiber-Reinforced Materials", Reprint from ASTM Special Publication No.580, 1975.

3. Read, B. E. and Dean, G. E., "The Determination of Dynamic Properties of Polymers and Composites", John Wiley & Sons, 1978.

4. Du Pont Co., "Du Pont 982 Dynamic Mechanical Analyzer", E-42397.

5. Du Pont Co., "DMA Standard Data Analysis Program", Dec., 1984.

6. Ferry, J. D., "Viscoelastic Properties of Polymers", Third Edition, John Wiley & Sons, 1980.

7. Snowdon, J. C., "Vibration and Shock in Damped Mechanical Systems", John Wiley & Sons, 1968.

8. SAS Institute Inc., "SAS Users' Guide: Basics", 1985.

9. SAS Institute Inc., "SAS User's Guide: Statistics", 1985.

10. SAS Institute Inc., "SAS/Graph User's Guide", 1985.

11. Heller, R. A. and Singh, M. P., "Random probability Techniques for Rocket Motor Service Life Prediction - Part I: Transportation Stresses in Rocket Motors", Virginia Tech, VPI-1-81.25, 1981.

12. Leaderman, H., "Reology-Theory and Applications", Academic Press, 1958.

13. Flugge, W., "Viscoelasticity", 2nd ed., Springer-Verlag, 1974.

14. Christensen, R. M., "Theory of Viscoelasticity", Academic Press, 1981.

15. Lear, J. D. and Gill, P. S., "Theory of Operation of the Du Pont 982 Dynamic Mechanical Analyzer", Du Pont Co.

16. Gill, P. S., Lear, J. D. and Leckenby, J. N., "Recent developments in Polymer Characterization by Dynamic Mechanical Analysis" in "Measurement Techniques for Polymeric Solids" edited by Brown, R. P. and Read, B. E., Elsevier Applied Science Publishers, 1984.

17. Nicholas, T. and Heller, R. A., "Determination of the Complex Modulus of a Filled Elastomer from a Vibrating Sandwich Beam", Experimental Mechanics, March, 1967.

18. Johnson, C. D. and Kienholz, A., "Finite Element Prediction of Damping in Beams with Constrained Viscoelastic Layers", Shock and Vibration Bulletin, Proc. 51, 1980.

19. Ungar, E. E. and Kerwin, B. M., Jr., "Loss Factors of Viscoelastic Systems in Terms of Energy Concepts", Journal of Acoust. Soc. of Am., Vol. 34, pp. 954, 1962.

20. Soni, M. L., "Finite Element Analysis of Viscoelastically Damped Sandwich Structures", Shock and Vibration Bulletin, Proc. 52, 1981.

21. Soni, M. L. and Boyner, F. K., "Finite Element Vibration Analysis of Damped Structures", AIAA Journal, 20 (5), 1982.

22. Nakra, B. C., "Vibration Control with Viscoelastic Materials-III", Shock and Vibration Digest, May, 1984.

23. Nakra, B. C., "Vibration Control with Viscoelastic Materials-II", Shock and Vibration Digest, Jan., 1981.

24. Nakra, B. C., "Vibration Control with Viscoelastic Materials-I", Shock and Vibration Digest, June, 1976.

25. Thomson, W. T., "Theory of Vibration with Application", 1981

26. Meirovitch, L., "Analytical Methods in Vibrations", MacMillan Co., 1967.

27. Steidel, R. F. Jr., "Introduction to Mechanical Vibrations", John Wiley & Sons, 1971.

28. Curtis, A. J., Tintling, N. G. and Abstein, H. R., "Selection and Performance of Vibration Tests" Shock and Vibration Info. Center, 1972.

29. Pilkey, W. and Pilkey, B., Editors,"Shock and Vibration Computer Programs - Reviews and Summaries", Shock and Vibration Information Center, 1975.

30. Gorman, D. J., "Free Vibration Analysis of Beams and Shafts", John Wiley, 1975.

31. Rieger, N. F., "The literature of Vibration Engineering", Shock and Vibration Digest, Jan., 1982.

32. Crandall, S. H., "Random Vibration", Applied Mechanics Review, 12, pp 739-742, 1959.

33. Crandall, S. H., "Random Vibration in Mechanical Systems", Academic Press, 1963.

34. Roberson, J. D., "An Introduction to Random Vibration" Edingburg University Press, 1963.

35. Lin, Y. K., "Probabilistic Theory of Structural Dynamics", Krieger, 1977.

36. Newland, D. E., "An Introduction to Random Vibration and Spectral Analysis", Longmans, London, 1975.

37. Elishakoff, I., "Probabilistic Methods in the Theory of Structures", 1983.

38. Shin, Y. S. and Au-Yang, M. K., editors, "Random Fatigue Life Prediction", PVP-72, ASME, 1983.

39. Bolotin, V. V., "Random Vibrations of Elastic Systems", Martinus Nijhoff Publishers, 1984.

40. Huang, T. C. and Spanos, P. D., editors, "Random Vibration" AMD-65, ASME, 1984.

41. Turner, M., Clough, R., Martin, H. and Topp, L., " Stiffness and Deflection Analysis of Complex Structures", Journal of Aeronautical Sci. ,23, pp. 805-823, 1956.

42. Zienkiwicz, O. C., "The Finite Element Method", McGraw-Hill, 1977.

43. Desai, C. S., and Abel, J. F., "Introduction to the Finite Element method", Van Nostrand, 1972.

44. Pilkey, W., Saczalski, K. and Schaeffer, H., eds., "Structural Mechanics Computer Programs, Surveys, Assessments and Availability", Univ. Press of Virginia, 1974.

45. Batoz, J. L., Bathe, K. J., and Ho, L. W., " A study of Three-Node Trigular Plate Bending Elements", Int. Journal for Numerical Methods in Engineering, 15, pp. 1771-1812, 1980.

46. Wilson, E. L., Taylor, R. L., Doherty, W. P. and Ghaboussi, J., "Incompatible Displacement Model", Numerical and Computer methods in Structural Mechanics, edited by Fenves, S. J., et. al., Academic Press, 1973.

47. Irons, B. M., "A Frontal Solution Program for Finite Element Analysis", Int. Journal for numerial Methods in Engineering, 2-1, pp. 5-32, Jan., 1970.

48. NASA'S Computer Software Management and Information Center (COSMIC), "COSMIC Software Catalog", 1986 edition.

49. Engineering Information, Inc., "Engineering & Industrial Software Directory", 1985.

50. IMSL ,INC., "International Mathematics Subroutine Library".

51. Kohnke, P. C., "ANSYS Engineering Analysis System - Theoretical manual", Swanson Analysis Systems, Inc. 1986.

52. DeSalvo, G. J., Swanson, J. A., "ANSYS Engineering Analysis System - Users's manual", Swanson Analysis Systems, Inc. 1986.

53. Clough, R. W. and Penzien, J., "Dynamics of Structures", McGraw-Hill,

54. Lee, H. J. and Heller, R. A., "Determination of the Complex Modulus of a Solid Rocket Propellant", U.S. Army Missile Command, Technical Report, RK-CR-86, 1986.

55. Nashif, A. D., Jones, D. I. G. and Henderson, J. P., "Vibration Damping", John Wiley & Sons, 1985.

56. Du Pont Instruments, "Thermal Analysis Review: Dynamic Mechanical Analysis", E-16368, Wilmington, DE.

57. Heller, R. A., Singh, M. P., Thangjitham, S. and Zibdeh, H., "Random Probability Techniques for Rocket Motor Service Life Predictions" ,US Army Missile Command, Technical Report RK-CR-83, pp. 3-11, sept.,1983.

58. Reddy, J. N., "Introduction to the Finite Element Method", McGraw Hill, 1984.

59. Meirovitch, L., "Computational Methods in Structural Dynamics", Sijthoff & Noordhoff, 1980.

60. Bathe, K. and Wilson, E. L., "Numerical Methods in Finite Element Analysis", Prentice Hall, 1977.

61. Kluensener, M. F., and Drake, M. L., "Damped Structure Design Using Finite Element Method", Shock and Vibration Bulletin, Proc. 52. 1982.

62. Jeffries, R., "The Gigabyte Age", PC, Vol.4, No. 17, pp.95-98, Aug., 1985.

63. Trivette, D. B., "The Making of Microprocessor", LOTUS, Vol.2, No. 3, pp.72-75, March, 1986.

64. Jeffries, R., "On the Threshold of Supercheap Ram", PC, Vol.4, No. 26, pp.92-94, Dec., 1985

65. ASTM Standards E 756-83, "Standard Method for Measuring Vibration-Damping Properties of Materials", 1984.

66. Bogdanoff, J. L. and Kozin, F., "Probabilistic Models of Cumulative Damages", John Wiley, 1985.

APPENDIX A: COMPUTER PROGRAMS

A1. TTSP02 FORTRAN

```
C
C  FOR DMADATA 92,90,89,87,83 OF TPH8208 BY POINTWISE TIME-TEMP
C  SUPERPOSITION PRINCIPLE.
C
C
      DIMENSION TA(91),FRQ(91),E1(91),E2NEW(91),FRQNEW(91),E1NEW(91),
     $          TB(11),E2(91)
C
C
      READ(7,20) (TA(I),FRQ(I),E1(I),E2(I), I=1,91)
   20 FORMAT(91(4F10.6/))
      WRITE(8,30) (TA(I),FRQ(I),E1(I),E2(I),I=1,91)
   30 FORMAT(91(4(F10.6,5X)/))
C
C
      TB(1)= -20.
      TB(2)= -10.
      TB(3)=  0.0
      TB(4)=  10.
      TB(5)=  20.
      TB(6)=  30.
      TB(7)=  40.
      TB(8)=  50.
      TB(9)=  60.
      TB(10)= 70.
      TB(11)= 80.
C
      WRITE(8,40)
   40 FORMAT('C',/,'C',16X,'TB',15X,'FREQNEW',12X,'E1NEW',10X,
     $'E2NEW'/,'C')

      DO 90 J = 1,11
      DO 80 I = 1   , 91
C
C     TB IS THE TARGET TEMP.   E1NEW AND E2NEW IN MEGAPASCAL.
C
C
      E1NEW(I) = E1(I)*(TB(J)+273.)/(TA(I)+273.) * 1000.
      E2NEW(I) = E2(I)*(TB(J)+273.)/(TA(I)+273.) * 1000.
      AT =10.**((-20.5*(TA(I)+28.89 )/(206.7+(TA(I)+28.89)+0.01325*(TA(
     $    I)+28.89)**2))
     $    + ( 20.5*(TB(J)+28.89 )/(206.7+(TB(J)+28.89)+0.01325*(TB(
     $    J)+28.89)**2)))
```

```
      FRQNEW(I)=FRQ(I)*AT
      IF(FRQNEW(I) .GT. 5000.  .OR. FRQNEW(I) .LT. 1.0) GO TO 80
C
      WRITE(8,50) TB(J),FRQNEW(I),E1NEW(I),E2NEW(I)
   80 CONTINUE
   90 CONTINUE
C
   50 FORMAT(10X,4(F15.3))
      STOP
      END
```

A2. FIG35 SAS

COMMENT: E1 at constant temperature.

```
//xxxxxxx JOB xxxxxxxxxx,REGION=1500K
/*PRIORITY     STANDARD
/*JOBPARM      ACCTPG
//STEP1 EXEC   SASV
//SYSIN     DD *
GOPTIONS DEVICE = VPISASGV;
OPTIONS LINESIZE = 72;
PROC FORMAT;
      VALUE  CC  273 = 'TEMP273'
                 293 = 'TEMP293'
                 313 = 'TEMP313'
                 333 = 'TEMP333'
                 353 = 'TEMP353' ;
RUN;
DATA TPH022 ;

    B0 = -1.0815      ;
    B1 = -2209.6838   ;
    B2 = 2.105        ;
    B3 = 949179       ;
    B4 = -0.04108715  ;
    B5 = -413.6372    ;

   DO  TEMP = 273  TO 353 BY 20    ;
      DO FRQ = 2,5,10,15,20,30, 40 TO  500  BY  20  ;
      LNE1 = B0 + B1 / TEMP + B2 * LOG(FRQ) + B3 /(TEMP ** 2 )
             + B4 *((LOG(FRQ))**2)+ ( B5 / TEMP)* LOG(FRQ)  ;
      LN10E1 = 0.4343 * LNE1  ;
      OUTPUT;
      END;
   END;
RUN;
TITLE1 'STORAGE MODULUS-FREQ AT CONST TEMP' ;
FOOTNOTE1     'FIG35 SAS ,MEGAPASCAL-HERTZ-KELVIN   '  ;
SYMBOL1   I= JOINT  L=1  ;
SYMBOL2   I= JOINT  L=6  ;
SYMBOL3   I= JOINT  L=5  ;
SYMBOL4   I= JOINT  L=4  ;
SYMBOL5   I= JOINT  L=3  ;
COMMENT          SYMBOL6   I= JOINT  L=2  ;

PROC GPLOT   DATA = TPH022 ;
  PLOT  LN10E1 * FRQ = TEMP / VAXIS = 1.0 TO 2.5 BY 0.1  ;
```

```
  FORMAT TEMP CC. ;
RUN;
/*
//
```

```
A3.  CAN2D2 DATA
***
***  To find the El of Propellant by eigenvalue search
***
/PREP7
/GOPR
/TITLE, CAN2D2, FN AND MODES
KAN,2
ET,1,3        * BEAM
EX,1,30E6
DENS,1, 0.000728
R,1,0.005, 4.17E-8, 0.01, 1.2      ***  REAL DEPTH = 0.5 INCH ***

ET,2,42,,,3          ***** 2D EL    ***
EX,2, 18000    ********** SEARCH FOR El OF PROPELLANT  **************
NUXY,2,0.49
DENS,2,0.0001617
R,2, 0.5             ***** 0.5 INCH DEPTH INTO PAPER

ET,3, 21,,,4
R,3, 5.70E-6         *** 0.5 GRAM ACC                        ****
                     *** 0.5 GRAM CABLE, TOTAL 1 GRAM   ***
KAY,3,3

N,1
N,10,5.3125
FILL
NGEN,2,10,1,10,1,,0.276      ****(0.25 + 0.05 X2) = 0.26
                             **** (0.266 + 0.05 X 2 ) = 0.276 INCH
TYPE,1
MAT,1
REAL,1
E,1,2
EGEN,9,1,1
E,11,12
EGEN,9,1,10

TYPE,2
MAT,2
REAL,2
E,1,2,12,11
EGEN,9,1,19

TYPE,3
REAL,3
E,10
```

```
M,2,UY,10
M,12,UY,20
ITER,1,1
D,1,ALL
D,11,ALL

WFRONT,1
WSTART,1,11,10
WAVES

AFWR,, 1
FINISH
/EXEC
/INPUT,27
FINISH
/EOF
```

```
A 4. CAN2D3 DATA
***
***  To find the damping ratio by matching test amplification ratio
***
/PREP7
/GOPR
/TITLE, CAN2D3, HARMONIC ANALYSIS
KAN,6
ET,1,3        * BEAM
EX,1,30E6
DENS,1, 0.000728
R,1,0.005, 4.17E-8, 0.01, 1.2      ***  REAL DEPTH = 0.5 INCH ***

ET,2,42,,,3          ***** 2D EL    ***
EX,2, 18000    ********** SEARCH FOR E1 OF PROPELLANT  **************
NUXY,2,0.49
DENS,2,0.0001617
R,2, 0.5             ***** 0.5 INCH DEPTH INTO PAPER

ET,3, 21,,,4
R,3, 5.70E-6         *** 0.5 GRAM ACC                        ****
                     *** 0.5 GRAM CABLE, TOTAL 1 GRAM  ***
N,1
N,10,5.3125
FILL
NGEN,2,10,1,10,1,,0.276     ****(0.25 + 0.05 X2) = 0.26
                            **** (0.266 + 0.05 X 2 ) = 0.276 INCH
TYPE,1
MAT,1
REAL,1
E,1,2
EGEN,9,1,1
E,11,12
EGEN,9,1,10

TYPE,2
MAT,2
REAL,2
E,1,2,12,11
EGEN,9,1,19

TYPE,3
REAL,3
E,10

CP,1,UY,1,11          ********* KAN,6
```

```
M,1,UY,10
M,12,UY,20

D, 1,UX,0,0,,,ROTZ
D,11,UX,0,0,,,ROTZ
D, 1,UY, 0.0001                    ************** KAN,6    **********
                                   ******* BASE DISP = 0.0001 INCH ***

WFRONT,1
WSTART,1,11,10
WAVES

DMPRAT,0.133     ********* SEARCH FOR  ********************
KBC,1
KSE,1

HARFRQ,168,188
ITER,20,,1

AFWR             ************ NO DETAILS ***************
FINISH
/EXEC
/INPUT,27
FINISH

/POST26
FILE,10
DISP,2, 10,UY,UY10
DISP,3, 10,UY,PY10 ,1
PRVAR,2,3
FINISH
/EOF
```

```
A5.  CAN2D4 DATA
***
***  To find the energy ratio and then E2 of propellant
***
/PREP7
/GOPR
/TITLE, CAN2D3, HARMONIC ANALYSIS
KAN,6
ET,1,3        * BEAM
EX,1,30E6
DENS,1, 0.000728
R,1,0.005, 4.17E-8, 0.01, 1.2      ***  REAL DEPTH = 0.5 INCH ***

ET,2,42,,,3          ***** 2D EL    ***
EX,2, 18000    ********** SEARCH FOR E1 OF PROPELLANT  ************
NUXY,2,0.49
DENS,2,0.0001617
R,2, 0.5             ***** 0.5 INCH DEPTH INTO PAPER

ET,3, 21,,,4
R,3, 5.70E-6         *** 0.5 GRAM ACC                        ****
                     *** 0.5 GRAM CABLE, TOTAL 1 GRAM  ***
N,1
N,10,5.3125
FILL
NGEN,2,10,1,10,1,,0.276     ****(0.25 + 0.05 X2) = 0.26
                            **** (0.266 + 0.05 X 2 ) = 0.276 INCH
TYPE,1
MAT,1
REAL,1
E,1,2
EGEN,9,1,1
E,11,12
EGEN,9,1,10

TYPE,2
MAT,2
REAL,2
E,1,2,12,11
EGEN,9,1,19

TYPE,3
REAL,3
E,10

CP,1,UY,1,11          ********* KAN,6
```

```
M,1,UY,10
M,12,UY,20

D, 1,UX,0,0,,,ROTZ
D,11,UX,0,0,,,ROTZ
D, 1,UY, 0.0001                    ************** KAN,6    **********
                                   ******* BASE DISP = 0.0001 INCH ***

WFRONT,1
WSTART,1,11,10
WAVES

DMPRAT,0.133      ********* SEARCH FOR  ********************
KBC,1
KSE,1

HARFRQ,168,178
ITER,2 ,,1

AFWR              ************ NO DETAILS ***************
FINISH
/EXEC
/INPUT,27
FINISH

/POST26
FILE,10
DISP,2, 10,UY,UY10
DISP,3, 10,UY,PY10 ,1
PRVAR,2,3
FINISH

/STRESS
HARFRQ,168,178 ,0
ITER,2,,1
NSTRES,2
END
FINISH

/POST1
STRESS,SENE
SET,1,1
SSUM
ESEL,STIF,3
SSUM
ESEL,STIF,42
SSUM
```

```
RESET
STRESS,SENE
SET,1,2
PRSTRS
SSUM
ESEL,STIF,3
SSUM
ESEL,STIF,42
SSUM
FINISH

/STRESS
HARFRQ,168,178 ,90
ITER,2,,1
NSTRES,2
END
FINISH

/POST1
STRESS,SENE
SET,1,1
SSUM
ESEL,STIF,3
SSUM
ESEL,STIF,42
SSUM

RESET
STRESS,SENE
SET,1,2
PRSTRS
SSUM
ESEL,STIF,3
SSUM
ESEL,STIF,42
SSUM
FINISH
/EOF
```

```
A6.    FIG39B SAS
***
***  To print the E1, E2 and damping ratio of Propellant
***
OPTIONS LINESIZE = 72;
DATA TPH022 ;

    B0 = -1.0815      ;
    B1 = -2209.6838   ;
    B2 = 2.105        ;
    B3 = 949179       ;
    B4 = -0.04108715  ;
    B5 = -413.6372    ;

    C0 = -16.93447031             ;
    C1 =  5318.89297              ;
    C2 =  3.5053179               ;
    C3 =  0.0                     ;
    C4 = -0.0776937               ;
    C5 = -747.3686                ;
 COMMENT     ****************************

    C0 = -17.7658
    C1 =  5578.91877
    C2 =  3.6353179
    C3 =  0.0
    C4 = -0.08
    C5 = -781.3         ***************  ;

   DO  TEMP = 253  TO 353 BY 10 ;
      DO FRQ = 2,10,20  TO 500 BY 20 ;

      LNE1 = B0 + B1 / TEMP + B2 * LOG(FRQ) + B3 /(TEMP ** 2 )
           + B4 *((LOG(FRQ))**2)+ ( B5 / TEMP)* LOG(FRQ)  ;
      LN10E1 = 0.4343 * LNE1  ;

      LNE2 = C0 + C1 / TEMP + C2 * LOG(FRQ) + C3 /(TEMP ** 2 )
           + C4 *((LOG(FRQ))**2)+ ( C5 / TEMP)* LOG(FRQ)  ;
      LN10E2 = 0.4343 * LNE2  ;

      E1 = 10 ** LN10E1  ;
      E2 = 10 ** LN10E2  ;

      DMPRT = 10 ** (LN10E2 - LN10E1 ) ;

      OUTPUT;
      END;
   END;
```

```
PROC PRINT  ;
VAR  TEMP   FRQ  E1  E2  DMPRT  ;

RUN;
```

A7 . SHELL5 KAN2

```
***
***  To find f1 and mode shape #1 of rocket model
***

/PREP7
/GOPR
/TITLE, SHELL5 KAN2 EL MODAL ANSLYSIS, CHANGE FOR WAVE LIMIT = 200.
KAN,2
                                  *** STEEL CASING MAT PROPERTIES
ET,1,63,,,,,2                       * SHELL, KEYOPT(5) = 2 --> NODAL STRESS
EX,1,207E9                          * PASCAL, EY,EZ = EX,      PRINTOUT
NUXY,1,0.3                          * POISSON RATIO ,2 DEFAULTS
DENS,1,8300                         * KG/M**3
R,1,0.00152
                                  *** PROPELLANT TPH8208
ET,2,45,,,,1,2                       * 3D ISOPARAMETRIC EL, KEYOPT(5) = 2
EX,2,120E6                          *
NUXY,2,0.49
DENS,2, 1740                        *
                                    *
KAY,1,0   ***
KAY,2,5
KAY,7,5

CSYS,1                           ** CYLINDRICAL COORDINATE
N,101, 0.06274, 90                ** R,0,Z, R = .0635 - .00076 M
N,112, 0.06274, 90, 0.77          ** Z = 0.77 M,12 NODES,11 EL  *****
FILL
NGEN,10,100,101,112,1,0,-20,0
TYPE,1
MAT,1
REAL,1

EN,101,101,102,202,201             ** EL # 101
EGEN, 11,1,101                   ** GENERATE 11 ELS
ENGEN,100, 9,100,101,111

N,1101, 0.0235, 90
N,1112, 0.0235, 90, 0.77
FILL,1101,1112                   **
NGEN,10,100,1101,1112,1,0,-20

TYPE,2
MAT,2
EN,1101,1101,1102,1202,1201,101,102,202,201
EGEN,11,1,1101
ENGEN,100, 9,100,1101, 1111
```

```
44                              *** 180 NODES, 198 EL = 99 +99 EL
45
46    M,  102, UY,  112         *** ,1 ,UX ,UZ **** CONSIDER TO ADD
47    M,  302, UY,  312
48    M,  802, UY,  812
49    M, 1002, UY, 1012
50    M, 1102, UY, 1112
51    M, 1302, UY, 1312
52    M, 1802, UY, 1812
53    M, 2002, UY, 2012
54
55    M,  303, UX,  312, 3, UZ
56    M,  803, UX,  812, 3, UZ
57    M, 1303, UX, 1312, 3, UZ
58    M, 1803, UX, 1812, 3, UZ
59
60    ITER,25,1     *** ITERATION  IS DEFAULT FOR REDU SUBSPACE METHOD
1
                 **********  ANSYS INPUT DATA LISTING (FILE18)  **********

61    D,101,UX ,0,0,2001,100, UZ,ROTX,ROTY,ROTZ
62    D,101,UY ,0,0,2001,100     *** FOR KAN,2 ONLY, NOT FOR KAN,6
63
64              **  CPSIZE,20                      **
65              **  CPNGEN, 1,UY,101,2001,100      ** COUPLED D/F
66              **  D,101,UY ,1,0,2001,100         ** FOR KAN,6 ONLY, 1 OR 0.001
67
68    D,102,UX,0,0,  112,1,ROTY,ROTZ               ** SYM PLANE
69    D,1102,UX,0,0,1112
70    D,1002,UX,0,0,1012,1,ROTY,ROTZ               ** SYM PLANE
71    D,2002,UX,0,0,2012                           **
72    DSYS,1
73    NLIST,ALL
74
75
76    WFRONT,1
77    WSTART,101,1101,1000,10,100
78    WAVES
79    AFWR,,1
80    FINISH
81    /EXEC
82    /INPUT,27
83    FINISH
84    /EOF
```

A8. SHELL5 OUT2

```
***
*** To find f2, f3, f4, f5 and associated mode shapes
***
/PREP7
/GOPR
/TITLE, SHELL5 + 3D EL MODAL ANSLYSIS, 55555555555555555555
KAN,2
                                  *** STEEL CASING MAT PROPERTIES
ET,1,63,,,,,2                       * SHELL, KEYOPT(5) = 2 --> NODAL STRESS
EX,1,207E9                          * PASCAL, EY,EZ = EX,      PRINTOUT
NUXY,1,0.3                          * POISSON RATIO ,2 DEFAULTS
DENS,1,8300                         * KG/M**3
R,1,0.00152
                                  *** PROPELLANT TPH8208
ET,2,45,,,,1,2                 ******** 3D ISOPARAMETRIC EL, KEYOPT(5) = 2
EX,2,173E6                       *****
NUXY,2,0.49
DENS,2, 1740                        *
                                    *
KAY,1,0   ***
KAY,2,5
KAY,7,5

CSYS,1                           ** CYLINDRICAL COORDINATE
N,101, 0.06274, 90                ** R,O,Z, R = .0635 - .00076 M
N,112, 0.06274, 90, 0.77          ** Z = 0.77 M,12 NODES,11 EL  *****
FILL
NGEN,10,100,101,112,1,0,-20,0
TYPE,1
MAT,1
REAL,1

EN,101,101,102,202,201             ** EL # 101
EGEN, 11,1,101                  ** GENERATE 11 ELS
ENGEN,100, 9,100,101,111

N,1101, 0.0235, 90
N,1112, 0.0235, 90, 0.77
FILL,1101,1112                  **
NGEN,10,100,1101,1112,1,0,-20

TYPE,2
MAT,2
EN,1101,1101,1102,1202,1201,101,102,202,201
EGEN,11,1,1101
ENGEN,100, 9,100,1101, 1111
                                *** 180 NODES, 198 EL = 99 +99 EL
```

```
45
46   M,  102, UY,  112       *** ,1 ,UX ,UZ **** CONSIDER TO ADD
47   M,  302, UY,  312
48   M,  802, UY,  812
49   M, 1002, UY, 1012
50   M, 1102, UY, 1112
51   M, 1302, UY, 1312
52   M, 1802, UY, 1812
53   M, 2002, UY, 2012
54
55   M,  303, UX,  312, 3, UZ
56   M,  803, UX,  812, 3, UZ
57   M, 1303, UX, 1312, 3, UZ
58   M, 1803, UX, 1812, 3, UZ
59
60   ITER,25,1    *** ITERATION  IS DEFAULT FOR REDU SUBSPACE METHOD
1
          **********  ANSYS INPUT DATA LISTING (FILE18)  **********

61   D,101,UX ,0,0,2001,100, UZ,ROTX,ROTY,ROTZ
62   D,101,UY ,0,0,2001,100    ***
63
64             **  CPSIZE,20                      **
65             **  CPNGEN, 1,UY,101,2001,100  ** COUPLED D/F
66             **  D,101,UY ,1,0,2001,100     ** FOR KAN,6 ONLY, 1 OR 0.001
67
68   D,102,UX,0,0,  112,1,ROTY,ROTZ              ** SYM PLANE
69   D,1102,UX,0,0,1112
70   D,1002,UX,0,0,1012,1,ROTY,ROTZ              ** SYM PLANE
71   D,2002,UX,0,0,2012                          **
72              ***   DSYS,1
73              ***   NLIST,ALL
74
75              ***  WFRONT,1
76   WSTART,101,1101,1000,10,100
77   WAVES
78   AFWR                 *******
79   FINISH
80   /EXEC                *******
81   /INPUT,27
82   FINISH
83   /EOF
```

```
A9.   SHPSD11 OUT2
***
***   Random vibration of rocket motor, 20 - 200 Hz.
***
     11   /PREP7
     12   /GOPR
     13   /TITLE, SHPSD11, SHE + 3D EL, PSD ANALYSIS OF VISCOELASTIC STR
     14   KAN,6
     15                                *** STEEL CASING MAT PROPERTIES
     16   ET,1,63,,,,,2                *** SHELL, KEYOPT(5) = 2 --> NODAL STRESS
     17   ET,3,63,,,,,2                *** SHELL, KEYOPT(5) = 2 --> NODAL STRESS
     18   EX,1,207E9                   *** PASCAL, EY,EZ = EX,       PRINTOUT
     19   NUXY,1,0.3                   *** POISSON RATIO ,2 DEFAULTS
     20   DENS,1,8300                  *** KG/M**3
     21   R,1,0.00152
     22                                *** PROPELLANT TPH8208
     23   ET,2,45,,,,1,2                *** 3D ISOPARAMETRIC EL, KEYOPT(5) = 2
     24   ET,4,45,,,,1,2                *** 3D ISOPARAMETRIC EL, KEYOPT(5) = 2
     25   EX,2,120E6                    **
     26   NUXY,2,0.49
     27   DENS,2, 1740                  ** KG/M**3, = 0.064 LB/IN**3 = 0.0001656
     28                                 **
     29   CSYS,1                      ** CYLINDRICAL COORDINATE
     30   N,  1, 0.06274, 90           ** R,O,Z, R = .0635 - .00076 M
     31   N, 12, 0.06274, 90, 0.77     ** Z = 0.77 M,12 NODES,11 EL  *****
     32   FILL
     33   NGEN,10,12 , 1, 12,1,0,-20,0
     34   TYPE,1
     35   MAT,1
     36   REAL,1
     37
     38   EN,101,  1,  2, 14, 13      ** EL # 101
     39   EGEN, 11,1,101            ** GENERATE 11 ELS
     40   ENGEN,100, 9, 12, 101,111
     41
     42   N, 121, 0.0235, 90
     43   N, 132, 0.0235, 90, 0.77
     44   FILL,121 , 132              **
     45   NGEN,10, 12, 121, 132, 1,0,-20
     46
     47   TYPE,2
     48   MAT,2
     49   EN,1101, 121, 122, 134, 133,  1,  2, 14, 13
     50   EGEN,11,1,1101
     51   ENGEN,100, 9, 12,1101, 1111
     52
     53   TYPE,4                    ***
```

```
EMODIF,1101, 0          *
EMODIF,1501,0           *  3D EL
                        *
TYPE,3                  *
MAT,1                   *
REAL,1                  *  SHELL EL
EMODIF,101,0            *
1
          **********

EMODIF,501,0           ***

CPSIZE,20
CPNGEN,1,UY,  1, 229, 12
                         *** 240 NODES, 198 EL = 99 +99 EL
M,    1, UY
M,    2, UY,   12        ***
M,   26, UY,   36
M,   86, UY,   96
M,  110, UY,  120
M,  122, UY,  132
M,  146, UY,  156
M,  206, UY,  216
M,  230, UY,  240

M,   27, UX,   36, 3, UZ
M,   87, UX,   96, 3, UZ
M,  147, UX,  156, 3, UZ
M,  207, UX,  216, 3, UZ


D,  1,UX ,0,0, 229, 12, UZ,ROTX,ROTY,ROTZ
D,  1,UY ,1            ***


D,  2,UX,0,0,   12,1,ROTY,ROTZ           ** SYM PLANE
D, 122,UX,0,0, 132
D, 110,UX,0,0, 120,1,ROTY,ROTZ           ** SYM PLANE
D, 230,UX,0,0, 240                       **
DSYS,1
NLIST,ALL

WFRONT,1
WSTART,  1, 121, 120,10, 12
WAVES
BETAD, 1.3E-6       *** FOR FRQ RANGE 20--200 HZ,

DMPRAT, 0.0019       ***
```

```
 99   KBC,1
100   KSE,1                  *** STRAIN ENERGY
101
102   HARFRQ,10,90           *** INC = 10 HZ
103   ITER, 8,,1             ***
104   LWRITE
105
106   HARFRQ, 90, 92
107   ITER, 4,,1             *** INC = 0.5 HZ
108   LWRITE
109
110   HARFRQ, 92,93.5
111   ITER,15,7,1             *** INC = 0.1 HZ
112   LWRITE
113
114   HARFRQ,93.5, 94
115   ITER, 1,,1             *** INC = 0.5 HZ
116   LWRITE
117
118   HARFRQ,50,200          ******* WATCH CHANGES  *******
119   ITER, 3,,1             *** INC = 50 HZ
120   LWRITE
1
              **********  ANSYS INPUT DATA LISTING (FILE18)  **********

121
122   AFWR,,1
123   FINISH
124   /EXEC                 *****
125   /INPUT,27
126   FINISH
127
128         ******** THE FOLLOWING IS PROCESSING
129   /STRESS
130   HARFRQ,10,90 ,0    ****  INC = 10 HZ
131   ITER,8 ,,0         ****
132   POSTR,1,3,,4
133   NSTRES,8
134   END
135
136   HARFRQ, 90,92 ,0
137   ITER, 4,,0             *** INC = 1 HZ
138   POSTR,1,3,,4
139   NSTRES,4
140   END
141
142   HARFRQ, 92,93.5 ,0
143   ITER,15,,0             *** INC = 0.1 HZ
```

```
144   POSTR,1,3,,4
145   PONF,7
146   NSTRES,15
147   END
148
149   HARFRQ, 93.5,  94 ,0
150   ITER,1 ,,0              *** INC = 0.5 HZ
151   POSTR,1,3,,4
152   NSTRES,1
153   END
154
155   HARFRQ, 50,200          *** WATCH CHANGES  *****
156   ITER, 3,,0              *** INC = 50 HZ
157   POSTR,1,3,,4
158   NSTRES,3
159   END
160   FINISH
161
162   /POST26
163   DISP,3, 12,UY,UY12          *** TIP TOP UY
164   DISP,4,  6,UY,UY06           *** NEAR MID TOP UY
165   PSDDAT,2, 20,7.5 , 60,11.25, 100,15, 300,15, 500,15      ****
166   PSDDAT,2, 700,0.15
167         ***   ((M/SEC**2)**2) / HZ    *** RMS ACC = 9.3 G
168   PSDCAL, 9, 3, 2,  PSD-, UY12
169   PSDCAL,10, 4, 2,  PSD-, UY06
170   PRVAR,  2, 3, 9, 4, 10
171                   **********************
172   ESTR,3,  101,  21, SX(I       *** EL COORDINATE SYS, I-J SIDE = X SIDE
173   ESTR,4,  101,  26, SY(J
174   PSDCAL, 9, 3, 2,  PSD-,  SX(I
175   PSDCAL,10, 4, 2,  PSD-,  SY(J
176   PRVAR,  2, 3, 9, 4, 10
177                   **********************
178   ESTR,3,  101,  69, S1(I
179   ESTR,4,  101,  71, S3(I
180   PSDCAL, 9, 3, 2,  PSD-,  S1(I
1
              **********  ANSYS INPUT DATA LISTING (FILE18)  **********

181   PSDCAL,10, 4, 2,  PSD-,  S3(I
182   PRVAR,  2, 3, 9, 4, 10
183             **********************
184   ESTR, 3, 501,  11, SXY          *** REDEFINE VARIABLE 3
185   ESTR, 4, 511,  11, SXY          *** REDEFINE VARIABLE 4
186   PSDCAL, 9, 3, 2,  PSD-,  SXY
187   PSDCAL,10, 4, 2,  PSD-,  SXY
188   PRVAR,  2, 3, 9, 4, 10
```

```
          **********************
ESTR, 3, 1101,   37, SX(M           ***
ESTR, 4, 1101,   81, S1(M           ***
PSDCAL, 9, 3, 2,  PSD-,  SX(M
PSDCAL,10, 4, 2,  PSD-,  S1(M
PRVAR,  2, 3, 9, 4, 10
                  **********************
ESTR, 3, 1501,    4, SXY            ***
ESTR, 4, 1511,    4, SXY            ***
PSDCAL, 9, 3, 2,  PSD-,  SXY
PSDCAL,10, 4, 2,  PSD-,  SXY
PRVAR,  2, 3, 9, 4, 10
FINISH

/POST1
    ** STRESS,S1SH,63,129      *** PRINCIAL STRESS 1,3 AND 2 X MAX. SHEAR
    ** STRESS,S3SH,63,131      *** TOP CENTROID OF SHELL
    ** STRESS,SISH,63,132      ***
    ** STRESS,S1SO,45,101      *** PRINCIAL STRESS 1,3 AND 2 X MAX. SHEAR
    ** STRESS,S3SO,45,103        *** 3D SOLID ELEMENT
    ** STRESS,SISO,45,104        ***
    ** SET,3,17                *** FOR 92.7 HZ *****
    ** PRSTRS
                          ***
STRESS,SENE
SET,3, 7
PRSTRS
SSUM
ESEL,STIF,63
SSUM
ESEL,STIF,45
SSUM

RESET
STRESS,SENE
SET,1, 3
PRSTRS
SSUM
ESEL,STIF,63
SSUM
ESEL,STIF,45
SSUM

RESET
STRESS,SENE
SET,5, 3
PRSTRS
SSUM
```

```
    237   ESEL,STIF,63
    238   SSUM
    239   ESEL,STIF,45
    240   SSUM
1
                  **********  ANSYS INPUT DATA LISTING (FILE18)  **********

    241   FINISH
    242
    243   /STRESS
    244   HARFRQ,10,90 ,90  ****  INC = 10 HZ
    245   ITER,8 ,,0        ****
    246   POSTR,1,3,,4
    247   NSTRES,8
    248   END
    249
    250   HARFRQ, 90,92 ,90
    251   ITER, 4,,0            *** INC = 1 HZ
    252   POSTR,1,3,,4
    253   NSTRES,4
    254   END
    255
    256   HARFRQ, 92,93.5 ,90
    257   ITER,15,,0            *** INC = 0.1 HZ
    258   POSTR,1,3,,4
    259   PONF,7
    260   NSTRES,15
    261   END
    262
    263   HARFRQ, 93.5, 94, 90
    264   ITER,1 ,,0            *** INC = 0.5 HZ
    265   POSTR,1,3,,4
    266   NSTRES,1
    267   END
    268
    269   HARFRQ, 50,200, 90    *** WATCH CHANGES  *****
    270   ITER, 3,,0            *** INC = 50 HZ
    271   POSTR,1,3,,4
    272   NSTRES,3
    273   END
    274   FINISH
    275
    276   /POST26
    277
    278   DISP,3, 12,UY,UY12          *** TIP TOP UY
    279   DISP,4,  6,UY,UY6           *** NEAR MID TOP UY
    280   PSDDAT,2, 20,7.5 , 60,11.25, 100,15, 300,15, 500,15      ****
    281   PSDDAT,2, 700,0.15
```

```
282          ***   ((M/SEC**2)**2) / HZ    ***
283    PSDCAL, 9, 3, 2,  PSD-, UY12
284    PSDCAL,10, 4, 2,  PSD-, UY6
285    PRVAR,  2, 3, 9, 4, 10
286                      **********************
287    ESTR,3,  101,  21, SX(I       *** EL COORDINATE SYS, I-J SIDE = X SIDE
288    ESTR,4,  101,  26, SY(J
289    PSDCAL, 9, 3, 2,  PSD-,  SX(I
290    PSDCAL,10, 4, 2,  PSD-,  SY(J
291    PRVAR,  2, 3, 9, 4, 10
292                      **********************
293    ESTR,3,  101,  69, S1(I
294    ESTR,4,  101,  71, S3(I
295    PSDCAL, 9, 3, 2,  PSD-,  S1(I
296    PSDCAL,10, 4, 2,  PSD-,  S3(I
297    PRVAR,  2, 3, 9, 4, 10
298             **********************
299    ESTR, 3, 501,  11, SXY           *** REDEFINE VARIABLE 3
300    ESTR, 4, 511,  11, SXY           *** REDEFINE VARIABLE 4
1
                **********  ANSYS INPUT DATA LISTING (FILE18)  **********

301    PSDCAL, 9, 3, 2,  PSD-,  SXY
302    PSDCAL,10, 4, 2,  PSD-,  SXY
303    PRVAR,  2, 3, 9, 4, 10
304             **********************
305    ESTR, 3, 1101,  37, SX(M          ***
306    ESTR, 4, 1101,  81, S1(M          ***
307    PSDCAL, 9, 3, 2,  PSD-,  SX(M
308    PSDCAL,10, 4, 2,  PSD-,  S1(M
309    PRVAR,  2, 3, 9, 4, 10
310                     **********************
311    ESTR, 3, 1501,   4, SXY           ***
312    ESTR, 4, 1511,   4, SXY           ***
313    PSDCAL, 9, 3, 2,  PSD-,  SXY
314    PSDCAL,10, 4, 2,  PSD-,  SXY
315    PRVAR,  2, 3, 9, 4, 10
316    FINISH
317
318    /POST1
319        ** STRESS,S1SH,63,129     *** PRINCIAL STRESS 1,3 AND 2 X MAX. SHEAR
320        ** STRESS,S3SH,63,131     *** TOP CENTROID OF SHELL
321        ** STRESS,SISH,63,132     ***
322        ** STRESS,S1SO,45,101     *** PRINCIAL STRESS 1,3 AND 2 X MAX. SHEAR
323        ** STRESS,S3SO,45,103       *** 3D SOLID ELEMENT
324        ** STRESS,SISO,45,104       ***
325        ** SET,3,17                *** FOR 92.7 HZ *****
326        ** PRSTRS
```

```
                                ***
STRESS,SENE
SET,3, 7
PRSTRS
SSUM
ESEL,STIF,63
SSUM
ESEL,STIF,45
SSUM

RESET
STRESS,SENE
SET,1, 3
PRSTRS
SSUM
ESEL,STIF,63
SSUM
ESEL,STIF,45
SSUM

RESET
STRESS,SENE
SET,5, 3
PRSTRS
SSUM
ESEL,STIF,63
SSUM
ESEL,STIF,45
SSUM
FINISH

/EOF    ********************************************************
```

```
A10.   SHPSD16 OUT
***
***  Random vibration of rocket motor, 200 - 750 Hz.
***
     10   /PREP7
     11   /GOPR
     12   /TITLE, SHPSD16, SHE + 3D EL, PSD ANALYSIS OF VISCOELASTIC STR
     13   KAN,6
     14                                  *** STEEL CASING MAT PROPERTIES
     15   ET,1,63,,,,,2                  *** SHELL, KEYOPT(5) = 2 --> NODAL STRESS
     16   ET,3,63,,,,,2                  *** SHELL, KEYOPT(5) = 2 --> NODAL STRESS
     17   EX,1,207E9                     *** PASCAL, EY,EZ = EX,      PRINTOUT
     18   NUXY,1,0.3                     *** POISSON RATIO ,2 DEFAULTS
     19   DENS,1,8300                    *** KG/M**3
     20   R,1,0.00152
     21                                  *** PROPELLANT TPH8208
     22   ET,2,45,,,,1,2                  *** 3D ISOPARAMETRIC EL, KEYOPT(5) = 2
     23   ET,4,45,,,,1,2                  *** 3D ISOPARAMETRIC EL. KEYOPT(5) = 2
     24   EX,2,173E6                      **
     25   NUXY,2,0.49
     26   DENS,2, 1740                    ** KG/M**3, = 0.064 LB/IN**3 = 0.0001656
     27                                   **
     28   CSYS,1                        ** CYLINDRICAL COORDINATE
     29   N,  1, 0.06274, 90             ** R,O,Z, R = .0635 - .00076 M
     30   N, 12, 0.06274, 90, 0.77       ** Z = 0.77 M,12 NODES,11 EL  *****
     31   FILL
     32   NGEN,10,12 , 1, 12,1,0,-20,0
     33   TYPE,1
     34   MAT,1
     35   REAL,1
     36
     37   EN,101,  1,  2, 14, 13      ** EL # 101
     38   EGEN, 11,1,101             ** GENERATE 11 ELS
     39   ENGEN,100, 9, 12, 101,111
     40
     41   N, 121, 0.0235, 90
     42   N, 132, 0.0235, 90, 0.77
     43   FILL,121 , 132              **
     44   NGEN,10, 12, 121, 132, 1,0,-20
     45
     46   TYPE,2
     47   MAT,2
     48   EN,1101, 121, 122, 134, 133,  1,  2, 14, 13
     49   EGEN,11,1,1101
     50   ENGEN,100, 9, 12,1101, 1111
     51
     52   TYPE,4
```

```
53   EMODIF,1101, 0          *
54   EMODIF,1501,0           *  3D EL
55                           *
56   TYPE,3                  *
57   MAT,1                   *
58   REAL,1                  *  SHELL EL
59   EMODIF,101,0            *
60   EMODIF,501,0           ***
1
            **********

61
62   CPSIZE,20
63   CPNGEN,1,UY,  1, 229, 12
64                           *** 240 NODES, 198 EL = 99 +99 EL
65   M,    1, UY
66   M,    2, UY,   12       ***
67   M,   26, UY,   36
68   M,   86, UY,   96
69   M,  110, UY,  120
70   M,  122, UY,  132
71   M,  146, UY,  156
72   M,  206, UY,  216
73   M,  230, UY,  240
74
75   M,   27, UX,   36, 3, UZ
76   M,   87, UX,   96, 3, UZ
77   M,  147, UX,  156, 3, UZ
78   M,  207, UX,  216, 3, UZ
79
80
81   D,  1,UX ,0,0, 229, 12, UZ,ROTX,ROTY,ROTZ
82   D,  1,UY ,1            ***
83
84
85   D,  2,UX,0,0,   12,1,ROTY,ROTZ          ** SYM PLANE
86   D, 122,UX,0,0, 132
87   D, 110,UX,0,0, 120,1,ROTY,ROTZ          ** SYM PLANE
88   D, 230,UX,0,0, 240                      **
89   DSYS,1
90   NLIST,ALL
91
92   WFRONT,1
93   WSTART,  1, 121, 120,10, 12
94   WAVES
95       ***  BETAD, 1.2E-7   *** FOR FRQ RANGE 20--200 HZ,
96
97   DMPRAT, 0.0078
```

```
  98   KBC,1
  99   KSE,1                    *** STRAIN ENERGY
 100
 101   HARFRQ,150,450             *** INC = 50 HZ
 102   ITER, 6,,1               ***
 103   LWRITE
 104
 105   HARFRQ,464.8, 514.8
 106   ITER,10,,1               *** INC =  5  HZ
 107   LWRITE
 108
 109   HARFRQ,500, 700
 110   ITER, 4, ,1               *** INC = 50  HZ
 111   LWRITE
 112
 113   HARFRQ,720, 750
 114   ITER, 3,,1               *** INC = 10 HZ
 115   LWRITE
 116
 117   AFWR,,1
 118   FINISH
 119   /EXEC                 *****
 120   /INPUT,27
1
                ***********  ANSYS INPUT DATA LISTING (FILE18)  ***********

 121   FINISH
 122         ******** THE FOLLOWING IS PROCESSING  *************
 123   /STRESS
 124   HARFRQ,150,450,0         ****  INC = 50 HZ
 125   ITER,6 ,,0               ****
 126   POSTR,1,3,,4
 127   NSTRES,6
 128   END
 129
 130   HARFRQ, 464.8, 514.8, 0
 131   ITER,10,,0               *** INC = 5 HZ
 132   POSTR,1,3,,4
 133   PONF,5                   ****** NO NEED TO SPECIFY ******
 134   NSTRES,10
 135   END
 136
 137   HARFRQ, 500,700 ,0
 138   ITER, 4,,0               *** INC = 50  HZ
 139   POSTR,1,3,,4
 140   NSTRES, 4
 141   END
 142
```

```
    143   HARFRQ, 720, 750, 0
    144   ITER,3 ,,0            *** INC = 10 HZ
    145   POSTR,1,3,,4
    146   NSTRES,3
    147   END
    148   FINISH
    149
    150   /POST26
    151   DISP,3, 12,UY,UY12          *** TIP TOP UY
    152   DISP,4,  6,UY,UY06           *** NEAR MID TOP UY
    153   PSDDAT,2, 20,7.5 , 60,11.25, 100,15, 300,15, 500,15      ****
    154   PSDDAT,2, 750,0.15
    155         ***   ((M/SEC**2)**2) / HZ    *** RMS ACC = 9.55 G
    156   PSDCAL, 9, 3, 2,  PSD-, UY12
    157   PSDCAL,10, 4, 2,  PSD-, UY06
    158   PRVAR,  2, 3, 9, 4, 10
    159                     ************************
    160   ESTR,3,  101,  21, SX(I       *** EL COORDINATE SYS, I-J SIDE = X SIDE
    161   ESTR,4,  101,  26, SY(J
    162   PSDCAL, 9, 3, 2,  PSD-,  SX(I
    163   PSDCAL,10, 4, 2,  PSD-,  SY(J
    164   PRVAR,  2, 3, 9, 4, 10
    165                     ************************
    166   ESTR,3,  101,  69, S1(I
    167   ESTR,4,  101,  71, S3(I
    168   PSDCAL, 9, 3, 2,  PSD-,  S1(I
    169   PSDCAL,10, 4, 2,  PSD-,  S3(I
    170   PRVAR,  2, 3, 9, 4, 10
    171             **********************
    172   ESTR, 3, 501,  11, SXY            *** REDEFINE VARIABLE 3
    173   ESTR, 4, 511,  11, SXY            *** REDEFINE VARIABLE 4
    174   PSDCAL, 9, 3, 2,  PSD-,  SXY
    175   PSDCAL,10, 4, 2,  PSD-,  SXY
    176   PRVAR,  2, 3, 9, 4, 10
    177             **********************
    178   ESTR, 3, 1101,  37, SX(M           ***
    179   ESTR, 4, 1101,  81, S1(M           ***
    180   PSDCAL, 9, 3, 2,  PSD-,  SX(M
1
                  **********  ANSYS INPUT DATA LISTING (FILE18)  **********

    181   PSDCAL,10, 4, 2,  PSD-,  S1(M
    182   PRVAR,  2, 3, 9, 4, 10
    183                    **********************
    184   ESTR, 3, 1501,   4, SXY           ***
    185   ESTR, 4, 1511,   4, SXY           ***
    186   PSDCAL, 9, 3, 2,  PSD-,  SXY
    187   PSDCAL,10, 4, 2,  PSD-,  SXY
```

```
188   PRVAR,  2, 3, 9, 4, 10
189   FINISH
190
191   /POST1
192   STRESS,S1SH,63,129      *** PRINCIAL STRESS 1,3 AND 2 X MAX. SHEAR
193   STRESS,S3SH,63,131      *** TOP CENTROID OF SHELL
194   STRESS,SISH,63,132      ***
195   STRESS,S1SO,45,101      *** PRINCIAL STRESS 1,3 AND 2 X MAX. SHEAR
196   STRESS,S3SO,45,103        *** 3D SOLID ELEMENT
197   STRESS,SISO,45,104        ***
198   SET,2, 5                *** FOR 489.8  HZ *****
199   PRSTRS
200                           ***
201   RESET
202   STRESS,SENE
203   SET,1, 1
204   PRSTRS
205   SSUM
206   ESEL,STIF,63
207   SSUM
208   ESEL,STIF,45
209   SSUM
210
211   RESET
212   STRESS,SENE
213   SET,2, 5
214   PRSTRS
215   SSUM
216   ESEL,STIF,63
217   SSUM
218   ESEL,STIF,45
219   SSUM
220
221   RESET
222   STRESS,SENE
223   SET,4, 2
224   PRSTRS
225   SSUM
226   ESEL,STIF,63
227   SSUM
228   ESEL,STIF,45
229   SSUM
230   FINISH
231
232   /STRESS
233   HARFRQ,150,450,90     ****  INC = 50 HZ
234   ITER,6 ,,0            ****
235   POSTR,1,3,,4
```

```
  236   NSTRES,6
  237   END
  238
  239   HARFRQ, 464.8, 514.8, 90
  240   ITER,10,,0              *** INC = 5 HZ
1
                **********  ANSYS INPUT DATA LISTING (FILE18)  **********

  241   POSTR,1,3,,4
  242   PONF,5                  ****** NO NEED TO SPECIFY ******
  243   NSTRES,10
  244   END
  245
  246   HARFRQ, 500,700 ,90
  247   ITER, 4,,0              *** INC = 50  HZ
  248   POSTR,1,3,,4
  249   NSTRES, 4
  250   END
  251
  252   HARFRQ, 720, 750, 90
  253   ITER,3 ,,0              *** INC = 10 HZ
  254   POSTR,1,3,,4
  255   NSTRES,3
  256   END
  257   FINISH
  258
  259   /POST26
  260
  261   DISP,3, 12,UY,UY12          *** TIP TOP UY
  262   DISP,4,  6,UY,UY6           *** NEAR MID TOP UY
  263   PSDDAT,2, 20,7.5 , 60,11.25, 100,15, 300,15, 500,15      ****
  264   PSDDAT,2, 750, 0.15
  265         ***   ((M/SEC**2)**2) / HZ    *** RMS ACC = 9.55 G
  266   PSDCAL, 9, 3, 2,  PSD-, UY12
  267   PSDCAL,10, 4, 2,  PSD-, UY6
  268   PRVAR,  2, 3, 9, 4, 10
  269                     **********************
  270   ESTR,3,  101,  21, SX(I       *** EL COORDINATE SYS, I-J SIDE = X SIDE
  271   ESTR,4,  101,  26, SY(J
  272   PSDCAL, 9, 3, 2,  PSD-,  SX(I
  273   PSDCAL,10, 4, 2,  PSD-,  SY(J
  274   PRVAR,  2, 3, 9, 4, 10
  275                     **********************
  276   ESTR,3,  101,  69, S1(I
  277   ESTR,4,  101,  71, S3(I
  278   PSDCAL, 9, 3, 2,  PSD-,  S1(I
  279   PSDCAL,10, 4, 2,  PSD-,  S3(I
  280   PRVAR,  2, 3, 9, 4, 10
```

```
                ***********************
ESTR, 3, 501,  11, SXY            *** REDEFINE VARIABLE 3
ESTR, 4, 511,  11, SXY            *** REDEFINE VARIABLE 4
PSDCAL, 9, 3, 2,  PSD-,  SXY
PSDCAL,10, 4, 2,  PSD-,  SXY
PRVAR,  2, 3, 9, 4, 10
                ***********************
ESTR, 3, 1101,  37, SX(M           ***
ESTR, 4, 1101,  81, S1(M           ***
PSDCAL, 9, 3, 2,  PSD-,  SX(M
PSDCAL,10, 4, 2,  PSD-,  S1(M
PRVAR,  2, 3, 9, 4, 10
                      ***********************
ESTR, 3, 1501,   4, SXY            ***
ESTR, 4, 1511,   4, SXY            ***
PSDCAL, 9, 3, 2,  PSD-,  SXY
PSDCAL,10, 4, 2,  PSD-,  SXY
PRVAR,  2, 3, 9, 4, 10
FINISH

1
                **********  ANSYS INPUT DATA LISTING (FILE18)  **********

/POST1
STRESS,S1SH,63,129      *** PRINCIAL STRESS 1,3 AND 2 X MAX. SHEAR
STRESS,S3SH,63,131      *** TOP CENTROID OF SHELL
STRESS,SISH,63,132      ***
STRESS,S1SO,45,101      *** PRINCIAL STRESS 1,3 AND 2 X MAX. SHEAR
STRESS,S3SO,45,103        *** 3D SOLID ELEMENT
STRESS,SISO,45,104        ***
SET,2, 5                *** FOR 489.5 HZ *****
PRSTRS
                        ***
RESET
STRESS,SENE
SET,1, 1
PRSTRS
SSUM
ESEL,STIF,63
SSUM
ESEL,STIF,45
SSUM

RESET
STRESS,SENE
SET,2, 5
PRSTRS
SSUM
```

```
ESEL,STIF,63
SSUM
ESEL,STIF,45
SSUM

RESET
STRESS,SENE
SET,4, 2
PRSTRS
SSUM
ESEL,STIF,63
SSUM
ESEL,STIF,45
SSUM
FINISH

/EOF    ************************************************************
```

The vita has been removed from the scanned document